Role of *MMF1* Gene in Mannosylerythritol Lipid Secretion
and
Sustainable Biosurfactant Production from Brackish Water

by

Yuze Xu

A thesis submitted in partial fulfillment of the requirements for the degree of

Master of Science

Department of Biochemistry
University of Alberta

Abstract

This thesis investigates the secretion of mannosylerythritol lipid (MEL) in the JCM10317 strain of *P. antarctica,* and the potential for a more cost-effective, environmentally friendly production process for MEL.

The study demonstrates that the *Pa MMF1* gene is necessary for the secretion of di-acylated MEL-A/B/C when utilizing water-soluble carbon sources, and also identifies an unknown species of MEL. In addition, the amount of MEL in the cellular fraction of the knockout strain is equal to or more than that of the wild-type strain. A MEL species shift towards more hydrophobic MEL-A was also observed in the cellular fraction of *MMF1 KO* groups. This is the first study to investigate the relationship between the *MMF1* gene and MEL secretion in water-soluble carbon sources, providing new insights into the mechanisms of MEL secretion.

In the brackish water production experiment, the findings demonstrate that the JCM10317 strain can ferment MEL with unsterilized brackish water as a production medium, with waste canola cooking oil as a carbon source. By using a waste product instead of a food crop, and was directly added to the fermentative medium without pre-treatment. Unsterilized brackish water was utilized for MEL production with the addition of sodium chloride (NaCl). This process can convert a waste product into a value-added product, eliminate the need for sterilization, save energy costs, and reduce the need for specialized infrastructure, further contributing to sustainability efforts.

Overall, the findings of this thesis provide insights into the mechanisms of MEL secretion in *P. antarctica* and highlight the potential application of using unsterilized brackish water as a production medium in bioproduction. Further research is needed to fully understand the

mechanism of MEL secretion and the impact of brackish water and waste cooking oil on the MEL production process and the quality of the final product.

Preface

“Life is not easy for any of us. But what of that? We must have perseverance and above all confidence in ourselves. We must believe that we are gifted for something and that this thing must be attained.”

---Marie Curie

Battles and obstacles are an inevitable part of life's journey, constantly challenging our resilience and determination.

Embracing change wholeheartedly requires courage, as we confront the unknown and adapt to new circumstances.

Harnessing our inner strength, we face these changes head-on, persistently learning and growing throughout the process.

Confronting life's hurdles, we develop the essential skills and wisdom needed to overcome future challenges.

Evolving through adversity, we become more resilient and adaptable, prepared for whatever life brings our way.

Transitions, both difficult and smooth, ultimately shape our lives and contribute to our unique personal stories.

So, let us raise a glass to the power of perseverance and the beauty of overcoming adversity, knowing that these experiences are an integral part of our journey.

Acknowledgments

I would like to express my deepest gratitude to my supervisor, Dr. David Stuart, for his exceptional knowledge and guidance throughout my research journey. His unwavering support, both academically and emotionally, has been crucial in the completion of this thesis.

I am also immensely grateful to my committee members, Dr. Bernard Lemire and Dr. Martin Srayko, for their insightful advice, continuous encouragement, and constant support throughout this process. Their expertise has been invaluable in shaping my research.

I would like to extend my appreciation to all current and former lab members, including Brianna Greenwood, Laura Enekegho, Dr. Bonnie McNeil, Dr. Anagha Krishnan, Dr. Tabinda Shakeel, Christian Dykstra, and Xiaodong Liu, for their generous assistance and collaboration, I will always cherish the time we spent together.

Special thanks go to Anthony Cornish at the MBSU, Audric Moses at the Lipidomics Core Facility, and the University of Alberta Natural Resources Analytical Lab for their contributions to the experimental data.

I am especially grateful to my dear friend, Dr. Kalutota Samarasinghe, for the countless insightful discussions and memorable times we spent together at the University of Alberta.

I would like to acknowledge the faculty, staff, and students of the Department of Biochemistry for fostering an inspiring and supportive environment.

Last but not least, I extend my heartfelt appreciation to my family for their unwavering and immense support throughout my academic journey.

Table of contents

List of Tables

List of Figures

List of Abbreviations

Units

M	Molar
g	gram
L	Liter
mM	millimolar
mg	milligram
mL	milliliter
µM	micromolar
µg	microgram
µL	microliter
nM	nanomolar
ppm	parts per million

Abbreviations

6PG	6-phosphate-gluconate
6PGD	6-phosphogluconate dehydrogenase
6PGL	6-phosphate-gluconolactone
acetyl-CoA	acetyl coenzyme A
ACN	aconitase
BA	2-bromooctanoic acid
BG	butylene glycerol
bp	base pair (DNA)
BSA	bovine serum albumin
CS	citrate synthase
CWP	cheese whey permeate
CWW	cassava wastewater
DC-Chol	cholesteryl-3-β-oxycarboxyamidoethylenedimethylamine
ddH_2O	double distilled water

DHAP	dihydroxyacetone phosphate
D-MEL-B	diastereomer MEL-B
DNA	deoxyribonucleic acid
DOPE	1,2-dioleoyl-sn-glycero-3-phosphatidylethanolamine
DPC	dermal papilla cells
DPPH	1,1-diphenyl-2-picrylhydrazyl
E. coli	*Escherichia coli*
E4P	erythrose-4-phosphate
E4PK	erythrose-4-phosphate kinase
EDTA	ethylenediaminetetraacetic acid
Emt1	erythritol mannosyl transferase
ER	erythrose reductase
EtBr	ethidium bromide
F6P	fructose-6-phosphate
Fc receptor	fragment crystallizable receptor
FUM	fumarase
G3P	glycerol-3-phosphate
G6P	glucose-6-phosphate
G6PD	glucose-6-phosphate dehydrogenase
GA3P	glyceraldehyde-3-phosphate
GCK	glucokinase
GDP-mannose	guanosine diphosphate mannose
GFP	green fluorescent protein
GK	glycerol kinase
GLU	glucose
GPDH	glycerol-3-phosphate dehydrogenase
GPI	glucose-6-phosphate isomerase
GSL	glycosphingolipids
HIgG	human immunoglobulin G
HSA	human serum albumin
ICL	isocitrate lyase

IDH	isocitrate dehydrogenase
IDT	Integrated DNA Technologies
IgG	immunoglobulin G
IPF	ice packing factor
LC-FACS	long-chain fatty acid CoA synthetase
LC-MS	liquid chromatography–mass spectrometry
LiAc-PEG	lithium acetate-polyethylene glycol
M1P	mannose-1-phosphate
M6P	mannose-6-phosphate
Mac1	mannosylerythritol acyltransferase 1
Mac2	mannosylerythritol acyltransferase 2
MAL	mannosylarabitol
Mat1	mannosylerythritol lipid acetyltransferase 1
MBC	minimum bactericidal concentration
MCFA	medium-chain fatty acid
MDH	malate dehydrogenase
ME	mannosylerythritol
MEL	mannosylerythritol lipid
MFS	major facilitator superfamily
MIC	minimum inhibition concentration
Mmf1	mannosylerythritol lipid major facilitator 1
MML	mannosylmannitol lipid
MPGT	mannose-1-phosphate guanylyltransferase
MPI	mannose-6-phosphate isomerase
MRL	mannosylribitol lipid
MS	malate synthase
NADPH	reduced nicotinamide adenine dinucleotide phosphate
NAE	α -naphthyl acetate esterase
NBT	nitroblue tetrazolium
NCAE	naphthol AS-D-chloroacetate esterase
NEB	New England Biolabs

NMR	nuclear magnetic resonance
ODH	2-oxoglutarate dehydrogenase
-OH	hydroxyl group
PaE	*Pseudozyma antarctica* Esterase
PCR	polymerase chain reaction
pH	potential of hydrogen
PHEMA	poly (2-hydroxyethyl methacrylate)
PKC	protein kinase C
PMA	phorbol 12-myristate 13-acetate
PMM	phosphomannomutase
PPP	pentose phosphate pathway
PRFFA	post-refinery free fatty acids
PTS1	peroxisome targeting signal 1
R5P	ribose-5-phosphate
RNA-Seq	RNA sequencing
RPE	ribulose-5-phosphate 3-epimerase
RPI	ribulose-5-phosphate isomerase
Ru5P	ribulose-5-phosphate
S7P	sedoheptulose-7-phosphate
SCS	succinyl-CoA synthetase
SDH	succinate dehydrogenase
SDS	sodium dodecyl sulfate
SpA	*Staphylococcus aureus protein A*
SS	soapstock
TAL	transaldolase
TCA cycle	tricarboxylic acid cycle
TEWL	transepidermal water loss
TK	transketolase
TLC	thin layer chromatography
T_m	melting temperature
TPI	triosephosphate isomerase

UA	ustilagic acid
WCO	waste cooking oils
X5P	xylose-5-phosphate
Xu5P	xylulose-5-phosphate
v/v	volume by volume
w/v	weight by volume

Chapter 1

1. Introduction

Biosurfactants are natural and eco-friendly compounds used in various applications, ranging from the food and cosmetic industries to the petroleum industry. These compounds are produced by microorganisms such as bacteria and yeast. They have gained great attention in the surfactant industry due to their unique physicochemical properties, biodegradability, and low toxicity. One of the most promising biosurfactants is the Mannosylerythritol Lipid (MEL), which has a wide range of applications due to its stability, emulsifying, and antibacterial properties. This research will be focused on MEL, and its producer, *Pseudozyma antarctica* JCM 10317.

1.1. Discovery of MEL, MEL structure, and role of MEL in nature

1.1.1. Early discovery of MEL

Ustilaginomycetes are a class of parasitic fungi known to be producers of some important compounds, such as ustilagic acid (UA) [1]. During the screening process of high ustilagic acid-producing strains of *Ustilago zeae*, Haskins, et al. identified extracellular globules of an oil-like material were detected at high yields. The oily compound was separated from the cultures with ethyl ether, and the aqueous phase along with cell debris could be discarded, leaving a colorless extract with a final yield of 15 g/L was isolated from the extracellular fraction and 1.9 g/L from the cell fraction [1]. Analysis of the oily compound by methanolysis yielded mannose, erythritol, acetic acid, and saturated and unsaturated long-chain fatty acids [2]. The mannose and erythritol were found to be present in equal molar quantities, suggesting that the compound contained D-mannoside-meso-erythritol with acetic acid and fatty acid covalently bound to the sugar compound [2]. Based on the chemical analysis, this compound was named mannosylerythritol lipid (MEL).

1.1.2. Structural analysis of MEL

A more detailed structural analysis was performed a decade after the identification of MEL [3]. Thin-layer chromatography (TLC) and infrared spectra suggested that unesterified hydroxyl groups are present in the structure. Hydrolysis of MEL-A demonstrated that there are 4 ester groups on mannose, which suggested that all of the fatty acid tails were linked to the mannose ring. The fatty acid chains were also analyzed in this study: the majority were found to be C16:0 followed by C14:0, together accounting for over 55% of the total incorporated fatty acid. Based on this study, the general structure of MEL was determined and classified as a new class of glycolipids naturally produced by microorganisms [3].

1.1.3. The general structure of MEL

Mannosylerythritol lipids (MELs) consist of a hydrophilic sugar moiety, with a mannosyl group linked to erythritol through a glycosidic linkage, and the hydrophobic moiety usually composed of two acyl chains and zero to two acetyl groups, acyl chains are attached to the C2' and C3' position of mannosyl group via an ester linkage, with acetylation at C4' and C6' (**Fig. 1.1**) [3].

Common MELs can be classified based on the degree of acetylation. MEL-A is the di-acetylated form, while MEL-B and MEL-C are the mono-acetylated forms with mono-acetylation at C6' and C4', respectively, and MEL-D is the unacetylated form [3][4].

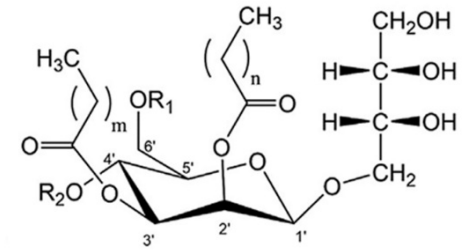

MEL-A: R1=Ac; R2=Ac
MEL-B: R1=Ac; R2=H
MEL-C: R1=H; R2=Ac
MEL-D: R1=H; R2=H

Figure 1.1. The general chemical structure of MEL. m= 6 to 18 carbons; and n= 2 to 10 carbons. Modified from [11].

1.1.4. Variations of MEL structure

Beyond the general classifications above, MEL species display structural variations dependent on factors such as microbial production strain, feedstock assimilated, and cultivation conditions. As previously indicated, the hydrophilic component of MELs is β-D-mannopyranosyl-D-erythritol, and in most MEL producers, the diol of erythritol is in the *S* configuration [5][6]. In contrast, *Pseudozyma tsukubaensis* and *Pseudozyma crassa* produce a stereoisomer version of MELs, with diol of erythritol in the *R* configuration ((*R*)-MEL) [5][6]. Although erythritol is the default sugar alcohol component of MEL, other forms of MEL can be synthesized. If cells are cultured in the presence of sugar alcohols such as arabitol, ribitol, or mannitol, erythritol can be substituted with the added sugar alcohol to yield mannosylarabitol lipid (MAL), mannosylribitol lipid (MRL), and mannosylmannitol lipid (MML) [7][8]. The hydrophobic moiety of MEL consists of fatty acyl chains, other than the common di-acylated MEL, mono-acylated MEL, and tri-acylated MEL can be produced in different cultivation conditions or in response to genetic modifications [9][10]. The length and degree of saturation of the fatty acyl tails are highly dependent on the producing species and feedstock. This will be described in greater detail in subsequent chapters.

In summary: the structural variations observed in MEL species includes 1) the stereoisomer configuration of erythritol; 2) the substitution of erythritol with other sugar alcohol; 3) the number of acyl chains; and 4) the acyl chain length and saturation degree. (**Fig. 1.2**)

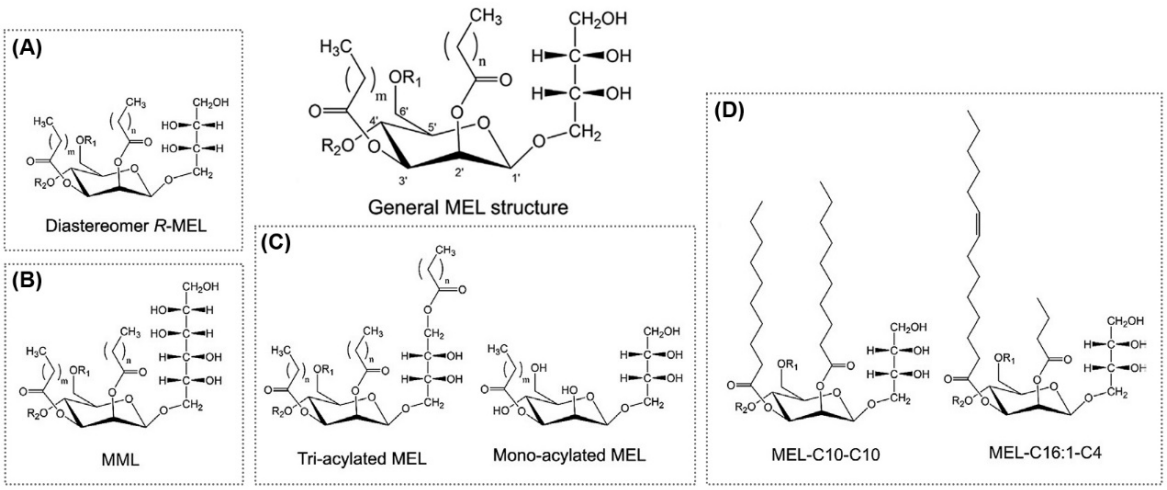

Figure 1.2. Structural variation of unconventional MEL. Structural variation exists in the following ways: (A) diastereomer (R*)*-MEL with opposite diol configuration on erythritol; (B) substitution of erythritol with other sugar alcohol (mannitol as an example); (C) acetylation degree of MEL; and (D) species-dependent and feedstock-dependent acyl chain length and saturation degree. Modified from [11].

1.1.5. MEL-producing conditions

Following the identification of *Pseudozyma antarctica* T-34 as a MEL producer, efforts were made to determine the optimal MEL-producing conditions in batch culture using shake flasks [4]. Kitamoto, et al. found that soybean oil was identified as a superior carbon source, along with other plant-derived oils, and the yield of MELs increased directly with oil concentration in the culture medium up to 8% v/v and then reached a plateau [4]. Nitrogen limitation was considered a critical factor for stimulating MEL production. Among the sources of nitrogen tested, $NaNO_3$ was most effective at a concentration of 0.2% w/v. Other acidic nitrogen salts, such NH_4Cl or $(NH_4)_2SO_4$ had the effect of lowering the pH of the culture medium, and this resulted in a lower product yield [4]. Supplementation of these minimal medium conditions with yeast extract at 0.1% greatly enhanced the yield, presumably because it provided essential vitamins and trace elements. MEL biosynthesis was tested over a range of temperature conditions, and the ideal temperature was determined to be 30 °C, any further increase in temperature reduced the final yield. Based on this research by Kitamoto, et al., the basic production medium and conditions of MEL were established.

1.1.6. Role of MEL in nature

A variety of *Ustilaginomycete* yeasts that secrete MEL have been identified, but the role of MEL in nature is not entirely clear. However, the phenotype of mutants that are unable to produce MEL gives some potential insights into its function. *P. antarctica* is an excellent MEL producer, and the initial strain of this species was originally isolated from the bottom of Lake Vanda in the Antarctic [110]. A closely related strain *P. antarctica* T-34 was used as the recipient for a deletion of the *EMT1* gene, a mutation that prevents the strain from synthesizing MEL (discussed in Chapter 1.2.3). It is also notable that the wild-type and mutant strain were able to grow in culture with a similar doubling time at 25^{o}C. In contrast, while the wild-type strain was able to

proliferate effectively at 4ºC with a doubling time of approximately 72 hours and reached a dry cell mass of > 6 g/L in 21 days, the *emt1* mutant that was unable to produce MEL displayed significantly reduced growth at the lower temperature and was unable to achieve a dry cell mass of even 2 g/L in 21 days [12]. This suggests that MEL production contributes to cold tolerance displayed by *P. antarctica* [12]. Although it has not been demonstrated experimentally, the role of MEL could be similar to other biosurfactants produced by yeasts. Firstly, they could facilitate the assimilation of water-insoluble substrates into the cell. Secondly, they can provide a competitive advantage in nature since MEL shows antimicrobial activity [13]. Thirdly, MEL might play a role in the morphological changes in some MEL-producing strains. For *P. antarctica* T-34, four-fifths of wild-type cells transitioned from yeast form to fungal form with pseudo-hyphae formation in two days, while in *emt1* knockouts, the transition was not observed, and the addition of MEL in the medium allowed this morphology transition [12]. Most MEL-producing strains are plant pathogens. Therefore, the role of MEL associated with propagation was investigated. *P. antarctica* T-34 strains defective in MEL production showed a significantly smaller colony size than the wild-type strains on wheat leaves, and a significant reduction of hyphae formation was also observed. Enlargement of the colonized area and morphological transition were observed when MEL was added exogenously, suggesting MEL plays an important role in propagation on plant surfaces [14]. In contrast, when MEL defective strains of *Ustilago maydis* MB215 were directly injected into corn seedlings, tumor formations and other symptoms are indistinguishable from wild type, suggesting MEL is not essential for virulence [15].

In summary, the potential role of MEL in nature includes 1) cold tolerance; 2) assimilation of hydrophobic carbon; 3) competitive advantage from antimicrobial activity; 4) morphological transition; and 5) plant surface colonization.

1.2. Genes required for MEL biosynthesis are organized into a cluster

MEL is a typical example of a secondary metabolite produced by a fungal species. The genes involved in secondary metabolite synthesis in yeasts are often organized in close proximity in the genome, forming a unique biosynthesis cluster [16]. Identification of the MEL biosynthesis cluster, conservation, and studies on individual genes will be discussed in this chapter.

1.2.1. Identification of a MEL biosynthesis cluster

The MEL biosynthesis cluster was first discovered and characterized in *Ustilago maydis* in 2006 [17]. It was previously known that MEL production in a different producer, *P. antarctica* T-34 is highly induced in nitrogen-limited conditions [4]. Therefore, they performed a genome-wide expression analysis using microarrays and prepared the total RNA before and after nitrogen starvation. In the experiment, the investigators identified a total of 582 genes that were induced more than 2.5-fold, with glycosyltransferase *EMT1* identified as the most highly induced with 25.5-fold upregulation. Bioinformatic filtering was performed, and all the genes that encode proteins involved in nitrogen uptake processes, such as the import of oligopeptides, amino acids, and nucleosides, were eliminated. Following this analysis, it was determined that four genes that are adjacent to *Um EMT1* were induced more than 2.5X in nitrogen-limiting conditions (*Um*03116, *Um*03115, *Um*03114, and *Um*10636). *Um*03115 was predicted to have transmembrane domains, with sequences that are highly conserved in major facilitator superfamily transporters, therefore, they predicted this protein, named Mmf1, is the transporter of MEL. The three other candidates all had high similarity with other fungal proteins of unknown function, and there are two short signature sequences that correspond to Pfam domains that are characteristic of the BAHD family of CoA-dependent acyl transferases, those three proteins were named Mat1 (*Um*03114), Mac1 (*Um*03116), and Mac2 (*Um*10636). Gene deletion studies performed with the individual candidate genes revealed that cells with either *Δemt1*, *Δmac1*, *Δmac2* were unable to synthesize MEL, cells carrying *Δmmf1* were unable to produce extracellular MEL, and *Δmat1* only produced the MEL-D isoform. Overall, this allowed a pathway for MEL biosynthesis to be proposed for *Ustilago maydis* (**Fig. 1.3**).

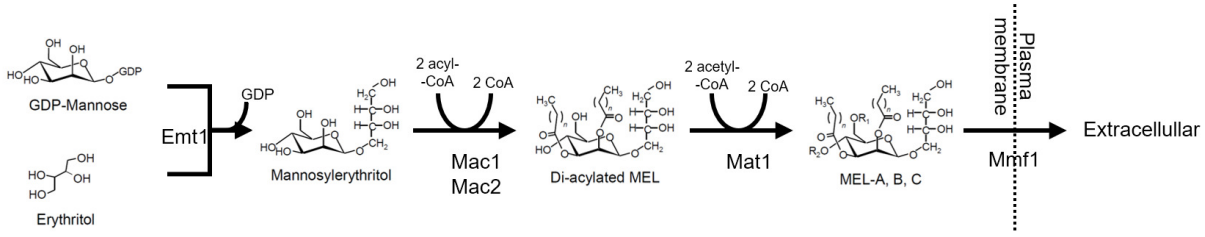

Figure 1.3. The proposed biosynthetic pathway for MEL. Formation of Mannosylerythritol with GDP-Mannose and erythritol, catalyzed by putative mannosyltransferase Emt1; transfer of acyl group to C2' and C3' of mannose ring, catalyzed by putative acyltransferase Mac1/Mac2;

transfer of acetyl group to C4' and C6' by putative acetyltransferase Mat1; export of MELs by putative exporter Mmf1. Modified from [17].

1.2.2. Conservation of the MEL gene cluster among MEL producers

Since the discovery of the MEL biosynthesis cluster in *U. maydis* [17], a similar gene cluster was found conserved in many closely related MEL-producing species, including *P. antarctica* with differences in the arrangement of genes within the cluster [18] (**Fig. 1.4**). Surprisingly, four of five genes with the exception being the putative transporter, were found in a cluster in the ascomycetes *Aspergillus nidulans* genome, but not in its closely related species *Aspergillus fumigatus* and *Aspergillus oryzae* [17]. In the fungal genome, primary metabolism genes are rarely clustered, while genes involved in secondary metabolites are preferentially clustered together, such as trichothecene [19] and gibberellin biosynthesis pathways [20]. One suspicion is that gene clusters for secondary metabolites, such as the MEL biosynthesis cluster, may have been introduced from a different organism through horizontal gene transfer. Although horizontal gene transfer is a relatively rare event in fungi, examples of similar gene clusters found in the distantly related ascomycetes *A. nidulans* [17] and *Geotrichum candidum* [22], and many other MEL-like glycolipid-producing species that are distantly related to *Pseudozyma* clade such as *Schizonella melanogramma* [116], and *Kurtzmanomyces sp.* [23] provide evidence to support this hypothesis. However, the origin of such gene cluster, and the horizontal transfer event, including the order and history of the MEL gene cluster, is hard to verify due to the complex nature of the mechanism.

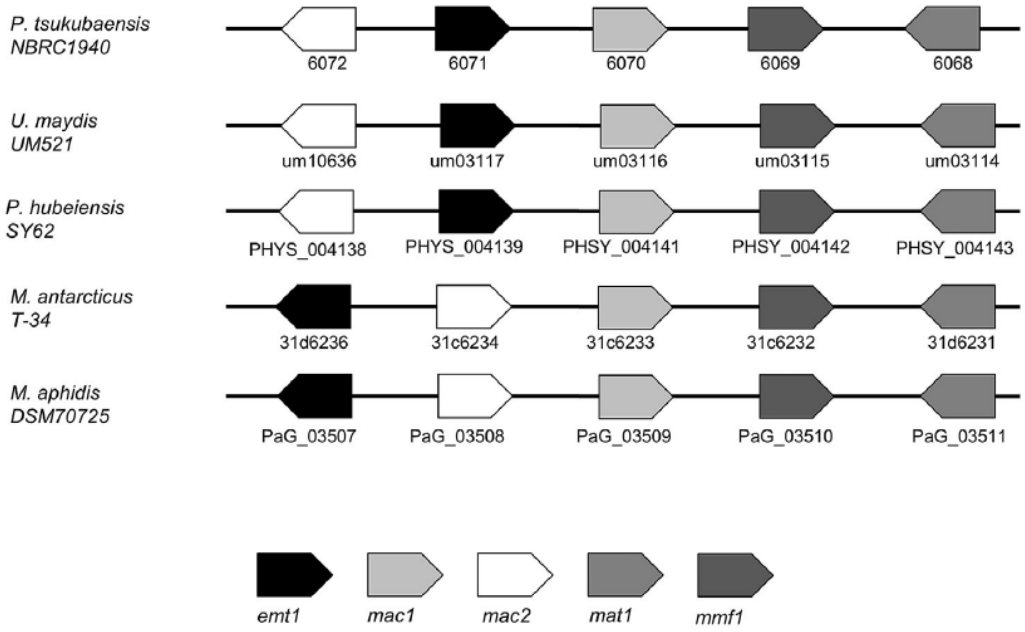

Figure 1.4. MEL biosynthesis cluster in different MEL-producing strains. All 5 genes are organized in close proximity, but the orientation and order are different. *emt1*, erythritol-mannosyl-transferase 1; *mac1* and *mac2*, mannosylerythritol-acyl-transferases; *mat1*, mannosylerythritol-acetyl-transferase 1; *mmf1*, mannosylerythritol-major-facilitator 1. Taken with permission from [11].

1.2.3. *EMT1*, a glycosyl-transferase for the synthesis of mannosyl-erythritol

1.2.3.1. Knockout studies of *EMT1*

The function of the enzyme encoded by *U. maydis EMT1* was determined through a combination of bioinformatics and gene deletion studies [15]. Bioinformatic studies identified 40 protein coding sequences with certain degrees of similarity to glycosyltransferases in *U. maydis.* Genes encoding glycosyltransferase with known function were eliminated from the analysis, and those remaining were subjected to a gene deletion. A knockout of *Um EMT1* in both *U. maydis* FB1 and *U. maydis* MB215 strains eliminated the strain's ability to produce MEL while the production of Ustilagic acid (UA, another glycolipid) was not affected. Therefore, they suggested that *EMT1* may utilize GDP-mannose and erythritol to synthesize the sugar moiety for MEL. Based on the DNA sequence alignments and gene synteny, it was anticipated that the

enzyme encoded by *EMT1* would function in the initial step of MEL biosynthesis in other MEL producers. Gene deletion studies with *Pseudozyma* species *P. antarctica* T-34 [12] and *P. tsukubaensis* NBRC1940 [24] supported this hypothesis. All of the gene deletion studies showed a similar result: Emt1 is essential for MEL production.

1.2.3.2. *Emt1* determines the stereoisomer and composition of the sugar moiety of MEL

Emt1 catalyzes the conjugation of the sugar alcohol erythritol to the mannose ring to yield the hydrophilic moiety of MEL. Hence this enzyme is critical for determining the optical configuration and composition of the final product. Common MEL-producing microorganisms synthesize 4-O-β-D-mannopyranosyl-(2S,3R)-erythritol (*S*-form) of MELs, whereas *P. tsukubaensis* produces only MEL-B with mannopyranosyl-(2R,3S)-erythritol (*R*-form) as the sugar moiety [24]. Amino acid sequence analysis revealed that *Pt EMT1* from *P. tsukubaensis* showed high sequence identity with other MEL producers (69%-72%). However, the sequence alignments revealed three regions with low identity with the 9 *S*-form MEL-producing strains on the phylogenetic tree (**Fig. 1.5**). The role of Emt1 in determining MEL stereoisomer forms was confirmed by expressing *Pt EMT1* in *P. antarctica* carrying *Pa Δemt1*. Analysis of the secreted MEL-A structure using nuclear magnetic resonance (NMR) demonstrated that the diastereomer *R*-form MEL-A was the sole product. Thus, replacing *Pa EMT1* with *Pt EMT1* is sufficient to switch the production of *S*-form MEL-A to *R*-form MEL-A, supporting the hypothesis that Emt1 plays a crucial role in determining the sugar conformation in MEL biosynthesis.

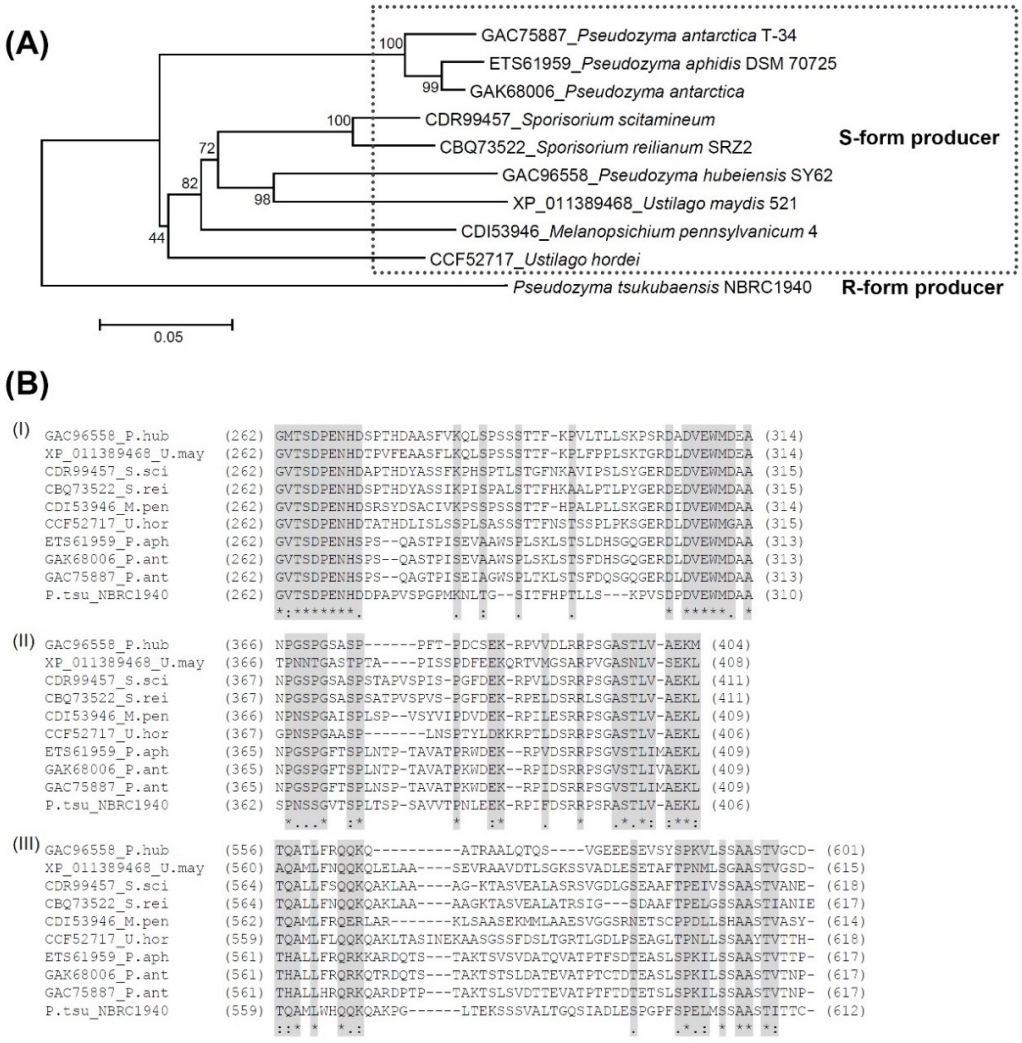

Figure 1.5. Phylogenetic analysis and amino acid sequence of *Pt* Emt1 (A) phylogenetic analysis among *P. tsukubaensis* NBRC1940 and other MEL-producing strains based on the Emt1 amino acid sequence. (B) Detailed view of three low-identity regions of *Pt* Emt1 amino acid sequences and nine other homologous proteins. GAC96558_P. hub: *Pseudozyma hubeiensis* SY62. XP_011389468_U. may: *Ustilago maydis* 521.CDR99457.1_S. sci: *Sporisorium scitamineum*. CBQ73522_S. rei: *Sporisorium reilianum* SRZ2. CDI53946_M. pen: *Melanopsichium pennsylvanicum* 4. CCF52717_U. hor: *Ustilago hordei*. ETS61959_P. aph: *Pseudozyma aphidis* DSM70725. GAK68006_P. ant: *Pseudozyma antarctica* JCM10317. GAC75887_P. ant: *Pseudozyma antarctica* T-34. P. tsu_NBRC1940: *Pseudozyma tsukubaensis* NBRC1940.

1.2.3.3. Localization of Emt1

Investigation of the cellular localization of MEL biosynthetic enzymes in *U. maydis* showed that *EMT1* tagged with GFP co-localized with vacuolar dye Celltracker Blue implying that Emt1 is in the vacuole (**Fig 1.10**) [25]. It needs to be clarified that this represents the true localization of Emt1 in cells since in this case, the investigators used a GFP-Emt1 fusion under the regulation of a heterologous constitutive promoter. Additionally, the *GFP-EMT1* fusion gene was integrated at a heterologous locus in a strain that was expressing the endogenous *EMT1*. Although vacuolar localization should not be discounted by this alone, it might make more sense to find Emt1 in the cytoplasm where it would have access to erythritol generated by the pentose phosphate pathway, and GDP-mannose also generated in the cytoplasm of most yeast and fungi.

1.2.3.4. Utilization of other sugar alcohols by Emt1

The production of unconventional MEL with different sugar alcohol moieties has also been investigated. By feeding four different MEL *S*-form producing yeasts (*P. parantarctica* JCM11752, *P. antarctica* JCM10317, *P. antarctica* T-34, *P. rugulosa* NBRC 10877) with 4% olive oil and 4% D-mannitol, a new species of MEL was detected along with the conventional MELs on thin layer chromatography (TLC). Structural analysis with NMR demonstrated that the unknown glycolipid was mannosyl-D-mannitol lipid [7]. A follow-up study utilized the same principle of feeding *P. parantarctica* with oil in addition to four different sugar alcohols: xylitol, D-ribitol, D-arabitol, and L-arabitol. Interestingly, novel glycolipid was only detected when feeding ribitol and D-arabitol [8]. Another study conducted with *P. tsukubaensis* JCM16987 (*R*-form producer) showed that *P.tsukubaensis* can only incorporate L-arabitol while not utilizing D-arabitol (diol orientation identical to R form of ME) [26]. These investigations demonstrate that mannosyltransferase Emt1 is able to transfer the mannosyl group to sugar alcohols with a similar structure, but the orientation of the diol group near the glycosidic linkage must be identical to that in erythritol (**Fig. 1.6**).

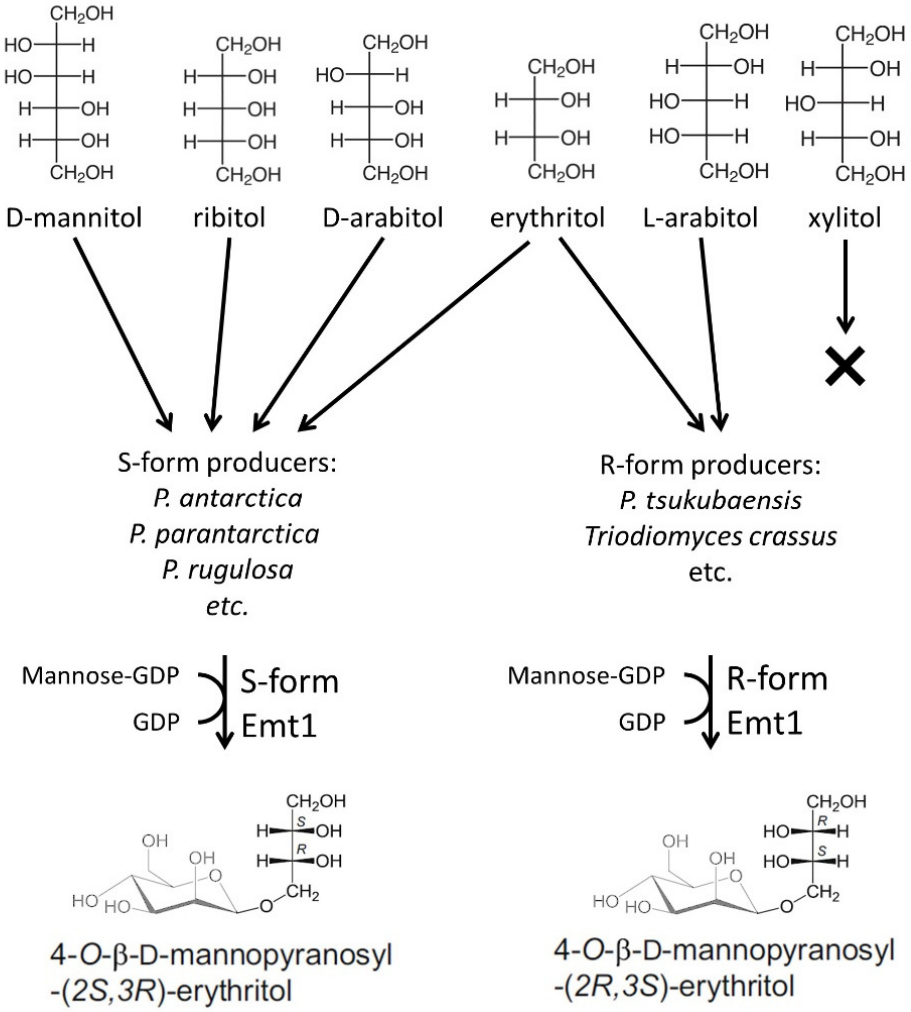

Figure 1.6. The proposed scheme of selective substitution of erythritol by other sugar alcohols. *S*-form/*R*-form Emt1 is specifically selecting sugar alcohol substitutes with the respective diol orientation similar to that of erythritol. Inspired by [26].

1.2.4. Mac1/Mac2 acyl-transferases is required for acyl-chain incorporation into MEL

1.2.4.1. Knockout studies of Mac1/Mac2

In the first investigations that identified the MEL biosynthesis gene cluster, the *MAC1* and *MAC2* genes in *U. maydis* were predicted to contain two short sequences that correspond to Pfam domain 02458, characteristic of the BAHD family of CoA-dependent acyltransferase from plants

[17]. Mac1 and Mac2 were found essential for MEL production, and deletion of either *MAC1* or *MAC2* genes resulted in complete loss of MEL production in *U. maydis* based on TLC analysis (**Fig. 1.7**). These observations lead to the conclusion that Mac1 and Mac2 are not redundant to each other, and may have high regioselectivity towards either 2' -OH or 3' -OH of mannosyl group.

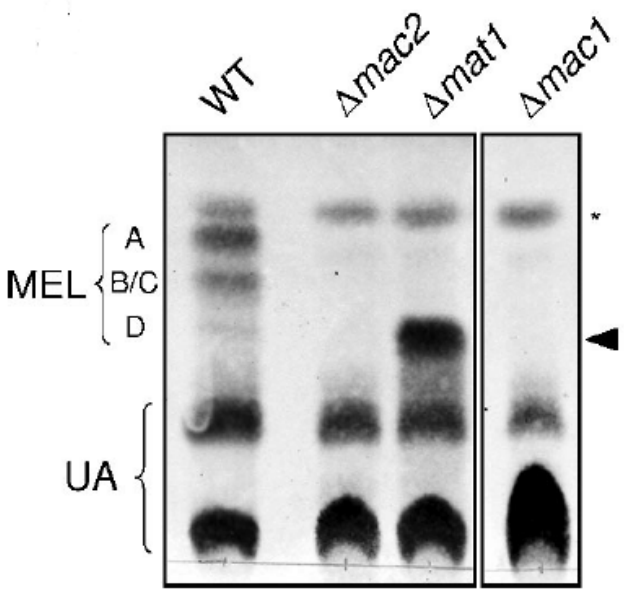

Figure 1.7. Thin layer chromatography analysis of MEL produced from *Ustilago maydis* with *Δmac1, Δmac2* or *Δmat1* mutation. Either *Δmac1* or *Δmac2* results in a complete loss of MEL production while not affecting the synthesis of ustilagic acid (UA). The *Δmat1* mutant strain only produces MEL D, indicated by the filled arrow. Figure taken with permission from [17].

1.2.4.2. Regioselectivity of Mac1/2

A follow-up study on cross-species complementation of Mac2 in *U. maydis* demonstrated the regioselective property of Mac2 [27]. *U. hordei*, a MEL producer, was found to have a putative MEL gene cluster with high amino acid similarity to other MEL producers. When cultured in MEL-producing conditions, the majority of product generated by *U. hordei* is mono-acetylated MEL-B/C with a preference for a short chain (C4) acyl tail at the 2' position and a medium chain (C12-C16) acyl tail at the 3' position of the mannosyl ring with a strong preference of C16.

When heterologously expressing either *U. hordei* Mac1 or *U. hordei* Mac2 in *U. maydis* with deletion of both the endogenous *ΔUm mac1* or *ΔUm mac2* genes, both strains are able to synthesize MEL. The structural analysis of MEL produced from *ΔUm mac2* [GFP-*UhMAC2*] cells showed significantly more C16 fatty acid chain and less C12 side chain at C3' position (similar to MEL produced by *U. hordei*) [27] (**Fig. 1.8**). This suggests that 1) Mac2 is specifically acylating C3' of mannosylerythritol, and 2) acyl chain length profile is a result of enzyme specificity/preference.

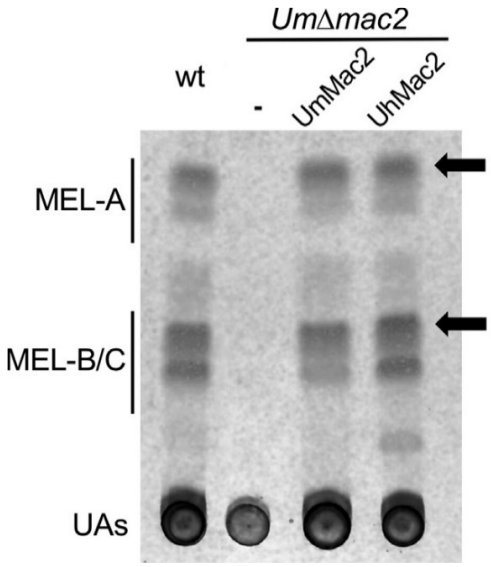

Figure 1.8. Complementation of *Uh Mac2* or *Um Mac2* expressed in *Ustilago maydis* with *Δmac2* background. Expression of *Uh* Mac2 resulted in the production of faster migrating MELs (arrows), indicating a more hydrophobic form of MEL was produced. Taken with permission from [27].

In line with the research above, a recent study conducted on *P. tsukubaensis* 1E5 demonstrated the same regioselectivity of Mac2 [28]. *P. tsukubaensis* carrying *ΔPt mac2* deletion was made through homologous recombination, and deletion of *MAC2* resulted in the production of C2' mono-acylated MEL-D. This showed that Mac1 and Mac2 are indeed regioselective: Mac1 targets 2' -OH, and Mac2 targets 3' -OH. They hypothesized that *P. tsukubaensis* mainly produces diastereomeric *R*-form of MEL, which might allow the stable formation of C2' mono-acylated MEL-D.

1.2.4.3. Localization experiment of Mac1/Mac2

Sequence analysis of Mac1 and Mac2 in *U. maydis* 521 showed that both proteins contain a PTS1-like sequence motif, which is characteristic for localization to the peroxisome (**Fig 1.10**) [25]. When Mac1 and Mac2 were fused with GFP and expressed in wild-type cells, the Mac1 and Mac2-GFP fusions were found localized in the peroxisome. In contrast, when the fusions were expressed in the *pex6* mutant strain (unable to recognize the PTS1 sequence), Mac1 and Mac2 remained in the cytosol. The acyl chain length of MEL was also affected by the intracellular localization of Mac1 and Mac2. When mistargeting Mac1 and 2 to the cytosol, LC-MS analysis of MEL showed a single peak representing C16 at the C2' position of the mannose ring and a C2 chain at the C3' position of the mannose ring as the major product, compared to a mixture of C12:C6, C14:C4, and C16:C2 from MEL produced by the wild-type strain. This result suggests that β-oxidation in the peroxisome is critical for the variety of acyl chain lengths that are incorporated into MEL, and mistargeting of Mac1 and Mac2 reduced the ability to capture acyl chains with variable lengths produced by partial β-oxidation in the peroxisome.

1.2.5. Mat1: an acetyl-transferase that modifies MEL

The *MAT1* gene sequence suggested that the enzyme encoded an acetyl-transferase activity and recombinant *U. maydis* Mat1 produced in *E. coli* has acetylase activity [17]. *In vitro*, recombinant Mat1 can acetylate MEL-D (unacetylated form) at the 4'-OH and the 6'-OH of the mannosyl ring [17], Deletion of the *MAT1* gene in *U. maydis* and *P. hubeiensis* independently resulted in the synthesis of only MEL-D, a species lacking acetylation [17] [29]. These investigations supported the idea that Mat1 played the role of acetylation of MEL. Expression of a GFP-Mat1 fusion in *U. maydis* demonstrated that the fusion localized to the plasma membrane of the cells (**Fig 1.10**) [25].

In the *mac2* knockout study performed in *P. tsukubaensis*, *Δ Pt mac2* strains were only able to produce mono-acylated MEL, and it was observed that this species was without any acetyl group modifications (mono-acylated MEL-D), in contrast with the di-acylated MEL-B produced by wild-type cells [28]. This result suggests that *Pt* Mat1 is unlikely to recognize mono-acylated MEL. In line with this result, *P. antarctica* T-34 produces mono-acylated MEL-D (unacetylated)

while simultaneously producing di-acylated MEL-A/B/C from glucose as carbon source (Chaper 1.3.3.2) [10], which further supports the hypothesis that Mat1 only recognizes di-acylated MEL in such strains, and helps with understanding the ordered events in the biosynthesis of MEL species.

1.2.5.1. Degree of acetylation is dependent on the activity of Mat1

U. maydis preferentially produces MEL-A, while the majority of MEL from *U. hordei* were mono-acetylated MEL-B/C. To test if the difference is due to the properties of the encoded Mat1 or due to other factors such as lipid metabolism, a *U. maydis Δmat1* strain was created expressing either *Um MAT1* or *Uh MAT1* from a plasmid. As expected, MEL-D was produced as the sole product in the *mat1* deletion strain. *Um* Mat1-expressing strains are able to produce a mixture of MEL-A/B/C [27]. Interestingly, the expression of *Uh* Mat1 resulted in the production of mono-acetylated MEL only (**Fig 1.9**). Mat1 exhibited a similar product preference in *P. tsukubaensis*, where mono-acetylated MEL-B was the only product when cultivated in excess (12%) olive oil [30]. This product preference of Mat1 in different organisms provides a toolbox for selective production of MEL species in the future.

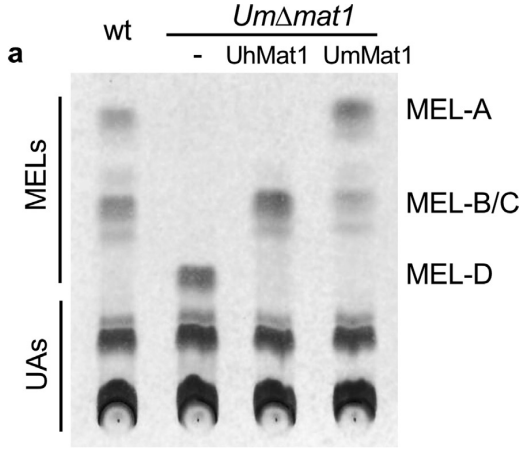

Figure 1.9. Complementation of *Uh* Mat1 and *Um* Mat1 expressed in *Ustilago maydis* with *Um Δmat1* background. Expression of *Uh* Mat1 resulted in the production of mono-acetylated MELs only (MEL-B/C). Taken with permission from [27].

1.2.6. Mmf1: a putative transporter for the export of MEL

The initial studies of the putative transporter Mmf1 were performed in *U. maydis*. The protein was identified along with other three proteins whose mRNAs were upregulated in nitrogen-limiting conditions and was flagged owing to the close proximity of its gene to the genomic sequence encoding the glycosyltransferase Emt1. The amino acid sequence of Mmf1 was predicted to have multiple transmembrane domains, with features representative of major facilitator superfamily transporters [17]. A *U. maydis* knockout mutant was unable to produce extracellular MELs, indicating it is essential for the export of MEL [17]. Mmf1 tagged with GFP was found on the plasma membrane of *U. maydis*, which again supports the hypothesis that Mmf1 is the transporter (**Fig 1.10**) [25].

However, a recent *Δmmf1* knockout study in *P. tsukubaensis* demonstrated a different result [31]. The MEL gene cluster of *P. tsukubaensis* showed a similar arrangement to *U. maydis*, and amino acid sequence alignment showed a very high identity (71%). Wild-type *P. tsukubaensis* cells mainly produce di-acylated MEL-B, traces of di-acylated MEL-D, and mono-acylated MEL-D. On the other hand, the *ΔPt mmf1* mutants produce a reduced amount of total MEL, but surprisingly also produce some extracellular MEL, with the majority product identified as a novel species of MEL: 2' mono-acylated MEL-B, followed by 2' mono-acylated MEL-D and di-acylated MEL-B. [31]

To summarize, the observation of an *MMF1* gene knockout in the *P. tsukubaensis* strain exhibited the following outcomes: (1) The presence of conventional MEL (di-acylated *R*-MEL-B) in the medium is still evident despite its considerably reduced yield relative to the wild-type *MMF1* strain. (2) A novel form of MEL (mono-acylated MEL-B) is detected, both within and outside the cell. (3) The overall production of MELs is notably diminished.

Based on this surprising result, two hypotheses were made: (1) Mmf1 is the transporter of MELs in *P. tsukubaensis*, and the decreased overall production of MEL was to prevent intracellular accumulation, as a result of disruption of *MMF1*. Since di-acylated MEL-B was retained in the cell for an extended time, other unknown esterases might cleave one of the acyl tails of di-acylated MEL-B (*Pt* Mat1 only acetylates di-acylated MEL-D), resulting in mono-acylated MEL-B. And, there might be another unknown transporter that transports the new species across

the membrane. (2) *Pt* Mmf1 is the transporter involved in the transport of acyl-CoA or mono-acylated MELs between organelles. The premature halt in the making of di-acylated MEL-B led to an accumulation of the mono-acylated intermediate.

Unless *P. tsukubaensis* has a different mechanism of MEL synthesis compared to *Ustilago maydis*, the second hypothesis is unlikely to be true. In *U. maydis*, the mechanism involves *Um* Mmf1 localizing on the plasma membrane, and both *Um* Mac1 and *Um* Mac2 localize in the peroxisome [25]. There is also no indication that a transporter is required for the trafficking of MELs between organelles.

When the Mmf1 amino acid sequences of ten MEL producers are aligned, there is a high similarity region spanning ~550 amino acids. However, the sequence at the amino terminus is significantly different in length, and the sequences display low identity to each other (**Fig. 1.11 A**), especially three examples, *P. hubeiensis*, *P. graminicola*, and *U. trichophora*. TMHMM transmembrane helix prediction software predicted that some overhangs are on the extracellular side (*P. hubeiensis*) while others have intracellular overhangs (*U. graminicola*, and *U. trichophora*). Such difference in topology may affect the function of *Mmf1*, and need to be studied in the future.

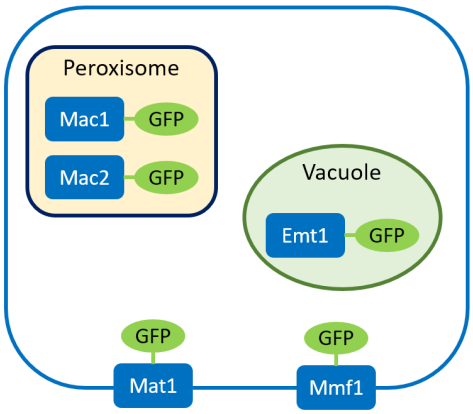

Figure 1.10. Schematic representation of MEL biosynthesis protein-GFP fusion localization within U. maydis. Emt1: erythritol mannosyl transferase; Mac1/2: mannosylerythritol acyltransferase 1/2; Mat1: mannosylerythritol lipid acetyltransferase; Mmf1: mannosylerythritol lipid major facilitator. Inspired from [25].

(A)

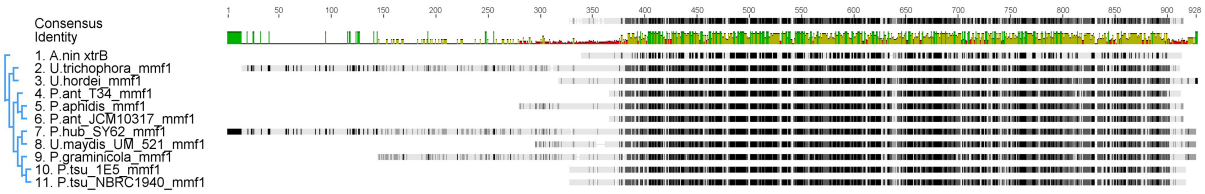

(B)

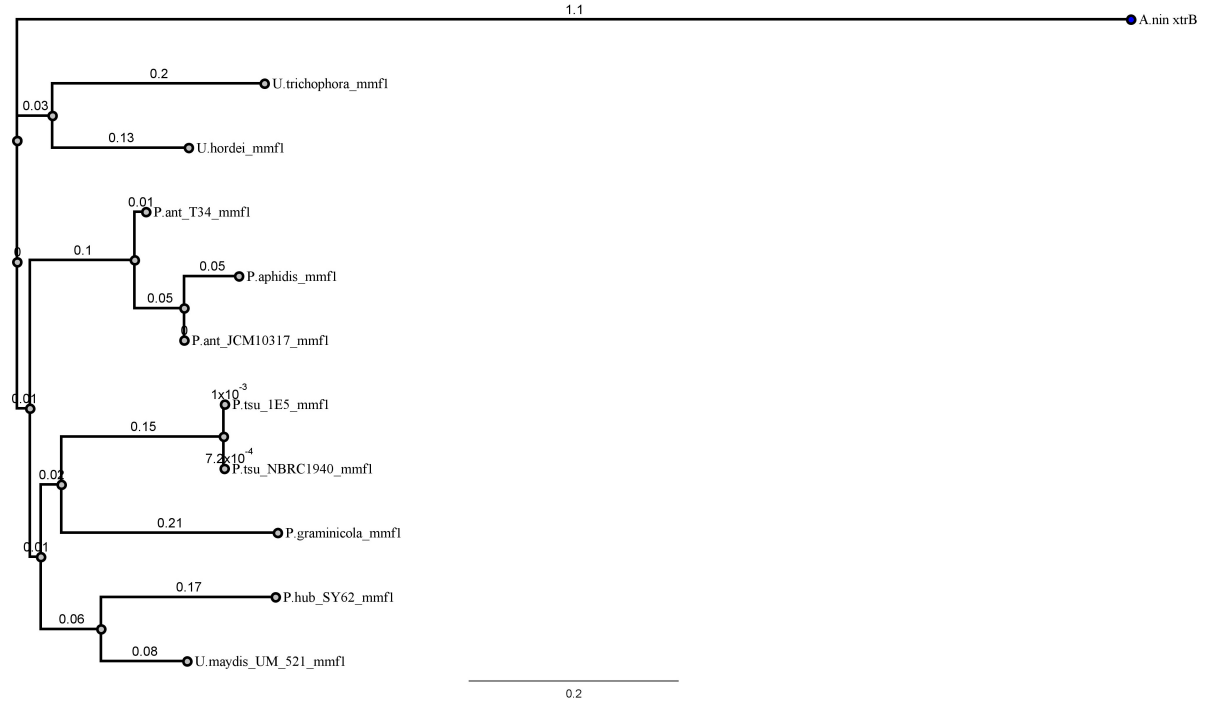

Figure 1.11. Sequence alignment and phylogenetic analysis of Mmf1 protein from different MEL producers. (A) Sequence alignment of Mmf1 amino acid sequence among MEL producers. Conservation plot is represented by identity column, with green has highest conservation and red with lowest. Darker black color in each protein sequence represent higher identity to consensus sequence. (B)The phylogenetic tree of Mmf1 proteins based amino sequence alignment. Abbreviations for organisms: P. ant_JCM10317: *Pseudozyma antarctica* JCM10317; P. ant_T34: *Pseudozyma antarctica* T-34; P. tsu_1E5: *Pseudozyma tsukubaensis* 1E5; P. tsu_NBRC1940: *Pseudozyma tsukubaensis*; P. aphidis: *Pseudozyma aphidis*; P. hub_SY62: *Pseudozyma hubeiensis* SY62. P. graminocola: *Pseudozyma graminocola*; U. maydis_UM521: *Ustilago maydis* 521; U. Hordei: *Ustilago hordei*; U. trichophora: *Ustilago*

trichophora. Outgroup: A. nin xtrB: *Aspergillus nidulans* FGSC A4 XP_660868.1. Figure generated with Geneious software.

1.3. Metabolism and gene regulation of MEL production

In all biotechnological processes involving the production of a specialized product, studying the pathway of precursor formation can give a lot of inspiration for means to increase the efficiency of product formation. For the synthesis of MEL, it is relatively simple, with hydrophilic two-sugar moiety, mannose and erythritol, and fatty acids forming the hydrophilic tail [1]. MEL can be produced at very high efficiency by different microorganisms with different carbon sources such as sugar [9], plant-derived oils [31], and other feedstocks [32][33]. The difference in metabolism pathways in different feedstock will be discussed.

1.3.1. Supply of precursors

1.3.1.1. Sugar moiety

Production of the hydrophobic sugar moiety of MEL is relatively simple when the feedstock is glucose. First, glucose was transported into the cell by the Hxt1 homolog transporter [35], activated by phosphorylation, and isomerized to fructose-6-phosphate (F6P). F6P can then be isomerized to form mannose-1-phosphate (M1P), then activated by mannose-1-phosphate guanylyltransferase (MPGT) to form GDP-mannose, one of the precursors of MEL. Erythritol can be derived from two different pathways, both involving the pentose phosphate pathway (PPP). The first pathway involves the oxidative phase of PPP, ribulose-5-phosphate (Ru5P), and NADPH is generated from glucose-6-phosphate (G6P) in the oxidative phase. In the context of erythritol synthesis, the final product of the non-oxidative phase is erythrose-4-phosphate (E4P) that can be subsequently dephosphorylated and reduced. The second pathway is much simpler: glyceraldehyde-3-phosphate (GA3P) and F6P from glycolysis are directly incorporated by transketolase to form Xylose-5-phosphate (X5P) and E4P [36]. E4P can be dephosphorylated to erythrose by the erythrose-4-phosphate kinase (E4PK), then converted to erythritol by erythrose reductase (ER) (**Fig. 1.13**) [37].

When using fatty acids as feedstock, gluconeogenesis plays an important role in making the precursor for the sugar moiety. Long-chain fatty acids were first converted to acetyl-CoA through β-oxidation; other than the energy-generating TCA cycle, the glyoxylate cycle allows conversion from acetyl-CoA to malate, which can then be converted to pyruvate and finally to glyceraldehyde-3-phosphate (GA3P) (**Fig. 1.12**) [38]. GA3P is the universal intermediate, connecting glycolysis, gluconeogenesis, and pentose phosphate pathway (**Fig. 1.13**). Which ultimately allows the production of GDP-mannose and erythritol from fatty acid as the sole carbon source.

From both glucose and fatty acids as carbon sources, the precursor GDP-mannose and erythritol can be made and combined to form mannosylerythritol (ME) by the mannosyltransferase Emt1.

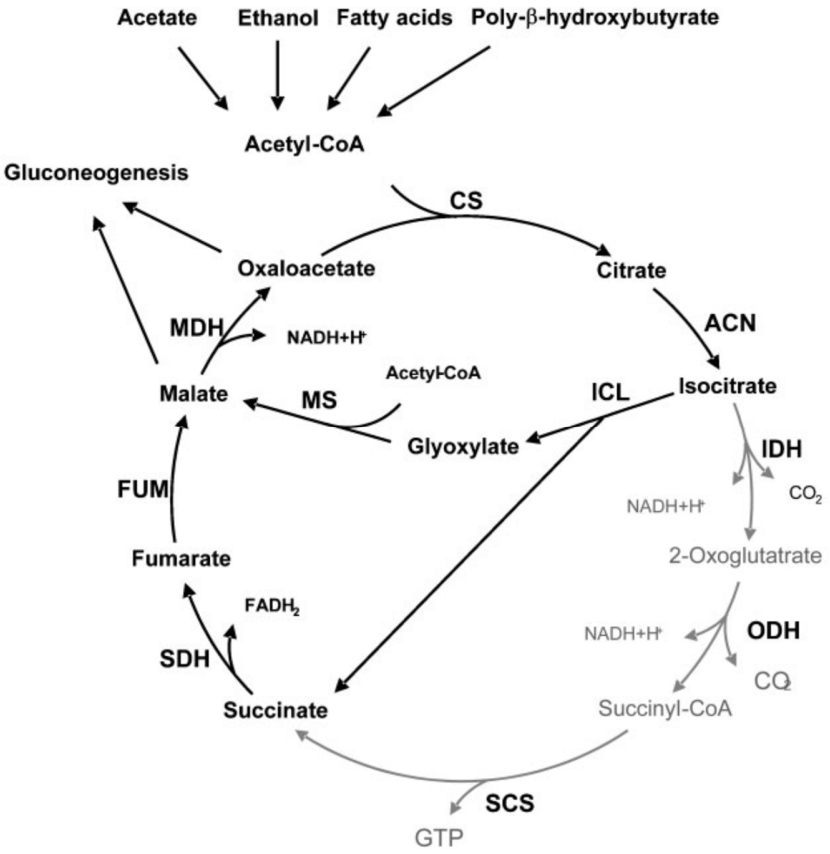

Figure 1.12. Glyoxylate citric acid cycle reactions. Acetyl-CoA can be generated from various metabolism reactions, including fatty acid metabolism. Glyoxylate cycle reactions bypass the CO_2-generating step. Black arrow, glyoxylate cycle; grey arrow, citric acid cycle Abbreviations:

CS, citrate synthase; ACN, aconitase; IDH, isocitrate dehydrogenase; ODH, 2-oxoglutarate dehydrogenase; SCS, succinyl-CoA synthetase; SDH, succinate dehydrogenase; FUM, fumarase; MDH, malate dehydrogenase; MS, malate synthase; ICL, isocitrate lyase. Taken with permission from [38].

1.3.1.2. Hydrophobic tail

Many experiments demonstrated that when using vegetable or other plant-derived oil as the sole carbon source, large quantities of MEL can be synthesized by different MEL producers. When using such feedstocks as carbon sources, the generation of medium-chain fatty acids (MCFA) incorporated into the mannose ring is relatively simple. Triglycerides were first hydrolyzed to long-chain fatty acids and glycerol by an extracellular esterase secreted by the cells (lipase 1 in *U. maydis*, and *P. antarctica* esterase (PaE)) [39][109], and fatty acids were then activated by long-chain fatty acid CoA synthase (LC-FACS). The long-chain acyl-CoA was then directed to the peroxisome, where partial β-oxidation or chain-shortening pathway plays a central role in the production of the medium-chain acyl-CoA (Chapter 1.3.3.1) (**Fig 1.13**) [25], preferentially utilized by Mac1 and Mac2 acyl transferases. The hydrophobic moiety can either be generated by the gluconeogenesis pathway discussed previously [38] or can be derived from glycerol (Chapter 1.3.2.1).

Alternatively, when utilizing water-soluble carbon sources as the sole feedstock for MEL production, the long-chain fatty acid can be derived from lipogenesis through acetyl-CoA as a precursor. These fatty acids are subsequently directed to the peroxisome, where β-oxidation occurs to shorten the chain length to medium-chain fatty acids (MCFA). These intermediates are utilized by Mac1 and Mac2 acyl transferases to synthesize the hydrophobic moiety (**Fig 1.13**). Detail will be discussed in Chapter 1.3.3.

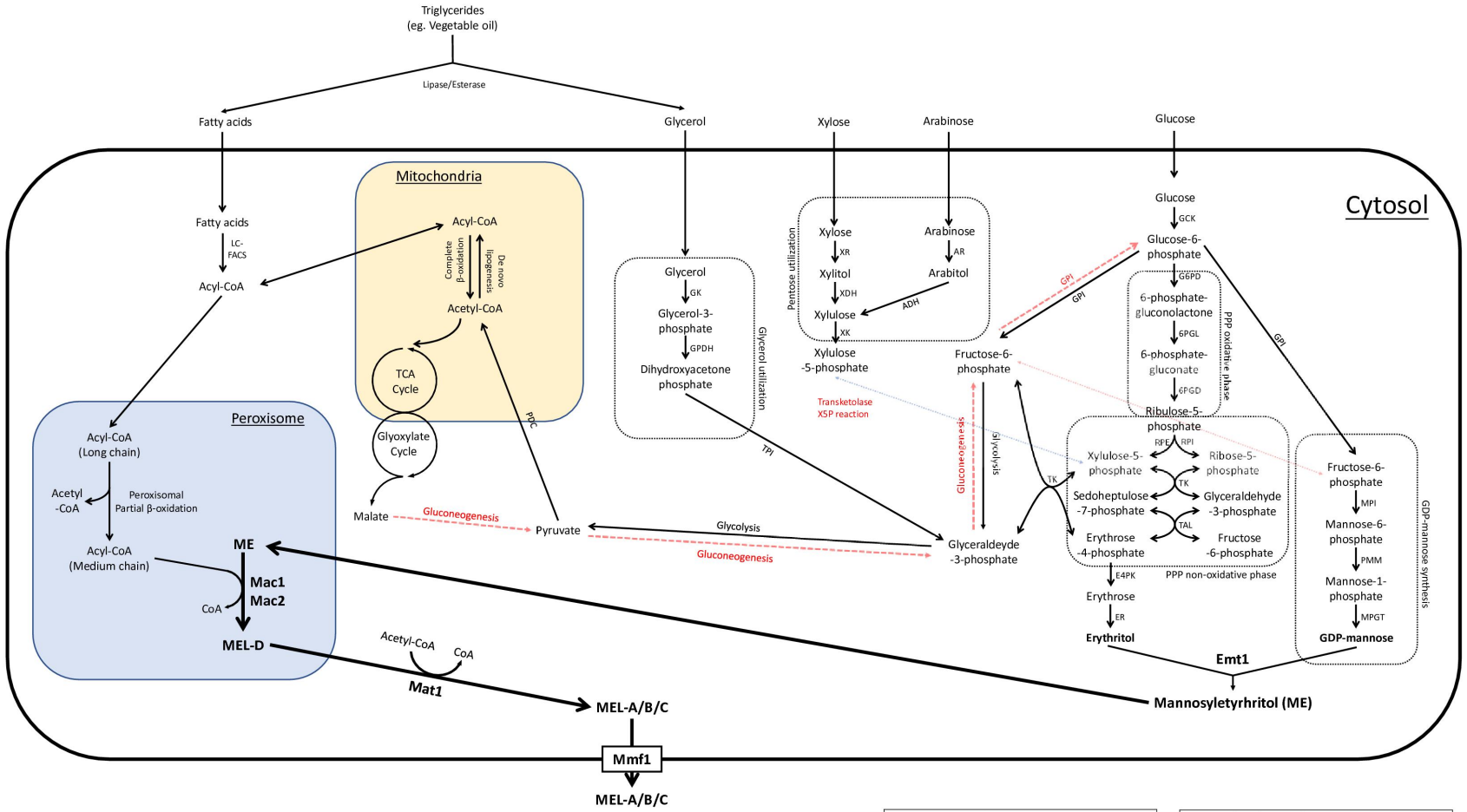

Lipogenesis	
PDC	Pyruvate dehydrogenase complex

Pentose Utilization pathway	
XR	Xylose reductase
XDH	Xylitol dehydrogenase
XK	Xylulose Kinase
AR	Arabitol reductase
ADH	Arabitol dehydrogenase

Glycerol pathway	
GK	Glycerol kinase
GPDH	Glycerol-3-phosphate dehydrogenase
TPI	Triosephosphate isomerase

Acetyl-Coa pathway	
LC-FACS	long-chain fatty acid CoA synthetase

MEL biosynthesis pathway	
Emt1	Erythritol mannosyl transferase
Mac1	Mannosylerythritol acyltransferase 1
Mac2	Mannosylerythritol acyltransferase 2
Mat1	Mannosylerythritol lipid acetyltransferase 1
Mmf1	Mannosylerythritol lipid major facilitator 1

Mannose-GDP pathway	
GPI	Glucose-6-phosphate isomerase
MPI	Mannose-6-phosphate isomerase
PMM	Phosphomannomutase
MPGT	Mannose-1-phosphate guanylyltransferase

Erythritol pathway	
E4PK	Erythrose-4-phosphate kinase
ER	Erythrose reductase

Pentose Phosphate pathway	
GCK	Glucokinase
G6PD	Glucose-6-phosphate dehydrogenase
6PGL	6-phosphate glucolactonase
6PGD	6-phosphogluconate dehydrogenase
RPE	Ribulose-5-phosphate 3-epimerase
RPI	Ribulose-5-phosphate isomerase
TK	Transketolase
TAL	Transaldolase

Figure 1.13. A detailed metabolic map from different carbon sources towards MEL production. Abbreviations of enzymes are listed below. Glycolysis and pentose phosphate pathway are critical for generating the precursor of the sugar moiety. Peroxisomal partial β-oxidation is important for supplying medium-chain fatty acid. Sugar and lipid metabolism are linked with mitochondrial β-oxidation, glyoxylate cycle, and gluconeogenesis. Inspired by [11].

1.3.2. Metabolic pathway leading from other precursors to MEL

1.3.2.1. Glycerol

Glycerol, either derived from the cleavage of triglycerides from plant-derived oil by extracellular esterase or added to the medium as the sole carbon source, can be used to synthesize MEL. The first step of the proposed carbon metabolism is to phosphorylate glycerol with glycerol-kinase, yielding glycerol-3-phosphate (G3P), and then further converted to dihydroxyacetone phosphate (DHAP) by glycerol-3-phosphate dehydrogenase (GPDH), and finally, yielding GA3P, the critical intermediate connecting glycolysis, gluconeogenesis, and lipogenesis, allowing the production of all precursors for MELs (**Fig 1.13**). Production of MELs from glycerol was demonstrated with *P. antarctica* JCM10317 [50].

1.3.2.2. Pentose

The utilization of 5-carbon sugars such as xylose and arabinose are of great interest for biosurfactant production since pentose can be derived from lignocellulosic waste along with glucose [34]. In the proposed pathway, both pentoses were first converted to their respective sugar alcohol form by reductase, followed by dehydrogenase, yielding xylulose, which can be phosphorylated to form xylulose-5-phosphate (X5P), an intermediate in pentose phosphate pathway, where it can be converted to erythritol or introduced into glycolysis, producing all precursors of MEL (**Fig 1.13**). The growth and MEL production of *P. antarctica* JCM10317 with xylose as the sole carbon source was demonstrated [40].

1.3.3. Fatty acid metabolism providing acyl chains for MEL synthesis

1.3.3.1. β-oxidation and chain shortening

A supply of medium-chain fatty acid (MCFA) is crucial for MEL synthesis, and the chain shortening pathway or partial β-oxidation plays a crucial role in MCFA synthesis [41]. In contrast to the complete β-oxidation in the mitochondria, the chain-shortening pathway is localized in the peroxisome [25], an organelle important for the synthesis of secondary metabolites [41].

A detailed series of studies on the role of fatty acid metabolism in MEL biosynthesis have been performed. The initial study carried out in 1993 utilized a *P. antarctica* T-34 strain fed with a series of fatty acid methyl esters (C11-C18) [43]. First of all, the growth rate exhibited a positive correlation with fatty acid chain length from C11 to C18, and cultures fed with C11 did not produce MEL. Strains cultured with longer chain lengths, even-numbered fatty acids (C12, C14, C16, C18) incorporated predominantly C10 acyl chains into the MEL produced regardless of the chain length of the initial feedstock. When odd-numbered substrates (C13, C15) were used as feedstock, the resulting fatty acid on MEL contained mainly odd-numbered chains (C9, C11). Hence, the conclusion is that acyl chains on MEL were always shortened by 2n carbons from the long-chain fatty acid feedstock.

Unsaturated MCFAs were only detected when using unsaturated long-chain fatty acids as feedstock, and the position of the double bond shifted toward the α-end in a 2n manner. This indicates that acetyl group removal is occurring on the α-end of the fatty acid.

The importance of the peroxisomal β -oxidation pathway for MEL biosynthesis was demonstrated with a β-oxidation inhibition study performed in 1998 [42]. *P. antarctica* T-34 preferentially produces MEL with the acyl chain length of C8, C10, and C12 [42]. 2-bromooctanoic acid (BA) was used as an inhibitor for partial β-oxidation, and the inhibition of MEL synthesis was significantly stronger than growth inhibition in a concentration-dependent manner in growing cells. Additionally, when cultures were co-incubated with BA and fatty acids with different chain lengths (C12-C18), cultures of the yeast supplied fatty acids with shorter chain length were significantly less inhibited by BA in MEL production than groups fed with longer fatty acids. From these results, it can be presumed that longer chains (C18) require more partial β-oxidation activity for MEL synthesis, while shorter chains do not necessitate strong

activity. Overall, these results demonstrated that the chain-shortening pathway is critical for MCFA synthesis, which is preferentially incorporated into MEL.

The effect of inhibiting the *de novo* synthesis of fatty acids on MEL production was also studied [46]. Cerulenin, an inhibitor of *de novo* fatty acid synthesis, caused only a weak reduction in MEL synthesis and growth when cells were fed on long-chain fatty acid methyl esters, while more significant with C12 and C13 feedstocks. This result indicates that MCFAs on MELs are derived from the chain-shortening of long-chain fatty acid rather than *de novo* synthesis of medium-chain fatty acids.

Overall, all evidence suggests that when long-chain fatty acids were fed, MEL lipid moiety MCFAs were generated from the partial chain-shortening pathway in peroxisome and *de novo* synthesis of fatty acids are not essential.

1.3.3.2. Mono/tri-acylated forms of MEL

P. antarctica T-34 produced mono-acylated MEL-D along with di-acylated MELs when using a high concentration of glucose (10%) as the sole carbon source, and the yield of MEL was much lower than when cells were provided with vegetable oils as feedstock [10]. Since previous experiments demonstrated that most of the MCFAs are from partial β-oxidation but not *de novo* synthesis when long-chain fatty acids were present, the hypothesis is that lower total yield and production of mono-acylation of MEL was due to the limitation of *de novo* synthesis of MCFA from acetyl-CoA, and mono-acylated MEL might be an intermediate for di-acylated MEL synthesis. Interestingly, all of the mono-acylated MEL is acylated at the C3' position of the mannose moiety. Previous experiments demonstrated a spatial preference that Mac1 targets the C2' position and Mac2 targets the C3' position of the mannose ring. Thus, this experiment potentially suggests the order of the MEL biosynthesis pathway: acylation at C3' first by Mac2, followed by acylation at C2' by Mac1.

Another experiment of feeding *P. antarctica* T-34 and *P. rugulosa* NBRC 10877 with excess vegetable oil (12%) showed the production of more hydrophobic glycolipid [9]. The structural analysis demonstrated that those were tri-acylated MEL with an additional long-chain acyl tail on the terminal hydroxyl group of erythritol. Since the chain length of the additional acyl tail

(C18:1) is significantly different from MFCAs at other positions (C8-C10), the authors suspected that the tri-acylated MEL was produced by extracellular lipase activity. *In vitro* production of tri-acylated MEL was demonstrated successfully by treatment of purified di-acylated MEL-A with Novozym 435 (*P. antarctica* lipase B fixed on resin, [47]) and methyl oleate.

This research opened a gateway for enzymatic post-synthesis modification of purified MELs. Later, (*S)*-MEL-D [49], and (*R*)-MEL-D [48] were produced in this manner, which opened the possibility of obtaining more hydrophilic MELs for applications where higher water solubility is required.

1.3.4. Regulation of MEL biosynthesis cluster

Generally, all MEL-producing species require a high carbon/nitrogen ratio in order to produce MEL. But MEL production is also carbon source dependent for some species. For example, *P. antarctica* can produce MEL with glucose [10], glycerol [50] and vegetable oil [51], while *P. aphidis* can only produce MEL in presence of hydrophobic carbon sources such as soybean oil [52]. Such differences suggest that the regulation of MEL synthesis is triggered differently. The regulation of MEL gene cluster and general metabolism genes in MEL biosynthesis will be discussed in this section.

1.3.4.1. Nitrogen availability

Nitrogen limitation was demonstrated to be a critical factor for MEL production in many different species. The yield of MEL is greatly enhanced in nitrogen-limiting conditions. Although there is no evidence for conserved motifs, several GATA sequences were identified in the promoter region of all five genes in the MEL synthesis cluster in *U. maydis*, suggesting a potential GATA-dependent transcription factor homolog to the general nitrogen dependent transcriptional regulator (AREA from *A. nidulans*) is controlling the transcription of MEL genes. The homolog of AREA, *Um* 04252 was found in *U. maydis* genome [15], but there are no further studies about the nitrogen-dependent regulatory mechanism, and more extensive investigations need to be done to understand the mechanism of MEL gene induction.

1.3.4.2. Carbon sources

Nitrogen limitation is considered a critical factor for most species in the production of glycolipid surfactant production, including MEL, but carbon sources affect MEL production in a species-dependent manner. The first study focused on comparing the difference in transcriptional regulation between two prominent MEL producers: *U. maydis* and *P. antarctica* in glucose and vegetable oil as carbon sources [53]. Even though both species exhibited a high degree of genome synteny, the expression of genes (evaluated using the DNA microarray method) related to fatty acid metabolism is significantly higher in oily conditions compared to glucose feedstock in *P. antarctica*. In addition, in *P. antarctica*, MEL biosynthesis cluster genes were highly expressed in both feedstocks. However, *U. maydis*, a maize pathogen that utilizes starch in its natural habitat, exhibited a much lower expression of MEL genes with vegetable oil as feedstock. This result is consistent with the previous observations that *U. maydis* preferentially produces MEL in glucose as carbon source [53], and demonstrated that MEL gene regulation is species-dependent, which makes sense given the differences in their typical environment.

Another evidence of carbon source-dependent regulation of MEL biosynthesis was from transcriptome profile analysis of *P. aphidis* when cultured with (i) excess soybean oil with glucose as a secondary carbon source, and (ii) identical conditions with no soybean oil [55]. When there was no presence of oil, the extracellular MEL production was significantly suppressed. The transcriptome analysis (using RNA-Seq) demonstrated that four out of five genes in the MEL biosynthesis cluster (except *PaG* MAT1) were highly induced in oily conditions, with *PaG EMT1* encoding mannosyltransferase with the strongest induction close to 40-fold. [55] These observations suggest that the MEL biosynthesis cluster genes in *P. aphidis* were clearly induced by the presence of hydrophobic carbon sources, and *PaG MAT1* might have a different regulatory mechanism.

1.3.5. Regulation of metabolism

In the transcriptome analysis of *P. aphidis* (MEL production induced with oily carbon sources), genes related to five classes of metabolic processes were significantly upregulated along with MEL gene clusters in the presence of hydrophobic carbon source [55]. The first category is related to cell growth, corresponding to morphology changes such as size expansion, filamentous growth, and accumulation of inclusion bodies for hydrophobic carbon storage. Eleven genes

related to nitrogen assimilation and metabolism represent the second class, which conforms with the nitrogen limitation condition required for MEL production. The third category is transport proteins related to the assimilation processes of inorganic ions, which might be important for functions in metabolism for MEL precursor synthesis and cell growth. Several genes related to lipid metabolism were identified and classified into the fourth category. Among those, genes for a lipase (*PaG_02330*) and 3-hydroxyacyl-dehydrogenase (*PaG_01112*) were significantly induced. The first gene might be related to the assimilation of oily carbon sources, and the second one plays an integral role in the β-oxidation pathway, both critical for MEL biosynthesis. The last group of genes can be classified with functions related to plant fungal infection. One particular gene (*PaG_10058*) showed high similarity to plant expansins, a non-enzymatic protein that induces the extensibility of plant cell walls and assists fungal infection [106]. In summary, genes related to morphological changes, nutrient assimilation, metabolism, and secretion of effector proteins were observed for *P. aphidis* upon induction with hydrophobic carbon sources.

A more detailed transcriptome analysis of metabolism genes related to the production of MELs was performed in *P. antarctica* and *U. maydis* [107]. The critical difference between both MEL-producing organisms is that *P. antarctica* can efficiently produce MELs with both glucose and plant derived oils as a sole carbon source while *U. maydis* displayed poor growth and MEL synthesis in oily conditions. This study compared the induction level of classes of genes in vegetable oil vs in glucose. As expected, β -oxidation in both mitochondria and peroxisome was highly induced in both organisms in the presence of vegetable oil, and fatty acid synthesis was suppressed. However, in *P. antarctica*, glycolysis/gluconeogenesis and citric acid cycle were induced in oily conditions but not *U. maydis*. Among those genes, malate synthase (14d00059), the critical enzyme for gluconeogenesis, is highly induced in *P. antarctica*. This might explain the difference in carbon source preference between the two organisms. *P. antarctica* is able to efficiently generate sugar moiety components through the carbon supply by gluconeogenesis, while acetyl-CoA and energy are provided through the TCA cycle. The difference in metabolism could be a result of evolution by living in different environments. *P. antarctica* T-34 was isolated from plant leaves, and breakdown of cuticles, a waxy coating, is utilized with lipases and esterases assisted hydrolysis, followed by assimilation with the assistance of MELs. On the other hand, *U. maydis* is a maize pathogen, therefore utilization of starch-derived sugar is more important.

1.4. Applications

1.4.1. Antimicrobial activity

MEL is produced as a secondary metabolite in the late logarithmic phase and stationary phase, and in theory, the antimicrobial activity can provide producers advantages in competition in the natural environment. On the other hand, multidrug-resistant bacteria can cause major problems in the healthcare system and have become a global concern and there is a growing demand for novel antimicrobial agents. The antimicrobial activity of MELs from several producers was investigated and will be discussed in this section.

1.4.1.1. MEL-A/B as a gram-positive bacteria inhibitor

The antimicrobial activity of MELs was first investigated by Kitamoto et al. in 1993, MEL-A and MEL- B were produced from soybean oil, purified then tested separately [57]. Both glycolipids showed strong activity against Gram-positive bacteria such as *Bacillus subtilis*, *Micrococcus leteus*, *Mycobacterium rhodochrous*, and *Staphylococcus aureus*, while weakly against Gram-negative bacteria with exception of *Pseudomonas rivoflavina*, and inactive against fungus. The more hydrophobic MEL, MEL-A was more active on bacteria than MEL-B. Importantly, MELs demonstrated much greater antimicrobial activity than synthetic glycolipid surfactants such as Sucrose monocaprate (SE 10) and SPAN 20. Recently, Shu, et al demonstrated that MEL-A exhibited a remarkable potential in combating multidrug-resistant *Staphylococcus aureus*, with a minimum inhibitory concentration (MIC) of 256 μg/mL in bacterial suspension, and an impressive biofilm eradication rate of over 90% when combined with ultrasound treatment [127]. When feeding the *P. antarctica* T-34 strain with glucose, mono-acylated MELs were produced. When performing the same minimum inhibition concentration (MIC) assay, the number was much higher than conventional MEL. Mono-acylated MEL is less hydrophobic due to one less acyl chain on C2', and less effective against bacteria as expected [58]. There is a positive correlation between hydrophobicity of MELs and bactericidal activity against Gram-positive bacteria. The suspected mechanism of antimicrobial activity is due to solubilizing activity against cell membranes. Due to the surface structural difference between Gram-positive and Gram-negative bacteria, the activity is significantly weaker in Gram-negative

bacteria due to the extra lipopolysaccharide outer membrane. Although the activity is weaker than SDS, the MEL's biodegradability and low toxicity is a major advantage over chemical surfactants.

1.4.1.2. MEL-A as a food preservative

Bacillus cereus is a Gram-positive, foodborne pathogen that can produce toxins and cause gastrointestinal illness [59]. Shu, et al reported the investigation of the bactericidal activity of MEL-A produced from *P. aphidis* against *B. cereus* vegetative cells and spores. Purified MELs (80% MEL-A) demonstrated a MIC of 1.25 mg/mL and a minimum bactericidal concentration (MBC) of 2.5 mg/mL against *B. cereus*. Furthermore, intracellular constituent leakage and reduction of cell viability were observed, indicating an unbalanced intracellular environment is caused by MEL [60]. Taken together, the results of this study provide evidence for the potential of MEL as a safe and effective food preservative in the food industry, owing to its low toxicity and potent bactericidal properties.

1.4.1.3. Pesticidal property of MELs against plant pathogenic fungi

Kitamoto, et al reported the investigation of the pesticidal property of MELs (MEL-A/B/C; diastereomer MEL-B) by testing disease suppressive activity against various pathogenic fungi, as well as their impact on fungal growth on host plant surfaces [61]. First of all, the effect of MEL on conidia germination was investigated on surfactant-treated (0.1% w/w MELs) hydrophobic plastic surfaces to simulate plant surfaces. MEL-A and diastereomer MEL-B ((*R*)-MEL-B) showed a significant suppressive effect on *Blumeria graminis* (causing powdery mildew on wheat), while enhanced germination on *Glomerella cingulata* (causing anthracnose disease on strawberry). These results demonstrate that MELs have different conidial germination inhibiting effect depending on the fungal species [61]. Overall, this preliminary study demonstrated that MELs have the potential to suppress powdery mildew of wheat plants, with inhibition of conidia germination as the potential mechanism. The low toxicity property of MEL could give a great advantage over chemical pesticides in agricultural applications. Further research can be conducted to investigate the pesticidal properties of different types of MELs on various pathogenic fungi and to uncover the mechanisms underlying their antifungal activity, and

provide important insights for the potential utilization of these biomolecules as natural fungicides.

1.4.2. Cosmetic industry

1.4.2.1. Moisturization activity of dry skin

MELs have a similar structure to ceramide-3, which is an essential intracellular lipid of the outer epidermis cells (**Fig. 1.14**). A similar chemical structure implies that MELs may exhibit skin care properties [62]. An *in vitro* assay system using a human skin tissue model (TESTSKIN^{TM} developed by Toyobo) and treated with sodium dodecyl sulfate (SDS) solution to simulate damage was used to investigate the effectiveness of MELs on skin tissue recovery. MELs and ceramide-3 were applied under dry skin conditions, and all MEL species demonstrated excellent recovery effects (by relative viability) on damaged cells at 1% concentration [63]. In later studies, Yamamoto et al reported that MEL-A produced from olive oil demonstrated a significantly higher recovery rate than from soybean oil [64]. This might be a result of the unsaturated fatty acid composition of feedstock resulting in the difference in the unsaturated acyl chain of MELs, and eventually affecting the biological activity of MELs.

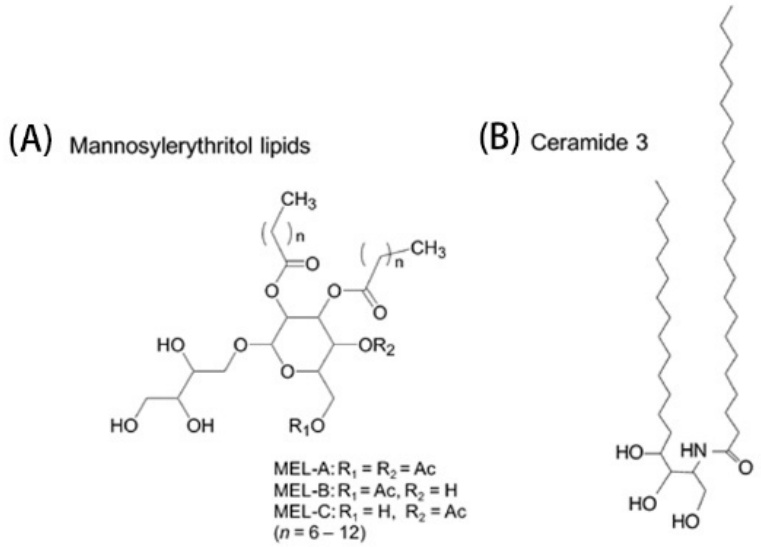

Figure 1.14. Chemical structure of (A) MEL; (B) Ceramide 3. Taken with permission from [63].

Diastereomer MEL-B ((*R*)-MEL-B) produced from *P. tsukubaensis* also demonstrated with excellent *in vitro* and *in vivo* water retention properties. (*R*)-MEL-B was prepared from vegetable oil as carbon source and dissolved at 1% or 5% (w/w) in water containing 5% 1,3-butylene glycerol (BG), a common solubilizer and humectant in the cosmetic industry. The solution containing (*R*)-MEL-B was applied to the forearm skin, and the water capacity of the stratum corneum was measured for a period of 2 hours. Skin treated with (*R*)-MEL-B solutions demonstrated a much higher water content in a concentration-dependent manner after 20 minutes and maintained for at least 2 hours [64]. The ability of (*R*)-MEL-B solution to control the loss of water by suppressing sweat was also investigated. The water loss was evaluated with trans-epidermal water loss (TEWL), and the area treated with water was compared to MEL solutions at different concentrations. A significant reduction in TEWL was observed in areas treated with MEL solutions in a concentration-dependent manner, and well maintained throughout the 2 hours.

The potential mechanism for (*R*)-MEL-B moisturizing activity is due to the orientation difference in erythritol moiety, which allows the formation of single-phase bicontinuous microemulsion with zero spontaneous curvature, different from other MELs that prefer the formation of micelle [65]. Such phase behavior may be critical in the maintenance of water barriers, strengthens the skin structure and result in the reduction of water loss.

1.4.2.2. Repair of damaged hair

Ceramides are also known to have protective properties on hair fibers against various agents. Due to the similarity in structure, the potential of MELs in hair care formulation was investigated [67]. MEL-A and (*R*)-MEL-B were prepared from *P. antarctica* T-34 and *P. tsukubaensis* NBRC 1940, and the hair was treated with SDS, bleached in hydrogen peroxide and ammonium solution to simulate chemical damage. The damaged hair was treated with a 0.5% solution of MEL dissolved in 4.5% lauryl glucoside (a common additive in shampoo) for 10 minutes followed by drying. MEL treatment significantly reduced cracks on the damaged hair surface and increased tensile strength, demonstrating a repairing effect. At the same time, the average friction coefficient and bending rigidity remained low, indicating that MEL treatment resulted in smooth

and flexible hair [67]. Overall, these data suggest that MELs demonstrate great potential as a new hair care ingredient.

1.4.2.3. Activation of papilla cells

Trans-differentiation of dermal papilla cells (DPC) is known to induce follicle formation, therefore, activation of DPC is considered a key factor for adult epidermis hair growth [69]. Different amounts of MEL-A (produced from *P. antarctica* T-34 with soybean oil) were then purified and mixed with cultured papilla cells in a papilla cell growth medium containing 10% bovine serum albumin (BSA) for 48 hours. The viability of papilla cells was significantly increased at low MEL-A concentrations, and an increase in MEL concentration resulted in a decrease in viability [68]. *In vivo* tests performed by topical administration of MEL-A on mice demonstrated a significant stimulation of hair growth [70]. Overall, these pieces of evidence suggest that MEL-A is likely to have great potential in hair loss treatment.

1.4.2.4. Antioxidation and protective effect on fibroblast cells

Oxidation damage is considered another major damage causing skin surface injury, thus leading to an increasing interest for the search for effective antioxidative agents in the cosmetic industry [71]. The antioxidant property of MEL species with differences in the fatty acid chains was tested using 1,1-diphenyl-2-picrylhydrazyl (DPPH) free radical scavenging assay and superoxide anion-scavenging assay. In both assays, MEL-C performed better than MEL-A/B, and MEL-C produced from *P. hubeiensis* (*Ph* MEL-C) with highest unsaturated fatty acid ratio demonstrated the highest scavenging activity [71]. These results suggest that the antioxidant activity of MEL is dependent on both the unsaturated fatty acid ratio, and the number/position of the acetyl group. The mechanism by which MEL exerts its antioxidant activity is not entirely clear, but it is thought to be related to the ability of its unsaturated fatty acid chains to scavenge free radicals and prevent oxidative damage.

The most active *Ph* MEL-C was used for *in vitro* tests on human skin fibroblast cells with hydrogen peroxide-induced oxidative stress. *Ph* MEL-C demonstrated a significantly higher cytoprotectivity (calculated with cell viability) than arbutin, although the radical scavenging activity was lower. This suggests that MEL could potentially have other biological protective

effects independent from radical scavenging activity. COX-2 is a marker protein in fibroblast cells induced by oxidative stress. The expression of COX-2 was significantly repressed by the treatment of both *Ph* MEL-C and arbutin [71]. From these results, *Ph* MEL-C demonstrated an antioxidant and protective effect on human fibroblast cells under oxidative damage.

1.4.3. Biomedical applications

Relevant applications of MELs in the clinical sector include (i) gene transfection and gene therapy studies since MELs can be one of the constituents of liposomes, which significantly enhances transformation efficiency in multiple cell lines; (ii) antitumor activity since MEL demonstrated differentiation-inducing/growth inhibition activity on HL60/K562 cell line and apoptosis-inducing effect on mouse melanoma cell line; and (iii) affinity binding system against immunoglobulin G, an important mediator of the human humoral immune response.

1.4.3.1. Gene transfection

The goal of gene therapy is to introduce genetic material into target cells. Traditionally, the most efficient methods for gene transfection are through viral vectors, however, the safety of such methods in clinical applications raises concerns, as some viral vectors are considered potentially oncogenic or immunogenic [73]. Due to this reason, cationic cholesterol liposome-mediated gene transfection was developed. However, transfection through this approach has limited success due to low efficiency, therefore the study of increasing transfection efficiency with MEL was investigated [72]. 1,2-Dioleoyl-sn-glycero-3-phosphatidylethanolamine (DOPE) was mixed in a 2:3 ratio with cationic cholesterol derivative cholesteryl-3b-carboxyamindoethylene-N-hydroxyethylamine (will be referred as derivative (I)), and mixed with different concentrations of purified MEL-A in liposome preparation. DOPE was mixed 3:2 ratio with Cholesteryl-3-β-oxycarboxyamidoethylenedimethylamine (DC-Chol) as another cationic liposome example with addition of MEL-A. First, the ideal concentration of MEL-A for transfection was determined by transfecting liposomes containing luciferase plasmid DNA to NIH3T3 cells. The transfection efficiency was determined by luciferase assay, and the addition of 10 nmol of MEL demonstrated a 5-fold increase in the transformation of the NIH3T3 cell line with both formulas, (DOPE+derivative(I) and DOPE+ DC-Chol) [72]. Transformation efficiency on the COS-7 monkey fibroblast-like cell line and HeLa cell line were also increased, demonstrating enhanced

transformation efficiency due to the addition of MEL-A was not cell line dependent. The diameter of liposomes was determined by a light scattering detector; the addition of MEL-A significantly reduced the average diameter of liposomes, suggesting the enhancement is partly due to the reduction of particle size, which minimized DNA-induced aggregation of liposomes.

1.4.3.2. Inducing differentiation in leukemia cell line HL60/K562

Glycosphingolipids (GSL) are reported as ubiquitous membrane components that modulate several activities, including cell growth, adhesion, and transmembrane signaling. A significant GSL component on the cell membrane was observed during oncogenesis, differentiation, and oncogenic transformation [76]. Even though there is a significant difference in the fatty acid chain length between GSL on HL60 vs MEL from *P. antarctica* (C16 vs C10) [57][77], owing to the general resemblance in glycolipid structure between MEL and GSL, soda, et al evaluated the ability of MEL to induce leukemia cell line HL-60 differentiation [74]. MEL was prepared from *P. antarctica* T-34 cell with soybean oil; the purified MEL was then co-incubated with HL60 for 5 days at different concentrations. It was shown that MEL inhibited insulin-dependent growth at 5 μM, complete inhibition of HL60 growth at 10 μM concentration, and resulted in cytotoxicity at 25 μM. For cell differentiation, cytochemical assessment was performed by naphthol AS-D-chloroacetate esterase (NCAE) staining which indicates differentiation towards granulocyte or α-naphthyl acetate esterase (NAE) towards T lymphocytes. The number of NCAE-positive cells was determined on day 2 and day 5, a time-dependent manner of differentiation was observed, and NCAE-positive cells reached 90% on day 5 [74]. Cell differentiation-associated properties were also assessed. NBT-reducing ability is often used as a marker for leukocytes which are known to exhibit toxicity on pathogenic bacteria or cancer cells; Fc receptor expression and phagocytic activity indicate the phagocytosis activity of differentiated granulocytes. There was a drastic increase in all activities at both concentrations on day 5 [74]. Furthermore, they demonstrated that individual components of MEL (ME, fatty acids, ME + fatty acids) were not able to trigger this differentiation, the differentiation is specific towards granulocyte (NCAE) but not monocyte (NAE), and differentiation is not trigger by other surfactants [74]. Overall, this research demonstrated that MELs were able to inhibit insulin-dependent growth while inducing differentiation-associated characteristics in granulocyte of the HL60 leukemia cell line. Later,

similar results of MEL activity were found for inducing the K562 leukemia cell line [78], which indicates the activity is not cell-line specific.

1.4.3.3. Induction of apoptosis in mouse melanoma cells

Apoptosis is considered a critical event since disrupted apoptosis regulation in oncocytes can result in uncontrolled proliferation [80]. Protein kinase C (PKC) family kinases are known to be key factors in activities such as cell differentiation, promotion of tumors, and apoptosis [81]. On the other hand, melanoma is known to be the deadliest type of skin cancer and considered resistant to chemotherapy [82], but the relationship between PKC and apoptosis in melanoma remains unclear. Zhao, et al. focused on the effect of MELs as inhibitors for melanoma proliferation [79]. The viability of mouse melanoma B16 cells were significantly inhibited by adding 10μM MEL and incubated for 48 hours, and flow cytometry revealed a significant increase in the percentage of apoptotic cells. However, when co-incubated with PKC activator phorbol 12-myristate 13-acetate (PMA), the pro-apoptotic effect of MEL was significantly quenched, suggesting the activity of MEL on the melanoma through regulation of PKC [79]. Overall, this study demonstrated that MEL is a novel mediator of apoptosis of melanoma cells through regulating PKC.

1.4.3.4. Affinity binding to Immunoglobulin G

Immunoglobulin G (IgG) is a monomeric immunoglobulin that represents the predominant isotype of antibodies in the human body, and plays a crucial role in hormonal response by binding antigens and recruiting immunocytes in pathogenic infection. The conventional ligand for IgG immunoaffinity chromatography is protein A of *Staphylococcus aureus* (SpA), which has two major drawbacks: the high cost of SpA, and the denaturation of IgG in an acidic condition during the elution process [84]. Some glycolipids from microorganisms demonstrated high affinity to immunoglobulins as a result of the “cluster effect” [85], therefore, individual MEL species (MEL-A/B/C) were purified from *P. antarctica* T-34 strain and fixed on poly (2-hydroxyethyl methacrylate) (PHEMA) beads and were tested as binding ligands for affinity chromatography [83]. The binding test demonstrated that human IgG (HIgG) displayed a concentration-dependent binding to MELs, and MEL-A showed a significantly higher binding affinity than the other two species. Recovery of IgG from MEL-A-PHEMA chromatography was

demonstrated in another study [86], where the binding affinity falls to a minimum with Na_2SO_4-free phosphate buffer at pH 7. The recovery test was conducted by using phosphate buffer followed by acetate buffer at pH 3.6 and was tested with different HIgG concentrations. The recovery of HIgG with two buffers was substrate concentration-dependent: at a lower substrate concentration, acetate buffer performs better, showing a negative correlation between substrate concentration and recovery rate; phosphate buffer showed a positive concentration-dependent manner, and the recovery rate drastically increase from 21% to 70% from 4 mg/mL to 5 mg/mL HIgG, and highest total recovery was at 9 mg/mL, with 93% recovery rate [86]. The effect of human serum albumin (HSA), the most abundant protein in plasma, on recovery performance was also assessed. At 9 mg/mL HIgG and 40 mg/mL HSA, the binding affinity was minimally affected (82% vs 84%) [86]. Overall, MEL-A linked to PHEMA beads demonstrated a high affinity towards HIgG and required a mild elution condition, thus may provide new techniques for IgG affinity separation.

1.4.4. Other applications

1.4.4.1. Laundry detergent

MELs have been demonstrated to have excellent structural stability in moderate high temperatures, and are stable over high pH ranges 8.0-12.0. With its environmentally friendly nature and excellent surface activity, MELs are attractive as a potential additive for laundry detergents, and their potential for this application has been investigated [87]. MELs were produced using *Pseudozyma* sp. NII 08165 with soybean oil, and extracted as crude MELs with ethyl acetate. The stain removal ability on fabric was measured by reflectometry, and Surf Excel ™ from Unilever (a common laundry detergent in South Asian countries) was used as a commercial washing detergent with or without MELs. The addition of crude MEL (5 mg/mL) with washing detergent improved the washing performance of multiple stains, including blood, ketchup, and chocolate [87]. Despite these positive results in the publication, the research may have limited value due to the less quantitative data obtained by reflectometry alone, and the actual improvement in cleaning power needed to be significant enough to justify the high cost of MELs. Acknowledging the value of their research, I suggest that further investigation is needed, such as investigating the performance of MELs with different types and concentrations of

contaminants, refining the formula of the detergent with MELs, and optimizing the conditions of the washing process.

1.4.4.2. MEL as anti-agglomerates in ice slurry systems

Ice slurry systems have been used extensively in air conditioning systems, water is converted to ice slurry during night off-peak time with much cheaper energy cost, and absorbs heat in the daytime [117]. However, ice particle agglomeration in the pipeline is a major issue and can cause complicated problems, lowering the cooling efficiency and stability of the system. Surfactants are widely used for preventing the agglomeration of solid materials in aqueous solutions. MEL-A produced from *P. antarctica* T-34 was purified and added to the ice slurry system and compared with other surfactants [88]. The ice packing factor (IPF), which is calculated as the volume of ice particles over the total system volume, was employed to evaluate the anti-agglomeration effect of an anti-agglomerate. A higher IPF corresponds to a more efficient energy storage capability and better anti-agglomeration effect. In small scale tests simulating commercial ice slurry air conditioning system, MEL-A demonstrated a promising result surpassing all other surfactants tested: MEL-A was able to reach a maximum IPF of 35% at 10 mg/L concentration [88]. MEL-A also demonstrates low toxicity and high biodegradability, which expands its application in the environmentally friendly ice slurry cooling system.

1.5. Efforts to improve the economics of commercial scale MEL production

MEL has demonstrated a great potential for applications in various fields, however, the cost of this biosurfactant is still high primarily due to the cost of feedstock and the production process. Feedstock for the production of MEL can be considered as two parts, the primary carbon source, for which the majority of the carbon will be converted into the final product; and secondary nutrient supply, that provides necessary ions, nitrogen, and micronutrients for maintaining cell function. The use of cheaper, renewable primary feedstocks such as lignocellulosic material, waste cooking oil, sugarcane juice, and oil refinery waste, and secondary feedstocks such as whey permeate and molasses for the production of MEL have been demonstrated with very promising results. Successful nutrient supply substitutions will be discussed in this section.

1.5.1. Primary carbon source substitutes

1.5.1.1. Edible oil post-refinery wastes

In the refinery process of vegetable oils, soapstock (SS) along with post-refinery free fatty acids (PRFFA) were generated in the neutralization step. Soapstock is an underutilized low-quality by-product, which consists of an alkaline aqueous emulsion of lipids, including free fatty acids and a mixture of other components such as tri-, di-, monoacylglycerols, sodium fatty acid salts, and over 50% water [89].

Soapstocks roughly represent 6% of crude vegetable oil refined and are regarded as a low-value side product since downstream processes are difficult [90]. Despite this, it might be an ideal feedstock for MEL production due to its high content in hydrophobic carbon sources, and relatively low cost.

Bioreactor culturing with SS as carbon source was attempted with *P. antarctica* ATCC 20509 and *P. apicola* ATCC 96134. In these experiments and yeast strains were supplied with either SS or PRFFA, along with glucose as a secondary carbon source. Micronutrients such as inorganic salts, and yeast extracts were added according to standard MEL production protocol, and sodium nitrate was used as nitrogen source [91]. When pH was adjusted to 5.5, both strains were able to efficiently produce MEL in a timely manner with both feedstocks. Indeed, *P. antarctica* ATCC 20509 reached a maximum yield of 13.4 g/L MEL production in 7 days [91].

1.5.1.2. Waste cooking oil

It is estimated that over ten million tons of waste cooking oils (WCO) are produced worldwide each year. These are generated in both household and food processing industries, and could cause serious negative impacts if not properly disposed and managed [92]. Biosurfactant production with waste cooking oil has been demonstrated previously, such as the production of sophorolipids by *Candida bombicola* [93], and the production of rhamnolipids by *Pseudomonas aeruginosa* 47T2 [94]. The ability of *P. aphidis* DSM 70725 to produce MEL using WCO as a carbon source was demonstrated in a culture medium supplemented with inorganic nitrogen source, and micronutrients [95]. This experiment using WCO resulted in a comparable yield (56 g/L) to soybean oil (60 g/L) [95]. The fatty acid side chain composition of the MEL products

exhibited a shift, with soybean oil showing C10:0 and C8:0 as the most abundant fatty acid chains. In contrast, using WCO as a feedstock resulted in predominantly C18:1 and C18:2 acyl-chain additions. Such difference might be caused by the chemical composition shift of the WCO owing to the prolonged heating process, but the detailed mechanism remains unknown. MEL biosynthesis by *P. aphidis* cultured with WCO as the carbon source was delayed relative to production from "clean" soybean oil, with peak MEL accumulation delayed by about 24 hours. Although the investigators did not provide an explanation for this, it may be that the WCO contains some byproduct such as peroxides and oxidation products from prolonged heating process that is inhibitory to cell growth or to one of the enzymatic steps in the MEL biosynthetic pathway and carbon metabolism.

1.5.1.3. Sugarcane juice

Sugarcane is processed in many places to yield sucrose-rich sugarcane juice [97]. The raw sugarcane juice thus has the potential to act as an ideal lower-cost substitute for refined sugar as a feedstock for industrial chemical synthesis. *Ustilago scitaminea* NBRC32730 was initially isolated from sugarcane plant [126], and was demonstrated to produce MEL-B from sucrose as the sole carbon source [96]. Upon incubation, the hydrolysis of sucrose was immediately observed, glucose was almost entirely consumed, while fructose remained at high levels until the end of production, and a final yield of 11.3 g/L MEL was observed. The optimum nitrogen source was also determined, by comparing various organic and inorganic nitrogen sources, urea at 1 g/L provided the best result of 20 g/L final yield [96].

1.5.1.4. Cassava waste water

Cassava wastewater (CWW) is the main residue in the process of making sour cassava starch (Polvilho azedo), a popular food in South American countries. The fermentative process of cassava starch lasts 30 to 90 days with lactic acid bacteria [98]. CWW usually looks cloudy due to suspended particles, and the major nutrients in CWW are fermentable carbohydrates (glucose, fructose), and starch, with minor components such as proteins, fibers, and lipids [99]. For MEL production, the CWW was first centrifuged to remove suspended particles, then sterilized to remove bacterial contamination from the previous fermentation, and used as a production medium for MEL without any additional substrates. *P. tsukubaensis* are able to yield 1.26 g/L

pure (*R*)-MEL-B in 84 hours [100]. Although the MEL yields from the starch waste is lower than from other hydrophobic carbon sources, the major advantage for water-soluble carbon source MEL production is the downstream purification processes of MEL. In this study, the MEL-B was recovered from the foam overflow with ultrafiltration, and the resulted MEL-B reached a purity of 30% and a recovery rate of 80% [100]. By completely avoiding the use of organic solvents for raw MEL extraction, this method makes such process scalable and thus potentially more economical, while reducing the environmental impact.

1.5.1.5. Xylan

Xylan is a type of polysaccharide composed of pentose sugars, predominantly xylose. This polymer is a structural component of plant cell walls and is abundant in hardwoods and agricultural wastes. Direct conversion of xylan to glycolipid without the addition of hydrolytic enzymes by *P. antarctica* PYCC5048 (=JCM10317) was investigated [34]. *P. antarctica* was able to grow on xylan as the sole carbon source but not cellulose, consistent with the secretion of xylanase. Xylobiose and xylose were detected rapidly with *P. antarctica* cultured in the medium with xylan as the carbon source [34]. The concentration of xylobiose peaked on day 1, and peak of xylose was delayed until day 2, and both disappeared again on day 4 [34]. Xylanase activity continuously increased in the whole period of the production. At the end of production, a yield of 1.3 g/L MELs were produced from 40 g/L xylan in 10 days [34], Although the MEL yield was lower than the observed 3.2 g/L from 40 g/L xylose, raw xylan has a significant advantage in cost compared to pure xylose.

1.5.2. Secondary nutrient substitutes

1.5.2.1. Cheese whey permeate

Cheese whey permeate (CWP) is a by-product of the cheese manufacturing industry. It is produced when cheese whey is passed through a filtration membrane that retains and concentrates the whey protein. Smaller molecules such as lactose, inorganic salts, and non-protein nitrogen pass through the membrane and form CWP [102][103]. It is an ideal substitution for a low-cost MEL production medium since it contains sugar, nitrogen source, inorganic salts, and other micronutrients. In a bioreactor culture containing soapstock as carbon source, and 200 mL/L CWP as a secondary nutrient source, *P. antarctica* ATCC 28323 synthesized up to 40 g/L

MEL in 144 hours [104]. However, one major drawback is that cheese whey permeate requires sterilization before adding to the MEL production medium, which increases the overall production cost.

1.5.2.2. Molasses

Molasses is one of the by-products generated from the sugarcane processing industry. During sugar preparation, the brown sticky liquid is generated during the repeated crystallization process and represents 2.2%-3.7% of raw sugarcane weight. Molasses generally contains 30%-35% sucrose, 10%-25% fructose, and minerals along with ~2% nitrogen [105], making molasses another ideal secondary nutrient supply for MEL production. *P. aphidis* DSM 70725 supplied with soapstock and 20g/L molasses with no addition of enriched nutrients, are able to produce over 90 g/L MEL over the course of a 10-day production [104]. This result demonstrated that molasses is one of the most promising substitutes as a secondary nutrient supply for MEL biosynthesis.

1.6. The *P. antarctica* JCM10317 strain as a producer of MEL.

The *Pseudozyma antarctica* strain used in this study is the JCM10317 strain. It is also referred to as ATCC 34888, CBS5955, and PYCC 5048 in other culture collections. This strain belongs to the *Ustilaginaceae* family of *Basidiomycota* division in the fungi kingdom. Most known MEL producers are conserved in the *Ustilaginaceae* family, including smut fungus *Ustilago maydis*, *Pseudozyma aphidis*, *Pseudozyma parantarctica*, etc. In 2015 taxonomic analysis revised the groupings of these yeasts in the *Ustilaginomycota* with the recommendation that the name *Pseudozyma* be replaced with *Moesziomyces* [75]. While acknowledging this recommendation, I have elected to retain the prior naming convention for this thesis in part to minimize confusion, as all literature and investigation prior to 2015 uses the *Pseudozyma* naming convention. *P. antarctica* JCM10317 was originally isolated from the sediment of a hypersaline lake: Lake Vanda in Antarctica in 1969 [110]. The yeast can tolerate harsh conditions and is able to grow at 10 °C while tolerating NaCl concentrations up to 10% w/v.

The draft genome of the JCM 10317 strain was published in 2014 [108]. The genome size is 18.1 Mb, with a G+C content of 60.9%. 6845 protein-coding genes were predicted with *U. maydis*

521 database, and 86.2% of genes were found homologous to *P. antarctica* T-34 strain. A nearly identical MEL cluster with the same organization of open reading frames was also found, five genes within the cluster were highly similar to the T-34 strain and shared over 90% of identity. *P. antarctica* T-34 was originally isolated from the exudate of a tree on Mt. Tsukuba in Japan. While it is not the focus of this thesis research, the high genome similarity between both organisms, while geographically separated, is consistent with divergence being driven by adaptation to life in starkly different environments.

MEL production with this strain is possible with a diverse collection of carbon sources. For production with sucrose, glucose, and olive oil at 10% w/v, the flask was supplied with 20 mL of medium with 0.3% w/v $NaNO_3$, 0.03% w/v $MgSO_4$, 0.03% w/v KH_2PO_4, 0.1% w/v yeast extract, pH 6.0. The resulting yield in 7 days of production at 25 ^oC is 1.61 g/L (glucose), 1.97 g/L (sucrose), and 12.98 g/L (olive oil), respectively [101] (**Fig. 1.15 A**). Production of MEL from xylose was demonstrated to be feasible, with a final yield of 3.2 g/L in 10 days [34]. Production with glycerol was also attempted, and it was demonstrated as the only *Pseudozyma* strain that is able to produce MEL-A/B/C with glycerol (**Fig. 1.15 C**). 10% glycerol and the same micronutrients listed above were supplied to the production medium, and the yield reached 3.7 g/L at 25 ^oC and 3.95 g/L when cultured at 30 ^oC [50]. Other than refined carbon supplies, JCM10317 strains are also demonstrated to utilize xylan as sole carbon source, the secreted xylanase and β-xylosidase facilitate the rapid breakdown of polymer to pentoses, and the final yield reached 1.3 g/L in 10 days at 28^oC [34].

(A)

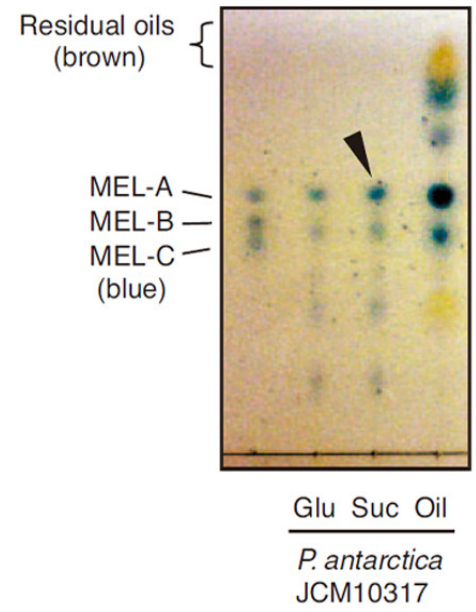

(B)

Fatty acid type	Composition (%) *P. antractica* JCM 10317	
	Sucrose	Olive oil
C6:0	—	—
C8:0	3.5	29.4
C10:0	38.9	45.1
C10:1	11.1	20.2
C12:0	30.8	3.2
C12:1	3.2	—
C12:2	1.9	—
C14:0	4.5	—
C14:1	—	—
C14:2	3.2	—
C16:0	1.6	—
C16:1	—	—
C16:2	—	—
C18:0	—	—
C18:1	—	—
C18:2	—	—
Unknown	1.3	2.1

(C)

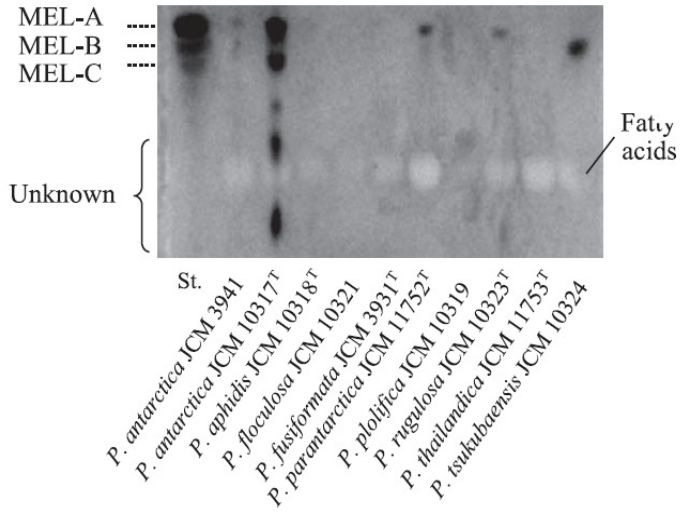

(D)

Fatty acid type	Composition (%) *P. antractica* JCM 10317 glycerol
C8:0	12.4
C8:1	–
C9:0	–
C10:0	28.6
C10:1	8.0
C10:2	2.5
C12:0	21.4
C12:1	–
C13:0	–
C14:0	11.4
C14:1	2.3
C14:2	5.5
C16:0	5.1
C16:1	1.7
Unknown	1.1

Figure 1.15. Properties of MELs produced from *P. antarctica* JCM10317. (A) Thin layer chromatography of secreted MELs by JCM10317 strain with 10% glucose, sucrose, and olive oil as carbon sources. TLC was performed with a solvent of chloroform: methanol: NH_4OH (65:15:2

ratio), and glycolipids were visualized by with spraying with anthrone reagent and heated at 90 °C. (B) Fatty acid profile of MELs produced from sucrose and olive oil by JCM10317 strain. (C) Thin layer chromatography of secreted MELs by *Pseudozyma* yeasts with 10% glycerol as carbon source. Method same as (A). (D) Fatty acid composition of MEL-A produced from glycerol by *P. antarctica* JCM 10317. (A)(B) taken with permission from [101]; (C)(D) taken with permission from [50].

With olive oil as used as carbon source, the fatty acid chain of MELs produced from the JCM 10317 strain is C10 dominant, with no chains longer than C12. However, with hydrophilic carbon sources such as sucrose, the fatty acid profile drastically changed in terms of chain length and unsaturation. While C10 remains dominant, there is a significant increase in C12 chains, and increase in the unsaturated fatty acids in the side chains such as C12:1 with sucrose and C14:2 with glycerol (**Fig. 1.15 B, D**). I personally suspect that when utilizing water-soluble carbon sources, there is reduced activity in the peroxisomal β-oxidation towards medium-chain fatty acids since all fatty acids have to be synthesized through lipogenesis from acetyl-CoA. Lipogenesis and β-oxidation are opposing pathways, it is unlikely that both of these reactions are stimulated at the same time, which eventually resulted in a lower partial β-oxidation activity, and longer fatty acid chain incorporated on MELs.

In summary, JCM 10317 strain has a published genome with annotation, demonstrated halotolerance and can utilize a variety of carbon sources including glycerol and xylose. Therefore, it is an excellent platform for studies involving genetic manipulation, and as industrial strains for the exploration of more economical production processes for MEL production.

1.7. Rationale and hypothesis

1.7.1. *MMF1* KO

The MEL biosynthesis cluster contains multiple proteins, including *MMF1*, for which limited information is available. Two gene deletion studies have been carried out, one on *Ustilago maydis* and the other on *Pseudozyma tsukubaensis*. The former indicated a correlation between *MMF1* and extracellular MEL production but lacked details. The latter study, specifically focused on *MMF1*, showed reduced MEL production and production of a previously unknown glycolipid. Interestingly, the study revealed extracellular di-acylated MEL-B production, at a

much lower yield. Although presumed to be a transporter based on homology and location, the exact function of *MMF1* is unknown, and further research is necessary. Additionally, phylogenetic tree analysis of *MMF1* in ten MEL producers has shown that the JCM10317 strain of *Pseudozyma antarctica* branches differently than both *P. tsukubaensis* and *U. maydis*, indicating possible differences in the function of *MMF1* between these species (**Fig. 1.11 B**). Furthermore, JCM10317 is capable of utilizing a variety of water-soluble carbon sources, unlike *P. tsukubaensis*, which rely on oily carbon sources. Consequently, the secretion of MEL is not required for carbon assimilation and production when grown in water-soluble carbon sources.

Based on this information, it is hypothesized that Mmf1 transports MEL across the cell membrane to the extracellular space, and that the knockout of *MMF1* gene in *P. antarctica* JCM10317 will abolish MEL secretion when grown in water-soluble carbon sources.

1.7.2. Brackish water MEL production

Although MEL is a useful and valuable surfactant, the current problem is that the bioreactor production of MEL using Pseudozyma yeasts requires a substantial amount of fresh water that needs sterilization, which can deplete valuable fresh water sources. However, on the bright side, seawater and brackish water - water that has more salinity than freshwater, but not as much as seawater, which contains 0.5g/L to 30g/L of dissolved salt - is readily available in estuaries around the world, but its usefulness is limited due to its salt content, and it is mostly used as coolant water in power plants, as well as in the oil and gas industry for hydraulic fracturing and drilling. Therefore, there is an ample supply of brackish water, but only a little demand for it. JCM10317 strain of *Pseudozyma antarctica* is a halotolerant yeast, initially discovered in the sediment of a hypersaline lake in Antarctica, implying that it can thrive in brackish water. Waste cooking oil has a significant supply and is relatively inexpensive, JCM10317 strain is able to utilize oily carbon sources for the production of MEL, and waste cooking oil was demonstrated for MEL production with *P. aphidis* DSM 70725 strain.

Based on these facts, the hypothesis is that *P. antarctica* JCM10317 are able to tolerate high salt concentration and can grow and produce MEL in unsterilized brackish water when provided with waste cooking oil as carbon source.

Chapter 2

2. Methods and materials

2.1. Materials

2.1.1. Restriction enzymes

Restriction enzymes were used to produce DNA fragments with a specific cut at the desired site for DNA cloning and southern blot analysis. All restriction digestions were executed in accordance with the manufacturer's instructions. Normally, restriction digestion of 20 µL consisted of 5 µL of plasmid DNA, 1X corresponding buffer, and 1 unit of restriction enzyme, the digestion was performed at a specified temperature for 1 hour for complete digestion, or based on experimental design. The total volume of the reaction varies based on the experimental design. Restriction enzymes used in this research are specified in table 2.3.

2.1.2. Thermal stable DNA polymerases

Q5 and Taq thermostable polymerases were used in this experiment for PCR reactions (2.3.3). Q5 and Taq were purchased from New England Biolabs (NEB), and reactions were performed according to the manufacturer's protocol.

2.1.3. Oligonucleotides

Oligonucleotides for PCR reactions were ordered from Integrated DNA Technologies (IDT), and double distilled water (ddH_2O) was added to solubilize oligonucleotides to reach a final concentration of 10 µM. The prepared oligonucleotides were stored at -20 °C for short-term and -80 °C for long-term storage. Primers used in this research were listed in table 2.2.

2.1.4. Reagents

Reagents used in this research were listed in table 2.1.

Table 2.1. List of reagents used in this research.

Name of reagents	Manufacturer

tryptone	Fisher Chemical
yeast extract	Fisher Chemical
NaCl	Fisher Chemical
agar	Fisher Chemical
ampicillin	Sigma-Aldrich
peptone	Fisher Chemical
dextrose	Fisher Chemical
adenine hemisulfate	Sigma-Aldrich
tryptophan	Sigma-Aldrich
hygromycin B	Invitrogen
glycerol	Fisher Chemical
canola oil	Crisco Pure Canola oil
ethidium bromide	Sigma
tris base	Fisher Scientific
glacial acetic acid	Sigma-Aldrich
EDTA	Fisher Scientific
agarose	Fisher Scientific
dNTP	Invitrogen
sodium nitrate, $NaNO_3$	Fisher Chemical
magnesium sulfate, $MgSO_4$	Fisher Chemical
potassium dihydrogen phosphate, KH_2PO_4	Baker Fine Chemical
ethyl acetate	Fisher Scientific
methanol	Fisher Scientific
chloroform	Fisher Scientific

ammonium hydroxide	Fisher Chemical
orcinol monohydrate	Sigma-Aldrich
sulfuric acid 98%	Sigma-Aldrich
lithium acetate	BDH Chemicals LTD
salmon sperm DNA	Sigma-Aldrich
polyethylene glycol (PEG) 3350	Bioshop Canada
sodium dodecyl sulfate (SDS)	Bio-rad
yeast nitrogen base (YNB)	Fisher Scientific
Denhardt's reagent 100X	G-Biosciences

Table 2.2. List of primers used in this research

Primer name	Sequence (5'→3')	Sense	T_m (°C)
VP15	ACGACGTTGTAAAACGACGGCCAGTGAATTCGCCTCGGAAAGATCCTTCTGG	+	58
P13H	TTTTGAGATGATGGATGGGGAG	-	56
P1H5	GTGTCACACTCCCCATCCATCATCTCAAAAATGGGTAAAAAGCCTGAACTCAC	+	57
H3T	GGGGAGGGAGACGTAGGGAGCGTACTTATTCCTTTGCCCTCGGACG	-	58
T5	GTACGCTCCCTACGTCTCCC	+	60
T3	CAACTCCGCGGTATTTTGAGC	-	58
P25	GGCTCAAAATACCGCGGAGTTGCCACCTCGGCCGCG	+	61
P23V	TGACCATGATTACGCCAAGCTTAGTGGAGATGCGATCGTTTATCGG	-	60
M13f	GTAAAACGACGGCCAGT	+	55

M13r	CAGGAAACAGCTATGAC	-	49
EMTD5	GACGTTGTAAAACGACGGCCAGTGAATTCAG CGTACATAGGCTATTGAGC	+	56
EMTD3	GACTCTATGACCATGATTACGCCAAGCTTACT TCTGGTTCTACTGGTACC	-	55
EGR5	CTTCAAGCTCAACAAGCCGAAGCGCAACCCG CCTCGGAAAGATCCTTCTGGCTTTC	+	62
EGR3	TTGAGCGGCGAGGTGAATCCTGGACTGCCCCA ACTCCGCGGTATTTTGAGCCC	-	61
ET5	AATGACAAAGTCCTCGCATCACGCATTCAC	+	63
ET3	GAATCTTTGACAAGCTCTTCGGAACAGTCATG	-	63
VM15	GTTGTAAAACGACGGCCAGTGAATT**CTCGAG** ATGGACGACAAGATTGCGCTGACGA	+	64
M1G3	AAAGCCAGAAGGATCTTTCCGAGGCCTGATG ATCAGTCCGGCGACCAGCG	-	65
PGPD5	GCCTCGGAAAGATCCTTCTGGCTTT	+	62
PPGK3	TGTGGAGATGCGATCGTTTATCGG	-	61
P2GFP5	CCCGATAAACGATCGCATCTCCACAATGAGTA AAGGAGAAGAACTTTTCAC	+	55
GFP3	CTATTTGTATAGTTCATCCATGCCATG	-	57
GTM5	TGGCATGGATGAACTATACAAATAGTCCGGTA GCTTTGGAGCCCT	+	61
TM3V	CTATGACCATGATTACGCCAAGCTTATGACCA TTGTCAATGCCAAGACGC	-	61
IM5	CTGATCGCACTCGTGTTTG	+	56
IM3	CGCCAGTATCGAAGTTTGAG	-	55
Probe 1f	AACATCCAAAGCCGAGTGGG	+	60

Probe 1r	TTCGGCAGATACCTCAGCG	-	59
Probe 2f	AAATAGAAGGGAGGCGCTTG 30bp downstream of the stop codon	+	58
Probe 2r	CAAGAGGGAGCTGGCCTTG +330 bp downstream of the stop codon	-	59

Primers with extra homology regions for homologic assembly are underlined, and sequence represent restriction sites are bolded. Primer melting temperatures (T_m) were estimated with SnapGene software by Dotmatics.

Table 2.3. List of restriction enzymes used in this research.

	Sequence (5'→3')	**Buffer**	**Manufacturer**
EcoR I	G^AATTC	NEB 3.1	Thermo Fisher
Hind III	AA^GCTT	NEB 2.1	NEB
Xho I	C^TCGAG	Cutsmart	NEB
Ssp I	AAT^ATT	NEB 2.1	NEB
Sac II	GATCT^C	NEB 1.1	NEB
Afl III	A^CRYGT	NEB 3.1	NEB

2.2. Growth medium

2.2.1. Lysogeny broth medium/plates (LB)

Add 10 g/L of Tryptone (Fisher), 5 g/L of yeast extract (Fisher), and 10 g/L of NaCl to 1L of ddH_2O. Autoclave the solution for 30 minutes. For agar plate medium, add 15 g/L of agar before autoclaving.

2.2.2. LB amp

Add 10 g/L of Tryptone (Fisher), 5 g/L of yeast extract (Fisher), and 10 g/L of NaCl to 1L of ddH_2O. Autoclave the solution for 30 minutes. Ampicillin was added to 100 mg/L final concentration after cooling to below 65 degrees. For agar plate medium, add 15 g/L of agar before autoclaving.

2.2.3. Yeast extract-Peptone-Dextrose medium/Plates (YEPD)

Add 10 g/L of yeast extract, 20 g/L of peptone, 20 g/L of dextrose (glucose), 30 mg/L of adenine hemisulfate, and 30 mg/L of L-tryptophan to 1L of ddH_2O. Autoclave the solution for 30 minutes. For agar plate medium, add 15 g/L of agar before autoclaving.

2.2.4. YEPD hygromycin (YEPD-Hygro)

Add 10 g/L of yeast extract, 20 g/L of peptone, 20 g/L of dextrose (glucose), 30 mg/L of adenine hemisulfate, and 30 mg/L of L-tryptophan to 1L of ddH_2O. Autoclave the solution for 30 minutes. Hygromycin was added to 300 or 500 mg/L final concentration after cooling to below 65 degrees Celsius. For agar plate medium, add 15 g/L of agar before autoclaving.

2.2.5. -Ura+Dex dropout medium

Dissolve 1.6 g/L of Difco Yeast Nitrogen Base, 5 g/L of ammonium sulfate, and a 2% glucose solution containing 2 g/L of amino acid drop-out mixtures in 1L of ddH_2O. Autoclave the solution for 30 minutes. For agar plate medium, add 15 g/L of agar before autoclaving. The drop-out mixtures of -uracil includes 0.5 g of adenine sulfate, 4 g of leucine, and 2 g of the required essential amino acids without uracil.

2.2.6. *P. antarctica* medium

2.2.6.1. *P. antarctica* seed medium

The seed medium was prepared by dissolving 1 g/L of yeast extract, 3 g/L of $NaNO_3$, 0.3 g/L of KH_2PO_4, 0.3 g/L of $MgSO_4$, and 40 g/L of glucose in 1L of ddH_2O. Autoclave the solution for 30 minutes to sterilize.

2.2.6.2. MEL production medium

The MEL production medium was prepared by dissolving 1 g/L of yeast extract, 3 g/L of $NaNO_3$, 0.3 g/L of KH_2PO_4, and 0.3 g/L of $MgSO_4$ in 1L of ddH_2O. Autoclave the solution for 30 minutes to sterilize. The carbon sources for production were added later. Filter-sterilized 50% glucose, 50% glycerol, and canola oil (10% v/v) were added to the production apparatus to desired concentration before production.

2.2.7. Brackish water WCO production medium

The brackish water sample was acquired from Iona beach (49°12'57.591" N;123°12'47.333" W) near Richmond, BC, Canada. To remove suspended dirt particles, it was filtered with Whatman filter paper (NO.1; Catalog # 1001 240) with pore size of 11 µm. 1 g/ L Yeast extract, 3 g/L $NaNO_3$, and 0.3 g/L KH_2PO_4 were added to the medium along with 10% waste cooking canola oil (acquired from La Poutine, Garneau, Edmonton). 29.22 g/L sodium chloride (0.5M) was added to the medium to inhibit bacterial growth.

2.3. General methods

2.3.1. Bioinformatics

The genome sequence for *P. antarctica* JCM10317 strain was acquired from GenBank (accession numbers BBIZ01000001 to BBIZ01000276) [108]. Plasmid sequences, primer sequences and melting temperature (T_m) was determined with Snapgene software. Protein sequences was acquired from NCBI (www.ncbi.nlm.nih.gov/). Geneious software was used to perform alignment of protein sequences and generation of phylogenetic tree.

2.3.2. Agarose gel electrophoresis

Agarose gel electrophoresis was commonly used in the experimental process to verify DNA fragments' size and purification. The agarose gel was prepared by 0.8% w/v agarose in 1X TAE and 5 µg/mL ethidium bromide (EtBr). The common preparation process is prepared by adding 2.4 g agarose gel in 300 mL 1X TAE (50X TAE stock: 242 g Tris base, 57.1 mL glacial acetic acid, and 100 mL 0.5M EDTA pH 8.0 in a final volume of 1L) heated to boil and supplemented 0.5 µg/mL EtBr (Sigma). The DNA was mixed with 10X loading buffer (Invitrogen), and

electrophoresis was carried out by applying 100V in 1X TAE buffer in BioRad Mini-Sub Cell GT Cell DNA electrophoresis apparatus. The DNA was visualized using BioRad Gel Doc XR+ imaging system with 10 μL 1kb plus DNA ladder (Invitrogen) or 1kb plus DNA ladder (NEB) as reference.

2.3.3. Polymerase chain reaction (PCR)

The polymerase chain reaction was normally carried out in a 100 μL reaction. Q5® High-Fidelity DNA Polymerase (New England Biolabs) was used for reactions with *P. antarctica* genomic DNA as a template, and other reactions were performed with Taq DNA Polymerase (NEB). In each reaction, 1 μL polymerase was added, buffer concentration was adjusted to 1X, and the final concentration of each primer and dNTP was 100 nM and 100 μM respectively. Common PCR reactions were performed in such process for Q5 polymerase: 98 °C for 5 minutes followed by 35 cycles of 1 minute at 98 °C, 1 minute at different annealing temperatures, and 72 °C for elongation with time depending on the product size. The denaturation temperature was adjusted to 95 °C for Taq polymerase.

2.3.4. Gel extraction/PCR product purification

DNA agarose gel extraction and PCR purification were performed with GenepHlow Gel/PCR Kit (Geneaid). After DNA electrophoresis, the correct band was cut and dissolved in 500 μl Gel/PCR Buffer and heated to 55 °C until the gel slice was dissolved. Samples were then transferred to the DFH column, washed with wash buffer, and eluted with 50 μL Elution buffer. The DNA samples were stored at -20 °C for short-term storage.

2.3.5. DNA sequencing

DNA sequencing in this experiment was done at the Molecular Biology Facility (MBSU) at the University of Alberta. The sequencing premix is 10 μL and contains a plasmid template of 57.5 ng/μL and primer of 0.25 μM, the data was generated by Applied Biosystems 3730 Genetic Analyzer.

2.3.6. Gibson assembly

Gibson assembly master mix was purchased from New England Biolabs. Gel-purified DNA fragment was first quantified with Nanodrop and mixed with the master mix in accordance with the manufacturer's protocol. Generally, 0.5 pmol of each DNA fragment was added to 5 μL of the master mix, and water was added to adjust the total volume to 10 μL. The reaction was incubated in a PCR machine at 50 degrees for 1 hour, then the mixture was transformed to *E. coli* DH5α cells as described later in this chapter.

2.3.7. Bacterial transformation and DNA recovery

2.3.7.1. Competent cell

The bacteria cell used in this experiment for plasmid propagation is DH5α *Escherichia coli* cell (*fhuA2 lac(del)U169 phoA glnV44 Φ80' lacZ(del)M15 gyrA96 recA1 relA1 endA1 thi-1 hsdR17*). Competent cells were prepared using the Inoue method described in the literature [120].

2.3.7.2. Bacterial transformation

The transformation of *E. coli* was performed as described in previous literature. Specifically, 100 μL of competent cells were incubated with 5 μL of plasmid DNA on ice for 1 hour. Subsequently, the cells were subjected to a brief heat shock step of 60 seconds at a temperature of 42 °C, then transferred back to ice for 2 minutes. The cells were then allowed to recover by incubation in LB medium for 1 hour at 37 °C. Finally, the cells were plated on appropriate antibiotic plates and incubated overnight in a 37 °C incubator.

2.3.7.3. Plasmid recovery from bacteria

Plasmid DNA recovery was performed with Geneaid Presto mini plasmid kit (#PDH300). Colonies from LB agar plates containing ampicillin were used to inoculate 3 mL of liquid LB Amp medium in a test tube. The culture was incubated overnight at 37°C in a reciprocating incubator. 1.5 mL of the overnight culture was transferred to an Eppendorf tube and centrifuged at 15000 x g for 1 minute at room temperature. The resulting supernatant was discarded, and the cell pellet was resuspended with PD1 buffer. The cells were lysed with 200 μL of PD2 buffer and neutralized with 300 μL of PD3 buffer. After centrifugation, the supernatant was transferred to the PDH column, washed with wash buffer, and eluted with 50 μL of elution buffer. The purified DNA product was quantified using a Nanodrop and stored at -20°C.

2.3.7.4. Rapid plasmid screening

The rapid bacterial plasmid screening method was employed to shorten the process of screening large numbers of plasmid candidates during the plasmid assembly process. Bacterial colonies were selected from respective selective plates and transferred to 96 well deep well plate (Axygen P-2ML-SQ-C-S) containing 1 mL of selective medium. The plates were then incubated in a shaking incubator at 37°C for 24 hours. A suspension of bacterial cells (100 µL) was transferred to a 1.5 mL microfuge tube and centrifuged at 15, 000x g for 1 minute. Next, a mixture of rapid screening buffer (0.2 M NaOH, 1% w/v SDS) and cell pellet (100 µL) was heated to 95°C for 2 minutes. The mixture was cooled down and centrifuged at maximum speed for another 2 minutes to remove debris. Subsequently, 15 µL of the supernatant was mixed with gel loading buffer, and agarose gel electrophoresis was performed to separate supercoiled plasmids by size.

2.3.8. *S. cerevisiae* transformation

The transformation of *S. cerevisiae* was adapted from [113]. A 25 mL culture of *Saccharomyces cerevisiae* was grown at 30°C overnight in YEPD medium. The culture was diluted in 50 mL fresh YEPD at OD_{600}= 0.1 and grown for ~4 hours until OD_{600} reached ~0.5. Cells were recovered with a Beckman Allegra 6r centrifuge at 2000 x g for 5 minutes. The supernatant was discarded, and the cell pellet was washed in 50 mL of sterile water. After recovery, the cell pellet was resuspended in 1 mL 0.1 M lithium acetate (0.1 M LiAc, 10 mM Tris HCl pH 8.0), and incubated at 30°C for 15 minutes with gentle agitation. For the transformation, 5 µg (less than 20 µL) of total DNA was added to 100 µL cell suspension along with 5 µL of 10 mg/mL salmon sperm DNA, and 300 µL of 40% w/v PEG 3350 solution and incubated at 30°C for 2 h. Heat shock was performed by placing the tube in the 42°C water bath for 10 minutes. The cells were collected by centrifugation at 15,000 x g for 3 minutes, the supernatant was discarded, and the pellet was washed twice with sterile water. Cells were resuspended in sterile water, transferred to YEPD medium, and incubated for 2 h at 30°C before plating on selective plate media.

2.3.9. Plasmid extraction from *S. cerevisiae*

Yeast cells were grown in 10 mL of selection medium for 2 days and then harvested by centrifugation at 2,000 x g for 5 minutes. The supernatant was discarded, and the resulting cell pellet was resuspended in 1.5 mL sterile water. The suspension was then transferred to a microcentrifuge tube and centrifuged at 15000 x g for 2 minutes. The supernatant was discarded, and the cell pellet was resuspended in yeast lysis buffer (10 mM Tris-HCl (pH 8.0), 1% SDS, and 50 mM EDTA). Acid-washed glass beads and 100 µL of 50:50 phenol: chloroform was added to the tube, which was then vigorously vortexed for 10 minutes. Next, 100 µL of TE buffer (1 mM EDTA, 10 mM Tris-HCl, pH 8.0) was added, and the mixture was centrifuged at maximum speed for 8 minutes. The aqueous phase was then transferred to a fresh tube and mixed with PD3 buffer, and the resulting mixture was subjected to the bacterial plasmid DNA recovery protocol as previously described. The recovered DNA was transformed into competent cells and selected on appropriate bacterial selection media.

2.3.10. Yeast genomic DNA preparation

2.3.10.1. Genomic DNA extraction

Yeast cells were harvested and resuspended in 300 µL of yeast lysis buffer (10 mM Tris-HCl (pH 8.0), 1% SDS, and 50 mM EDTA). Acid-washed glass beads were added, and the mixture was vortexed for 8 minutes, alternating with chilling on the ice every 2 minutes. The lysate was centrifuged at 15,000 x g for 8 minutes to separate the aqueous and organic phases, and the aqueous phase was transferred to a new tube. 300 µL of phenol was added, vortexed for 3 minutes, and centrifuged again. The aqueous phase was transferred to a new tube and treated vigorously with chloroform. The aqueous phase was transferred to a new tube. Genomic DNA was precipitated using 700 µL of ice-cold 100% ethanol, incubated at -20°C for 2 hours, and centrifuged at 15,000 x g for 3 minutes. The final DNA pellet was washed with 70% ethanol and resuspended in the plasmid elution buffer from the miniprep DNA extraction kit. The genomic DNA was stored at 4°C.

2.3.10.2. Yeast colony PCR genomic DNA preparation

The procedure employed for obtaining genomic DNA to confirm transformation was colony PCR. The procedure was previously reported in [114]. A yeast colony was initially resuspended in 200 µL of Colony PCR Lysis Buffer (200 mM LiAc, 1% SDS) with a toothpick. The suspension was then subjected to incubation at 70 degrees Celsius for 5 minutes. Following this, 600 µL of anhydrous ethanol was added to the mixture to precipitate genomic DNA, and the solution was centrifugated at 15000 x g for 5 minutes. The supernatant was eliminated, and the pellet was washed and centrifuged again with 70% ethanol before being dissolved in 100 µL of distilled water. The tube was then centrifuged at 15000 x g for 1 minute, and 1 µL of supernatant was utilized as the template for PCR reactions.

2.4. Plasmid construction

2.4.1. Construction of hygromycin cassette

YCplac33 plasmid was used in this study as the starting plasmid.

The *P. antarctica* hygromycin resistance cassette was first constructed on a plasmid before being used for other constructs. Primer sets VP15-P13H, T5-T3, and P25-P23V were used to amplify the *GPD1* promoter (*pGPD1*), *GPD1* terminator (*tGPD1*), and *PGK1* promoter (*pPGK1*) respectively from the genomic DNA of *P. antarctica*. P1H5-H3T primer set was used to amplify the hygromycin cassette from the pAG32 plasmid. As the listed sequences in the table, several primers have overhangs (~25 to 30 bp, see table) to each other in specific orders, thus providing homology for yeast homologous recombination. The plasmid used for this reaction is YCplac33 plasmid linearized with EcoRI and Hind III restriction enzyme with NEB 2.1 buffer. All the DNA components were examined with agarose gel for size and purified from the gel before the transformation. The gel-purified DNA was quantified with Nanodrop, mixed in a 1:1 molar ratio, and transformed with the lithium acetate-polyethylene glycol method.

After transforming all DNA fragments with the linearized plasmid, *Saccharomyces cerevisiae* was selected on a YEPD medium containing 300 mg/L hygromycin. Plasmid DNA was purified from yeast colonies and screened again for DNA size by PCR. And proceeded to the next step of creating constructs for *EMT1* KO and *MMF1* KO.

2.4.2. Construction of knockout plasmids

2.4.2.1. *EMT1 KO* constructs

Pa EMT1 gene (3360bp) was amplified from *P. antarctica* genomic DNA with EMTD5-EMTD3 primer pair with Q5 polymerase and contains homologous overhang to the plasmid. YEplac195 plasmid was digested with EcoRI and HindIII restriction enzyme with NEB 2.1 buffer to linearize the plasmid. Both DNA fragments were gel purified and assembled with Gibson assembly. The Gibson reaction mix was transformed into DH5α cells and selected on LB-Amp plates. DNA was extracted from the transformants and was screened by agarose gel electrophoresis and restriction digestion with EcoRI and HindIII. The assembled plasmid is named YEplac195-*EMT1*.

YEp195-*EMT1* was further digested with SmaI restriction enzyme in the middle of the *Pa EMT1* sequence (+1849 bp). Part of the previously constructed hygromycin cassette (*pGPD1*-HygR-*tGPD1*) was amplified with EGR5-EGR3 primer pair containing homology to digested YEplac195-*EMT1* and was gel purified. Both linear DNA fragments were assembled with Gibson assembly reaction and selected by agarose gel electrophoresis and restriction digestion verification. (**Fig 3.1**) The plasmid is named YEp195-*EMT1*::[Hyg] and was used as the template for PCR reactions amplifying the DNA fragment for homologous recombination knockout of *Pa EMT1.*

2.4.2.2. *MMF1 KO* construct

Four DNA fragments are required for the *MMF1* knockout plasmid. *MMF1* 1.1, and t*MMF1* fragments represent the first 1.1 kb from the start codon of *MMF1*, and 1 kb downstream of the stop codon was used as homologous region flanking the hygromycin cassette and GFP for homologous recombination knockout. *MMF1* 1.1 kb, Hygromycin cassette with *PGK1* promoter (*pPGK1*), GFP, and *tMMF1* was amplified with VM1.15-M1.1G3, PGPD5-PPGK3, P2GFP5-GFP3, and GTM5-TM3V primer with 25 bp homologous overhang in a specific order. YEplac195 plasmid was digested with EcoRI and HindIII restriction enzyme. All fragments were gel purified and mixed in a 1:1 molar ratio for the Gibson assembly reaction. The assembled plasmid was recovered from *E. coli*, and screened via restriction digestion and agarose gel electrophoresis. (**Fig 4.1**)

2.5. *P. antarctica*

2.5.1. Strains

Pseudozyma antarctica JCM 10317, now referred to as *Moesziomyces antarcticus*, was used in this experiment. The strain was acquired from American Type Culture Collection (ATCC 34888). Strains were prepared on YPD plates (10 g/L Yeast extract, 20 g/L peptone, 20 g/L glucose, and 15 g/L agar) and incubated at 30 °C for 3 days. Freezer stock was prepared by growing cells in YPD liquid medium (10 g/L Yeast extract, 20 g/L peptone, and 20 g/L glucose) for 2 days in a shaking incubator (200 RPM, 30°C), then mixed with an equal volume of 50% glycerol and stored in -80°C freezer.

2.5.2. Seed culture preparation

Initially, *P. antarctica* was cultivated in 25 mL of YPD medium for 48 hours at 30°C 200 rpm in 250 mL Erlenmeyer flasks. Then cells were cultivated in seed medium for 24 hours to reach early log phase to maximize the activity of MEL production in later steps. The seed medium was composed of 1 g/L Yeast extract, 3 g/L $NaNO_3$, 0.3 g/L KH_2PO_4, 0.3 g/L $MgSO_4$, and 40 g/L glucose with ddH_2O. 1 mL of cells from YPD were transferred to 25 mL of seed medium and then incubated for 24 hours at 30°C 200 RPM. Cells were centrifuged at 3,000 x g for 3 minutes and then resuspended in 5 mL water for MEL production.

2.5.3. *P. antarctica* antibiotic resistance against hygromycin

The background resistance of *P. antarctica* against hygromycin was tested in YEPD liquid and plate medium. For liquid medium, early log phase *P. antarctica* cells were taken from YEPD and inoculated into fresh YEPD medium containing 0 - 700 μg/mL hygromycin and incubated for 24 hours in standard condition. For YEPD-Hygro plates, 1 x 10^7 early log phase cells (determined by hemacytometer) were plated on YEPD plates containing 0 - 700 μg/mL hygromycin and incubated in standard condition for 48 hours.

2.5.4. Transformation of *P. antarctica*

Transformation of *P. antarctica* was adapted from *Saccharomyces cerevisiae* Li-Ac PEG 3350 mediated transformation method. The heat-shock temperature was determined with a gradient

PCR machine with temperature settings ranging from 30 - 43 degrees Celsius, and time from 15 to 60 minutes. The transformation was performed with the ideal heat shock temperature previously identified and selected on a YEPD-Hygro plate containing 500 µg/L hygromycin B.

2.5.5. PCR verification of knockouts

2.5.5.1. *EMT1*

Transformants of *EMT1* KO were first selected on YEPD-Hygro 500 plates. Positive growing colonies were then re-streaked on fresh plates, and colony PCR was performed on rapid-growing samples with primers targeting the hygromycin resistance gene (1084 bp). To verify if the transformed linear DNA fragment recombined at the correct location, genomic DNA was extracted from the candidates, and PCR was performed with EMTD5-HT3 (3879 bp) and P1H5-EMTD3 (2925 bp) primer set.

2.5.5.2. *MMF1*

Transformants of *MMF1* KO were first selected on YEPD-Hygro 500 plates. Positive growing colonies were then re-streaked on fresh plates, and colony PCR was performed on rapid-growing samples with primers targeting the hygromycin resistance cassette -*pPGK1* (3.7kb). Genomic DNA was extracted from the candidates, and the integrity of the whole construct was verified with the IM5-IM3 primer set (5.3 kb). To verify if the transformed linear DNA fragment recombined at the correct location, PCR was performed with VM15 HT3 (3545 bp) and P1H5-TM3V (4244 bp) primer set.

2.5.6. Southern blot of *MMF1 KO*

The goal of the Southern blot analysis is to definitively verify the genotype of *MMF1* knockout by investigating differences in DNA fragmentation patterns between wild-type and candidate *MMF1* knockout cells. The experiment involves the extraction of genomic DNA from wild-type and *MMF1* knockout cells, followed by the digestion of the DNA using various enzymes for varying durations. The ideal digestion time to produce “diffused smearing” pattern was chosen, and the DNA is separated by electrophoresis on a gel and imaged. The gel was depurinated with

0.25 M HCl for 7 minutes, and the DNA is denatured with 0.5 N NaOH and 1.5 M NaCl for two 20-minute incubations. This is followed by neutralization by soaking in 0.5 M Tris HCl pH 7.5, 1.5 M NaCl for 10 minutes. The DNA is then transferred to a ManaGraph nylon membrane using a wet capillary transfer using SSC buffer and crosslinked with UV crosslinker. The membrane is prehybridized with prehybridization buffer (6X SSC, 5X Denhardts, 0.4% SDS, and 50 µg/mL salmon sperm DNA) for 2 hours and washed before being incubated with a radioactive probe overnight. The probe and buffer were then removed and the membrane was washed with 2 x SSC buffer for 10-minutes at room temperature followed by a 15-minute wash in 0.2 X SSC buffer at room temperature. The membrane is then wrapped in saran wrap and imaged using Kodak AXR film. The membrane was stripped with probe stripping buffer (5 mM Tris-HCl, pH 8.0, 2 mM EDTA, 0.1X Denhardt's Reagent) for 2 hours at 65 degrees, and was re-probed with another probe.

2.5.6.1. Radioactive probe preparation

Two 300 bp DNA fragments were amplified from wild-type *MMF1* genomic DNA with primer set Probe 1f-1r and 2f-2r. 20 ng of a 300 bp DNA fragment from the *MMF1* sequence (Probe 1: -500 to -200 bp of stop codon; Probe 2: +30 to +330 bp of stop codon) were gel purified and used as substrate in a random priming reaction using random hexamer oligonucleotides (Invitrogen Laboratories). The 50 µL reaction included: 200 mM HEPES, 50 mM Tris-HCl, 5 mM $MgCl_2$, 10 mM β-mercaptoethanol, 0.4 mg/mL BSA pH6.8, 20 ng *MMF1* DNA, 5 OD_{260} units of random hexamers 20 µM dATP, 20 µM dTTP, 20 µM dGTP, 50 µCi α ^{32}P-dCTP (3000 Ci/mmol, 10 µCi/µL) (Perkin-Elmer Canada). This mixture was heated to 95 °C for 5 minutes and then rapidly cooled on ice prior to the addition of 3 U of the large fragment of *E. coli* polymerase I (Klenow fragment). This mixture was incubated at 25 °C for one hour and then the reaction was stopped by the addition of EDTA to a final concentration of 50 mM. The labeled probe DNA was separated from unincorporated a ^{32}P-dCTP by centrifugation through a Mini Biospin P6 gel filtration column. (Biorad laboratories). One-half of the recovered probe was added to the Southern blot hybridization.

2.6. MEL analysis

2.6.1. MEL production

For MEL production, *P. antarctica* was prepared as seed culture as previously described, and inoculated to production media with various carbon sources. The starting OD_{600} is adjusted to 0.5. Cultures were incubated for 7 days at 30°C and 200 RPM in an orbital reciprocating incubator. OD_{600} was measured in a 24-hour interval, and MELs were extracted as described later.

2.6.2. MEL extraction

For monitoring MEL production, 750 µl of mixed culture was extracted with an equal volume of ethyl acetate 2 times with vigorous shaking. The aqueous and organic phases were separated by centrifuge at 15,000 x g for 3 minutes. The organic phase was collected and air-dried at room temperature. The crude MEL was resuspended in 100 µl chloroform for TLC analysis. For monitoring secretion, the cellular and medium fraction were initially separated by centrifugation at 15,000 x g for 3 minutes, and the MEL extraction was performed on the cell pellet and medium fraction separately.

2.6.3. Thin layer chromatography

The enriched MELs extract was resuspended in chloroform depending on the volume of the original medium (1:7.5 Chloroform: Original medium). Silica gel 60 TLC plates (Millipore-Sigma Z740235; Millipore - Sigma 1.05626) were used for analysis with chloroform, methanol, and NH_4OH solvent system in a 65:15:2 (v:v:v) ratio. The MEL species on TLC plate was visualized by spraying the orcinol-H_2SO_4 reagent (0.1% orcinol, 5% H_2SO_4) and was heated in the oven for 5 minutes at 110 °C.

2.6.4. HPLC

High performance liquid chromatography (HPLC) by Lipidomics Core Facility at University of Alberta. The analysis was carried out on an Agilent 1100 instrument equipped with a quaternary pump and Alltech ELSD2000 Evaporative Light-Scattering Detector. Extracted MELs were dissolved in chloroform and separated using a method based on [111], using a binary gradient at 1.4 mL/min, on an Alltech Allsphere silica 100 x 4.6 mm column with 3 µm particle size (Mandel Scientific). Solvent A was dichloromethane, and solvent B was methanol. The total analysis time was 19 minutes per sample. The gradient was as follows: 0 min, 1%B; 0-2 min,

13%B; 2-10 min, 31%B; 10-16 min, 99%B; 16-17 min, 99%B; 17-18 min, 1%B; 18-19 min, 1%B. The detector settings were: drift tube, 60°C; gas flow, 2.5 L/min; gain, 1.

2.7. Brackish water production

2.7.1. NaCl tolerance test

Freshwater medium is prepared with 1 g/L Yeast extract, 3 g/L NaNO3, 0.3 g/L KH2PO4, and 0.3 g/L MgSO4, 4% glucose was added as carbon source, and sterilized. The P. antarctica cells were taken from the late log phase of the MEL seed medium and transferred to a fresh seed medium containing various amounts of NaCl (0.1 M, 0.2 M, 0. 5M, 1.0 M, 2.0 M) and cultured for 10 days at 30°C and 200 RPM in an orbital reciprocating incubator. The growth of cell was monitored by absorbance at OD600 with the Biochrom Ultraspec 3000, an UV/Visible spectrometer.

2.7.2. Brackish water analysis

Brackish water, which is a mixture of fresh water and salt water with a salinity between 0.5% and 3%, was acquired from Iona beach (49°12’57.591” N;123°12’47.333” W) near Richmond, BC, Canada, with a reported salinity of 1.44%~1.58%. Brackish water was filtered with Whatman filter paper (NO.1; Catalog # 1001 240) to remove suspended dirt particles. Natural Resources Analytical Lab at the University of Alberta analyzed the brackish water sample for carbon, phosphate, ion and micronutrient content.

2.7.3. Micronutrient subtraction experiment

Brackish water was first sterilized, then the micronutrients ($NaNO_3$, $MgSO_4$, KH_2PO_4) were subtracted one by one to determine if the addition of the specific micronutrient was necessary for MEL production when using brackish water as production medium. The MEL was produced with glucose as carbon source in a period of 4 days, and MEL was extracted at day 4.

2.7.4. NaCl bacterial inhibition experiment

Unsterilized brackish water was supplied with 1 g/L Yeast extract, 3 g/L $NaNO_3$, 0.3 g/L KH_2PO_4, and 10% waste cooking oil was added as the carbon source, various concentrations of NaCl were added to the medium (0 M-1 M, 0.1 M interval). *P. antarctica* cells were collected from the seed medium and inoculated to each 25 mL medium until OD_{600} reached 2.0. Production was carried out for 10 days at 30°C and 200 RPM in an orbital reciprocating incubator.

2.7.5. Brackish water/WCO production

For brackish water WCO medium, 1 g/L Yeast extract, 3 g/L $NaNO_3$, 0.3 g/L KH_2PO_4, then 29.22 g/L NaCl was added to increase the salinity by 0.5 M without sterilization. 10% v:v of waste cooking oil was added as the carbon source. With 25 mL of culture in 250 mL Erlenmeyer's flask, concentrated cells from the seed medium were added to the brackish water WCO medium until OD_{600} reach ~2. Production was carried out for 10 days at 30°C and 200 RPM in orbital reciprocating incubator.

2.7.6. Silica column purification

For whole culture extraction (10-50 mL), after production, cells were rested on a stable surface for 2 hours for cells to settle, the supernatant along with excess oil was removed, and the dense culture was extracted with an equal volume of ethyl acetate with vigorous agitation twice. The organic phase was air-dried at room temperature. The crude MEL was dissolved in chloroform before loading to a column of silica gel. The column was loaded with 12 mL of Silica gel 60 (0.063 - 0.200 mm) (Millipore 1.07734.1000). Chromatography was performed with 24 mL of 8:2 Chloroform: acetone, 24 mL 4:6 Chloroform: acetone, and finally 24 mL 0:10 Chloroform: acetone. Each fraction is 2 mL, and 36 fractions were collected. The fractions were evaporated at room temperature and dissolved in 200 µL chloroform for TLC analysis as described. Fractions were collected depending on the TLC result and chloroform was evaporated at room temperature.

Chapter 3

3. Establishing a transformation protocol for *Pseudozyma antarctica* JCM10317 using *EMT1* deletion as an experimental model.

3.1. Determination of *P. antarctica* sensitivity to hygromycin

Engineering a microbial strain such as *P. antarctica* requires the ability to manipulate the chromosomal DNA by deleting endogenous sequences and inserting heterologous DNA. Both of these processes are dependent upon the ability to select the desired transformants and so requires some form of readily selectable marker. Dominant drug resistance markers are beneficial for this purpose. Hygromycin B is a protein synthesis inhibitor that is toxic to a wide variety of prokaryotic and eukaryotic cells. To determine the sensitivity of *P. antarctica* to hygromycin, 1 x 10^6 early log phase cells were plated on YEPD-hygro plates with hygromycin concentrations ranging from 100 to 700 µg/mL. Inspection of the plates after 48 hours of incubation revealed that a hygromycin concentration of 500 µg/mL completely stalled colony formation (**Fig. 3.1**). Based on the observed sensitivity of the *P. antarctica* strain, a concentration of 500 µg/mL of hygromycin was used for subsequent experiments.

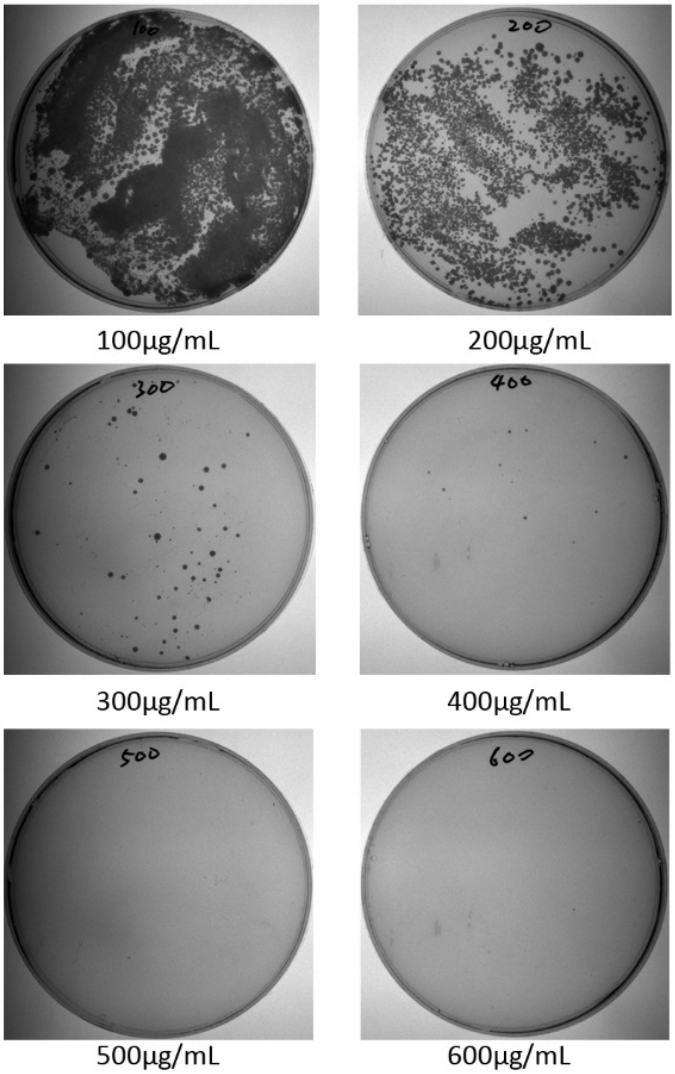

Figure 3.1. Antibiotic resistance of *P. antarctica* on YEPD-Hygro agar plate medium. 10^6 early log phase cells were plated on YEPD plates with hygromycin concentration from 100 to 700 µg/mL, and were incubated at 30°C for 48 hours.

3.2. Construction of P. antarctica - specific hygromycin resistance cassette.

The construction of a selectable genetic marker is a useful tool that may be used to perform gene deletion or insertion studies. Therefore, the first goal was to construct a genetic cassette containing an antibiotic resistance marker driven by a *P. antarctica* native promoter. A limited number of genetic elements from *P. antarctica* have been characterized. In order to generate a hygromycin

resistance gene with a native, strong, constitutively expressing promoter, the *GPD1* promoter (*pGPD1*) and *GPD1* transcriptional terminator (*tGPD1*) from the *P. antarctica* Glycerol-3-Phosphate Dehydrogenase gene were selected along with another promoter that is constitutively expressed in most yeasts, the *PGK1* promoter (*pPGK1*) from the Phosphoglycerate Kinase gene.

Methods that rely on homologous recombination of multiple linear DNA fragments with homology in appropriate order, were employed to construct this plasmid [118]. As listed in Table 3.1, individual gene fragments were first amplified using PCR reactions with respective primers, with several primers containing overhangs to each other in a specific order (**Fig. 3.2 A**). All fragments were successfully amplified (**Fig. 3.2. B**) with their expected sizes as demonstrated on agarose gel electrophoresis. Later, all four DNA fragments and linearized YCplac33 plasmid backbone were used to transform *S. cerevisiae* W303 cells. Colonies were first selected on uracil dropout plates to identify strains that had taken up the plasmid vector. The URA^+ colonies were then transferred to the YEPD-hygromycin plate to select for expression of the hygromycin resistance gene (**Fig. 3.2 C**). PCR reactions were performed using genomic DNA isolated from colonies that grew well on the YEPD-hygromycin plates as templates for M13 primer sets flanking the plasmid polylinker sequence (**Fig 3.2. D**). Positive candidates B1, B2, and F1 were chosen based on the appearance of a PCR product corresponding to the expected size of the correctly assembled hygromycin resistance cassette. These candidate plasmids were rescued from the *S. cerevisiae* by extraction of the genomic DNA followed by transformation of *E. coli*. The rescued plasmid DNA was subjected to DNA sequence analysis to confirm the sequence of the cassette that had been assembled into the YCplac33 plasmid. This plasmid is named YCplac33-[Hyg]-*pPGK1* plasmid and was used as starting plasmid for further experiments.

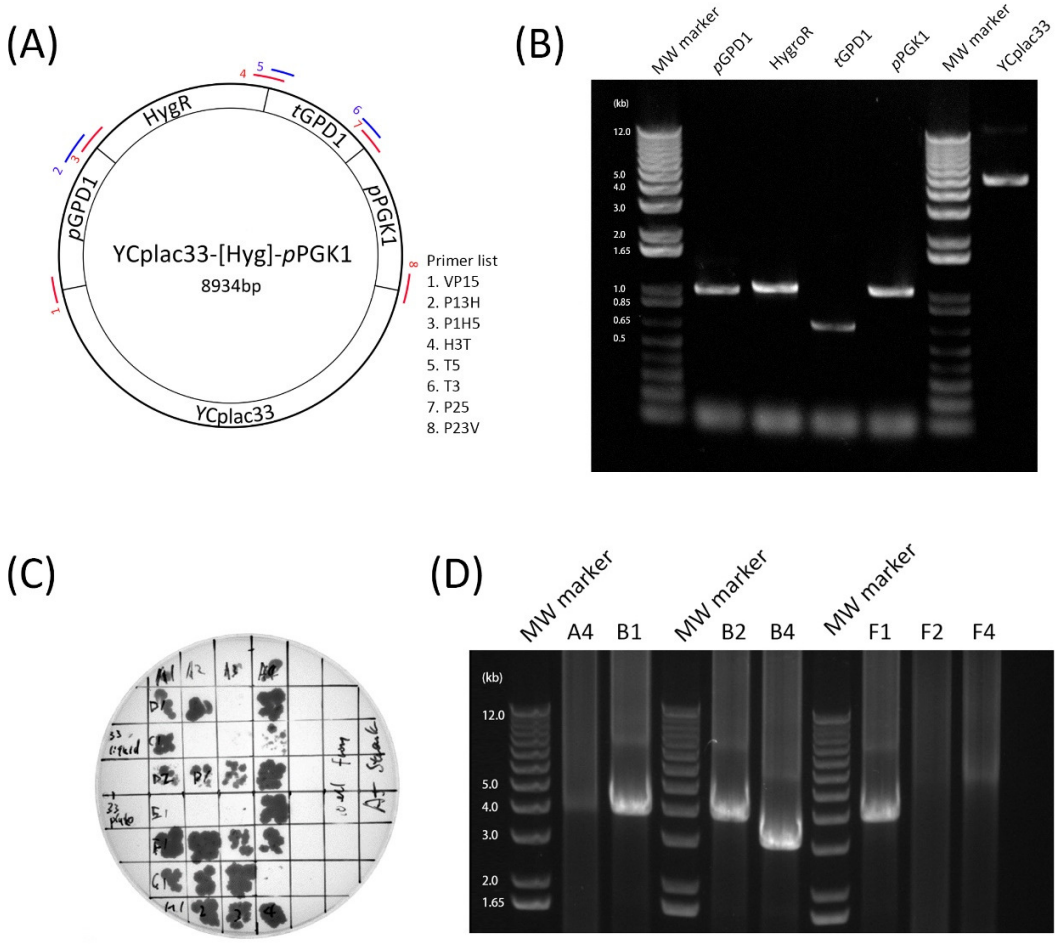

Figure 3.2. Assembly of YCplac33-[Hyg]-*pPGK1* plasmid containing a hygromycin resistance cassette for expression in *P. antarctica*. (A) Arrangement of elements on the YCplac33-[Hyg]-*pPGK1* plasmid. Primers: 1. VP15; 2. P13H; 3. P1H5; 4. H3T; 5. T5; 6. T3; 7. P25; 8. P23V. Primers in red contain homologous overhangs. (B) Agarose gel electrophoresis of individual DNA fragments for the assembly of the plasmid. The *GPD1* promoter (*pGPD1*=1022 bp), *GPD1* terminator (*tGPD1*=656 bp), and *PGK1* promoter (*pPGK1*=1044 bp) were amplified with *P. antarctica* genomic DNA as template, hygromycin resistance gene (HygroR=1084 bp) was amplified from plasmid pAG32 [115]. The YCplac33 plasmid (5502 bp) was linearized with EcoRI and HindIII restriction enzymes. 1kb plus ladder (Invitrogen) was used as a molecular weight reference. (C) *S. cerevisiae* cells were patched on YEPD Hygromycin plates for 48 hours at 30^{o}C, selecting for colonies carrying plasmids expressing the hygromycin resistance gene. (D)

The integrity of the assembled hygromycin cassette is examined with PCR reactions using M13 primer sets, with an expected size of 3734 bp. 1kb plus ladder (Invitrogen) was used as a reference.

3.3. Construction of DNA construct for *Pa EMT1* knockout

Following the construction of the *P. antarctica* hygromycin resistance cassette, the next goal was to make a DNA construct to use for homology-directed gene knockout using this selectable marker. *EMT1* is essential for MEL synthesis, and the inactivation of this gene abolishes MEL synthesis was demonstrated in several MEL producers. Therefore, *Pa EMT1* was chosen as the target for the initial knockout study. An *EMT1* mutant strain was also useful to obtain as it provides a negative control for MEL synthesis experiments for later studies.

An *EMT1* deletion vector was constructed using Gibson isothermal assembly [112]. First, the YEplac195 plasmid vector was digested with EcoRI and HindIII, and *Pa EMT1* was amplified with the EMTD5-EMTD3 primer set. The *EMT1* open reading frame amplified with these primers also included 25 bp of homology to the plasmid vectors cut ends. This allowed the *EMT1* fragment to assemble with the plasmid vector generating YEp195-EMT1. Next, YEp195-*EMT1* was linearized with SmaI restriction enzyme. The plasmid contained a unique site for this enzyme located in the center of the *EMT1* coding sequence. The hygromycin resistance cassette was amplified with EGR5 and EGR3 primer set and the two fragments were assembled again via Gibson assembly (**Fig. 3.3 B**), forming YEp195-*EMT1*::[Hyg] plasmid (**Fig. 3.3 A**).

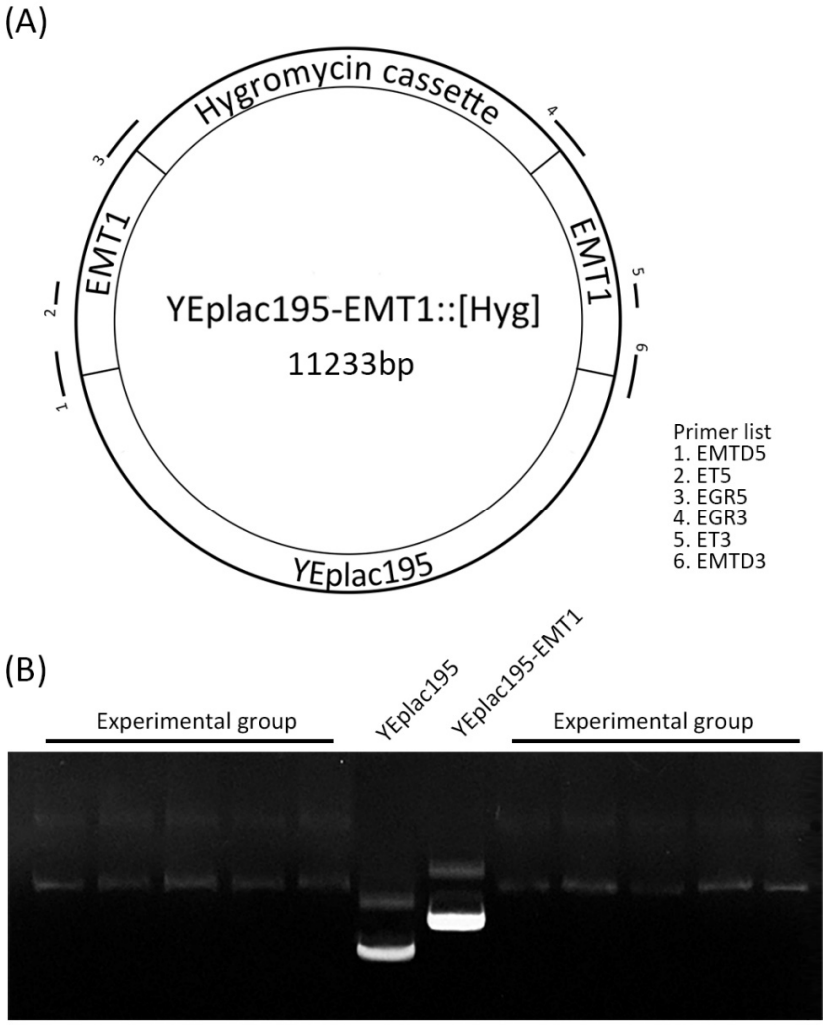

Figure 3.3. Assembly of YEp195-*EMT1*::[Hyg] plasmid. (A) Arrangement of elements on the YEplac195-*EMT1*::[Hyg] plasmid (11333 bp). Primers: 1. EMTD5; 2. ET5; 3. EGR5; 4. EGR3; 5. ET3; 6. EMTD3. EMTD5-EMTD3 primers contain homologic overhang to YEp195 plasmid, and EGR5-EGR3 primers contain homologic overhang to SmaI digested *Pa EMT1*. (B) Screening of assembled YEplac195-*EMT1*::[Hyg] plasmid. Agarose gel electrophoresis was performed on supercoiled plasmid samples to identify many plasmid samples quickly. YEp195 (5241 bp) and YEp195-*EMT1* plasmid (8567 bp) were used as the negative control.

3.4. Disruption of the *Pa EMT1* in *P. antarctica* JCM10317 strain blocks MEL synthesis

Previously, knockout studies were conducted with the *P. antarctica* T-34 strain, a sibling species to the JCM10317 strain. It was demonstrated that the transformation of linear DNA with homologous overhangs on both ends could replace the targeted gene with desired DNA construct [12]. Therefore, we attempted to conduct a comparable experiment on the JCM10317 strain using a similar approach. The DNA fragment for transformation was obtained from YEplac195-*EMT1*::[Hyg] using the ET5-ET3 primer set and contained 1127 bp homology at the 5' end and 1118 bp homology at the 3' end to *P. antarctica EMT1* genomic DNA (**Fig 3.4 A**). A standard *S. cerevisiae* Li-PEG transformation protocol [113] was used to perform the transformation, and resulting colonies were patched onto a fresh YEPD-Hygro 500 plates. Genomic DNA from eight candidate colonies was subjected to PCR analysis with the P1H5-H3T primer set and all tested positive for the presence of the hygromycin resistance cassette (**Fig 3.4 B**). To confirm that the transformed construct was recombined at the correct location, PCR reactions were performed with one primer hybridizing to sequences within the disrupting construct and another targeting sequences of the genomic DNA that are 5' and 3' respectively to the regions of homology included in the disrupting DNA construct (**Fig 3.4 C**). If the transformed DNA has recombined at the correct location, these primer sets will give a predictable amplification product, indicating a successful knockout. Agarose gel electrophoresis revealed that the H3 and H5 isolates were positive for the PCR screening, confirming that the *EMT1* gene was successfully disrupted in H3 and H5 candidates (**Fig 3.4 D**).

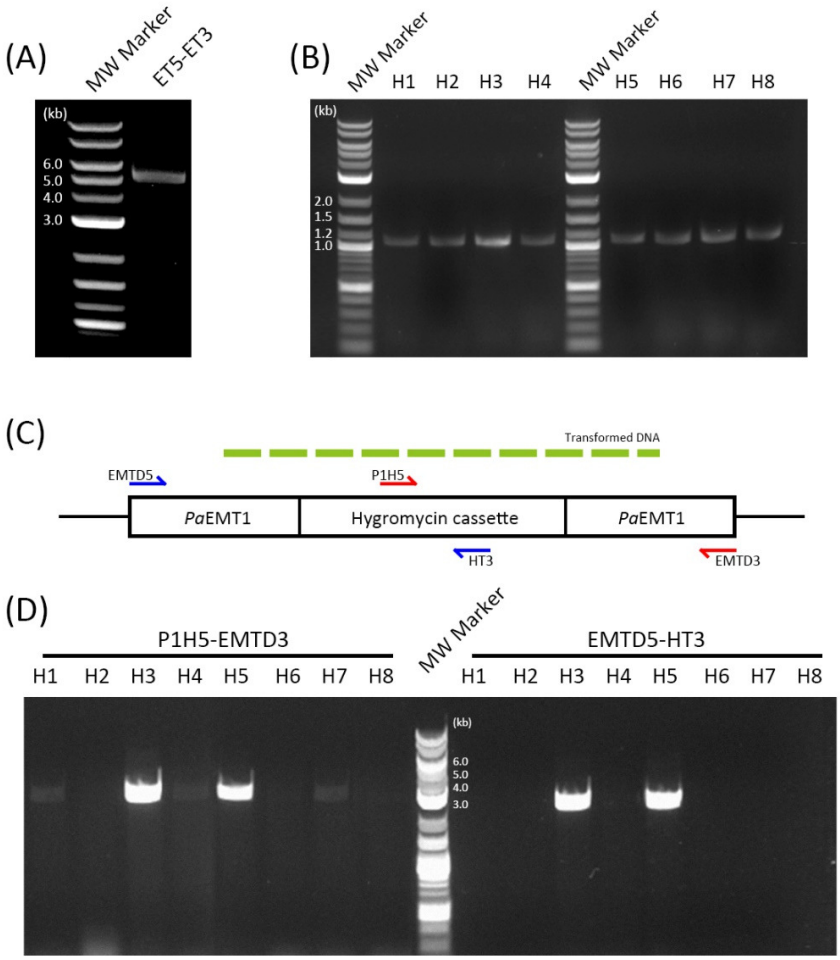

Figure 3.4. Transformation and screening of *EMT1* KO candidates of *P. antarctica*. (A) PCR amplification of linear DNA fragment with ET5-ET3 primers for transformation. (B) PCR screening for the hygromycin gene cassette from genomic DNA of *P. antarctica* candidates able to grow on YEPD-Hygro plates. P1H5-HT3 primers were used with an expected product size of 1084 bp. (C) The scheme for PCR screening of *EMT1* disruption. Blue primer: EMTD5-HT3 (3879 bp); Red primer P1H5-EMTD3 (3225 bp). Green dashed line: length of transformed DNA construct. (D) PCR verification of the *EMT1* gene disruption. PCR reactions were performed with Q5 polymerase, H3 and H5 candidates gave strong amplified product bands consistent with the correct integration of the disruption construct.

3.5. Analysis of MEL synthesis by JCM10317 with confirmed disruption of *EMT1*.

After confirming that the *EMT1* gene was disrupted in the H3 and H5 candidates, phenotype analysis was performed to investigate the effects of gene disruption on the MEL synthesis. *EMT1* wild-type cells and both knockout candidates were inoculated into MEL production medium with 4% glucose as the carbon source and cultured for a duration of four days. Wild-type cells were also inoculated into YEPD medium, where MEL synthesis is not induced, and served as a negative control. At the completion of the production trial, samples of the culture were collected, and the cells were removed by centrifugation. The resulting supernatant (culture medium) was extracted with ethyl acetate, and TLC was performed to detect the MEL species. The wild-type cells cultured in MEL production medium produced easily detectable quantities of MEL-A, MEL-B, and MEL-C (**Fig. 3.5**). The relative abundance of MEL species followed the same pattern as previously reported, where MEL-A and MEL-C were more abundant than MEL-B. In contrast, the wild-type cells cultured in YEPD medium did not produce detectable MEL, likely due to the abundant nitrogen in this rich medium (**Fig. 3.5**). Culture medium from the H3 and H5 *emt1::HYGRO* mutants contained no detectable MEL species (**Fig. 3.5**). This observation confirmed that it was possible to perform gene disruption by homologous recombination in *P. antarctica* making further genetic analysis of the strain possible. Additionally, this experiment demonstrates that Emt1 is an essential requirement for the production of MEL in the *P. antarctica* JCM10317 strain.

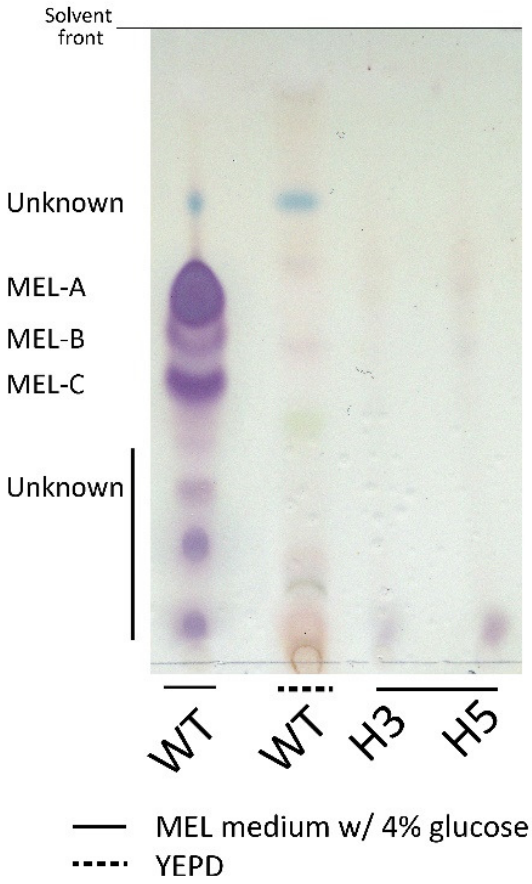

Figure 3.5. TLC analysis of MEL production by WT and *EMT1 KO*. Wild-type *EMT1* (WT) and mutant *emt1::HYGRO* (H3, H5) strains in YEPD or MEL production medium with 4% glucose for 4 days. The solid lines represent the MEL production, and the dotted line represents YEPD. Different MEL species produced by the WT strain in MEL production medium were successfully separated with TLC represented by the dark purple spots. No MEL was detected in WT cultured in YEPD (lane 2), or mutants H3, and H5 (lane 3, 4).

3.6. Improving transformation efficiency for the P. antarctica JCM10317 strain

The transformation efficiency observed in the *EMT1* gene disruption studies was remarkably low, with only 8 candidates obtained. This transformation efficiency is significantly lower than the efficiency reported in the *P. antarctica* GB-4(0) strain transformation using a protocol adapted

from the lithium acetate PEG-mediated transformation of *S. cerevisiae* [113][122]. The primary difference between the GB-4(0) and JCM10317 strains is their origin; while the GB-4(0) strain was originally isolated from rice husks in Tochigi prefecture in Japan, where the climate was mild, the JCM10317 strain was isolated from the sediment of hypersaline Lake Vanda in the Antarctic region [110]. It was hypothesized that the JCM10317 strain might be adapted to cold environments, and the heat shock step in the standard *S. cerevisiae* transformation protocol could significantly reduce cell viability.

To test this hypothesis, *P. antarctica* JCM10317 early log phase cells cultured in YEPD were diluted to $1x10^7$ cells/mL, and 100 µL of the culture was distributed into 200 µL tubes and transferred to a gradient PCR machine. The cells were treated at different temperatures and for durations from 15 to 60 minutes. Then 10 µL of cells from each condition were serially diluted and spotted onto YEPD plates. Observation of the plates after 48 hours of incubation at 30°C indicated that *P. antarctica* JCM10317 strains could tolerate 39.6 degrees for a shorter time period, while the viability was affected at 37 degrees when heated for 60 minutes (**Fig. 3.6 A**). Incubation at greater than 40°C for even 15 minutes caused a loss of cell viability (**Fig. 3.6 A**). These results indicate that the JCM10317 strain is relatively heat-sensitive, and the heat shock step in the standard yeast transformation will likely affect the viability of this strain.

The transformation efficiency of the JCM10317 strain with different heat shock temperatures was also determined. 5 µg of linear DNA fragment amplified with ET5-ET3 primer set was used as DNA input for a LiAc-PEG mediated transformation. The cells were heat shocked for 10 minutes at different temperatures using a gradient PCR machine, and following heat shock the cells were plated on YEPD-Hygro 500 to select for integration of the *emt1::HYGRO* gene disruption cassette. The colony formation was counted as colonies appeared on the plates using OpenCFU software set to a very low threshold to maximize sensitivity. As shown in (**Fig. 3.6 B)**, the CFU count displayed a downward trend as the temperature of heat shock increased, and the transformation efficiency was highest at 25 degrees and 30 degrees (essentially no heat shock). Also, when heat shocked at 41 and 42 degrees, the CFU count was lower compared to no DNA control, which agrees with the previous result that temperatures higher than 39.6 degrees seriously impact the viability of JCM10317 strain. There were approximately 116 CFUs counted on the no DNA group because the detection threshold was set to a very low value in OpenCFU software, and the tiny

colonies detected failed to grow when patched on to a fresh YEPD-Hygro 500 plate. Overall, this experiment demonstrated that the JCM10317 strain is unable to tolerate heat shock beyond 37 degrees for even a short time, and the transformation efficiency of the JCM10317 strain was improved by adjusting the heat shock temperature.

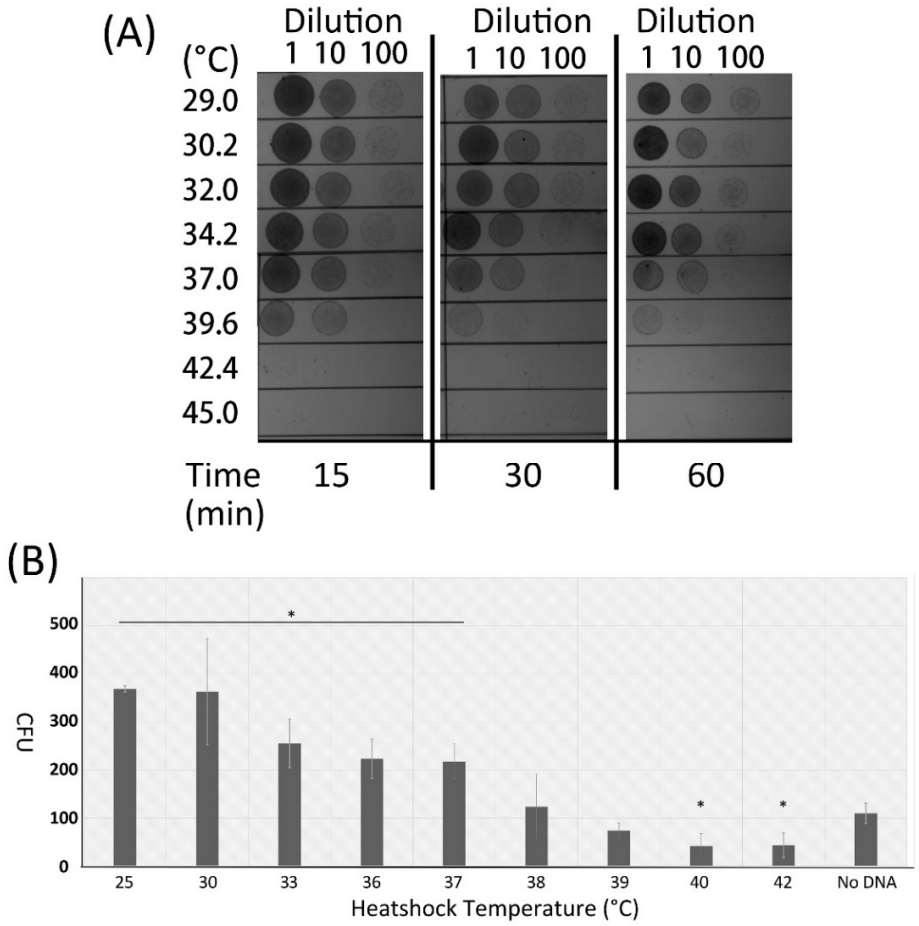

Figure 3.6. Transformation efficiency optimization for *P. antarctica* JCM10317. (A) Heat tolerance of *P. antarctica* cells was determined by heat treatment at different temperatures at different time intervals and then diluted and plated on YEPD plates. Original cell concentration: 1 x 10^7 cells/mL. (B) Transformation efficiency with different heat shock temperatures. *P. antarctica* cells were transformed with the linear DNA fragments of the hygromycin resistance cassette flanked by *EMT1* sequence and were selected on YEPD-Hygro 500 plates for 48 hours. Experiments were performed in triplicates, and CFU was determined with OpenCFU software.

Chapter 4

4. Identification of *MMF1* as essential for secretion of MEL by *P. antarctica* JCM10317

4.1. Construction of DNA construct for *PaMMF1* knockout

After successfully demonstrating the feasibility of targeted gene knockouts in the JCM10317 strain through the *EMT1* knockout experiment, our next goal was to knock out *MMF1*. *MMF1* has been proposed to encode the transporter of MEL based upon its proximity to the other MEL synthesis genes and its sequence similarity to other Major Facilitator Superfamily (MFS) transporters. To investigate the role of *MMF1* in MEL transport in *P. antarctica* JCM10317 a gene disruption strategy similar to that used on *EMT1* was applied. Initially, a plasmid containing the *MMF1* sequence flanking a selectable marker was constructed using the Gibson assembly technique. Subsequently, the linear fragment of the constructed sequence was used to transform *P. antarctica* JCM10317. Gene disruption vector YEplac195-*MMF1*::[Hyg]*pPGK1*-GFP (**Fig. 4.1 A**) was generated by amplification of the 5' 1.1 kb *MMF1* coding sequence from the start codon to position 1096 and the terminator region of *MMF1* (1047 bp of DNA downstream of the coding sequence) from wild-type *P. antarctica* genomic DNA. The hygromycin resistance cassette along with the *PGK1* promoter (3734 bp) was amplified from the YCp33-[Hyg]-*pPGK1* plasmid with PGPD5-PPGK3 primer set, and GFP (716 bp) was amplified from the pET30-R5-GFP plasmid with P2GFP5-GFP3 primer set. The plasmid backbone was the YEplac195 plasmid that was linearized with EcoRI and HindIII restriction enzymes. All individual fragments were gel-purified and quantified before being subjected to Gibson assembly reaction (**Fig. 4.1 B**).

Following the Gibson assembly reaction, candidate plasmids were screened for the expected size, and positive candidates were further verified through restriction digestion and PCR (**Fig. 4.1 C**). This construct deletes 531 bp of DNA sequence corresponding to 177 amino acid residues from the *MMF1* coding sequence replacing them with the hygromycin expression cassette.

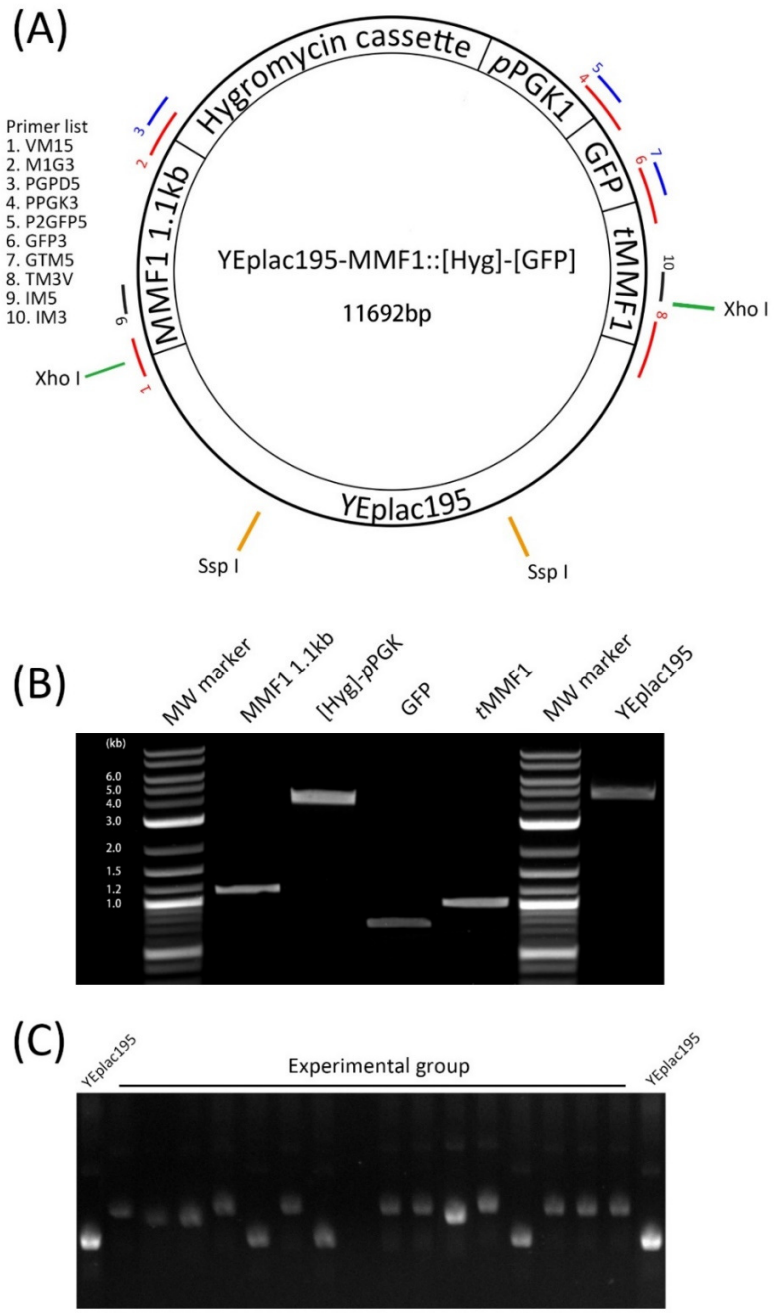

Figure 4.1 Assembly of YEp195-*MMF1*::[Hyg]-*pPGK1*-GFP plasmid. (A) Arrangement of elements on the YEp195-*MMF1*::[Hyg]- ***pPGK1*-**GFP plasmid (11692 bp). Primers: 1. VM15; 2. M1G3; 3. PGPD5; 4. PPGK3; 5. P2GFP5; 6. GFP3; 7. GTM5; 8. TM3V; 9. IM5; 10. IM3. Xho I restriction site were marked by green line, and Ssp1 site for fragmentation of plasmid backbone

were marked by orange line. (B) Agarose gel electrophoresis of individual DNA fragments for the assembly of this plasmid. *MMF1* 1.1kb (1150 bp), Hygromycin cassette +pPGK (3676 bp), GFP (717 bp) and *MMF1* terminator (*tMMF1*=1047 bp). YEplac195 plasmid (5190 bp) was linearized with EcoRI and HindIII restriction enzyme. 1kb plus ladder (NEB) was used as a reference. (C) Screening of assembled YEp195-*MMF1*::[Hyg]-GFP plasmid. Agarose gel electrophoresis was performed on supercoiled plasmid samples to identify as many plasmid samples as possible. YEp195 (5241 bp) were used as the negative control.

4.2. Inactivation of the *MMF1* gene in *P. antarctica* JCM10317

4.2.1. Transformation and PCR verification

Following the construction of the YEp195-*MMF1*::[Hyg]-*pPGK1*-GFP plasmid, the next experimental objective was to create a knockout of the *MMF1* gene through homologous recombination. The YEp195-*MMF1*::[Hyg]-*pPGK1*-GFP plasmid was digested using Xho I and Ssp I restriction enzymes, resulting in four fragments. Fragment 1, which is 6135 bp in length, contains the hygromycin resistance cassette with GFP and contained 1106 bp and 640 bp of homology to *Pa MMF1* on the 5' and 3' ends, respectively. The other three fragments were derived from the plasmid backbone at 2418 bp, 1802 bp, and 1337 bp, respectively (**Fig. 4.2 A**). Fragment 1 was then gel purified and used to transform the JCM10317 strain for *MMF1* KO.

After transformation using a temperature-adjusted protocol, 15 candidates were isolated from the YEPD-Hygro 500 plate. Genomic DNA was extracted from each candidate, and PCR with the PGPD5-PPGK3 primer set was used to examine the integrity of the hygromycin cassette. Of the 15 candidates, two candidates were tested positive (**Fig. 4.2 B**). PCR with the IM5-IM3 primer set, which binds within the transformed linear DNA sequence, was then used to determine the integrity of the entire construct, and candidate #7 was positive for this amplification (**Fig. 4.2 C**). Finally, the VM15-H3T and P1H5-TM3V primer sets were used, with each primer set containing one primer that binds to outside the transformed construct and another primer within the construct at either the 5' or 3' end, to verify if the recombination occurred at the correct location. Candidate #7 was demonstrated to have amplification with both primer sets, and was thus presumed to be *MMF1* gene disruption (**Fig. 4.2 D**). However, more definitive evidence is needed to verify the

KO of *MMF1*.

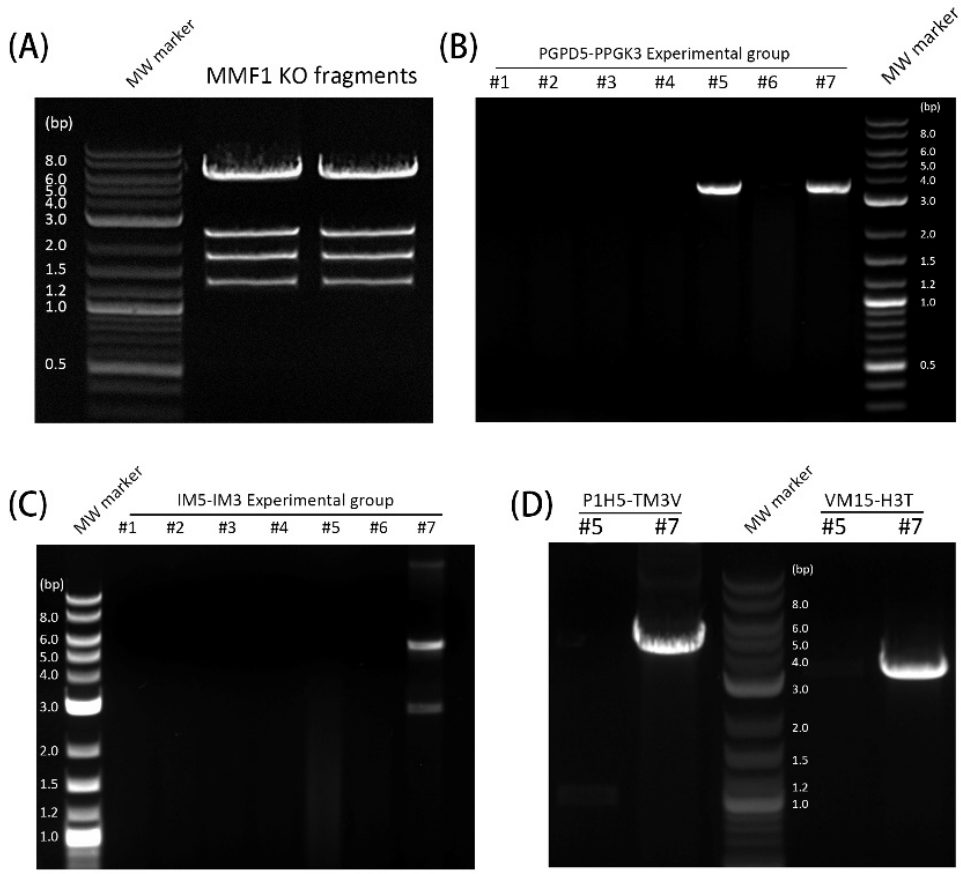

Figure 4.2. Transformation and screening of *MMF1 KO* candidates of *P. antarctica*. (A) Restriction digestion of YEplac195-MMF1::[Hyg]-*p*PGK1-GFP plasmid with Xho I and Ssp I for linear DNA fragment prior to transformation. (B) PCR screening of positively growing transformed P. antarctica cells on YEPD-Hygro plates. PGPD5 and PPGK3 primers were used with an expected size of 3676 bp. (C) PCR with the IM5-IM3 primer set, binds within the transformed linear DNA sequence with a expected size of 5365 bp to determine the integrity of the entire construct. (D) PCR verification of *MMF1 KO*. PCR reactions were performed with P1H5-TM3V and VM15-H3T primer and Q5 pol, candidates yielding strong bands for both primer sets indicate successful *MMF1 KO*.

4.2.2. Southern blot verification

As only one candidate was obtained from the knockout experiment, more definitive evidence was required to show that *MMF1* had been knocked out. Southern blot analysis can provide such evidence if the antibiotic resistance construct replaced the original sequence through homologous recombination. To this end, the DNA sequences at the region of interest for both wild-type (WT) and candidate #7 were analyzed, and two probes, each 300 bp in length, were prepared for Southern blot analysis.

Probe 1 targets a region of the *MMF1* coding sequence and should be completely removed if the transformed construct correctly recombined. Probe 2 targets the transcriptional termination region 30 bp 3' to the stop codon, which will be present for both *MMF1* wild-type and *MMF1* knockout (KO) with distinctive sizes after restriction digestion (**Fig. 4.3 A, 4.3 B**). XhoI, AflIII, and SacII were chosen as the restriction enzymes for Southern blot analysis since they produce distinct patterns with the designed probes.

Genomic DNA was extracted from both wild-type and candidate #7 and subjected to restriction enzyme digestion for varying durations (5 to 60 minutes) to determine the ideal digestion duration for a "diffuse smearing" pattern. The membrane was first probed with Probe 2, then stripped and probed with Probe 1, and the radioactive signal was detected by exposure of the membrane to Kodak AXR film.

For Probe 1 targeting the open reading frame of *Pa MMF1*, radioactive signals were shown for wild-type gDNA samples with expected patterns for each restriction enzyme (Sac II=3723 bp, Xho I=3033 bp, Afl III=3677 bp) (**Fig 4.3 D, F**). It is worth noting that the XhoI lane has two bands, and the higher molecular weight band is likely due to unintentional incomplete digestion at 1302 bp, resulting in a 4.1 kb band, but such incomplete digestion does not affect overall conclusion. No signals were detected in all *MMF1 KO* lanes, consistent with the loss of the *MMF1* open reading frame corresponding to this probe removed from the genomic DNA.

For Probe 2 targeting the terminator region of *MMF1*, both *MMF1* and *mmf1::HYGRO* are expected to give radioactive signals. For the *MMF1* strain Probe 2 gives identical hybridization signals for the three enzymes. For *mmf1::HYGRO*, the digestion pattern was identical to the predicted pattern for the three restriction enzymes (Sac II=2907 bp, Xho I=6898 bp, Afl III=1587 bp) (**Fig. 4.3 E,G**). Among the three restriction enzymes, XhoI with 6898 bp gives the definitive

answer that the transformed DNA construct was incorporated intact into the genomic DNA at the correct location, completely removing the native *MMF1* gene.

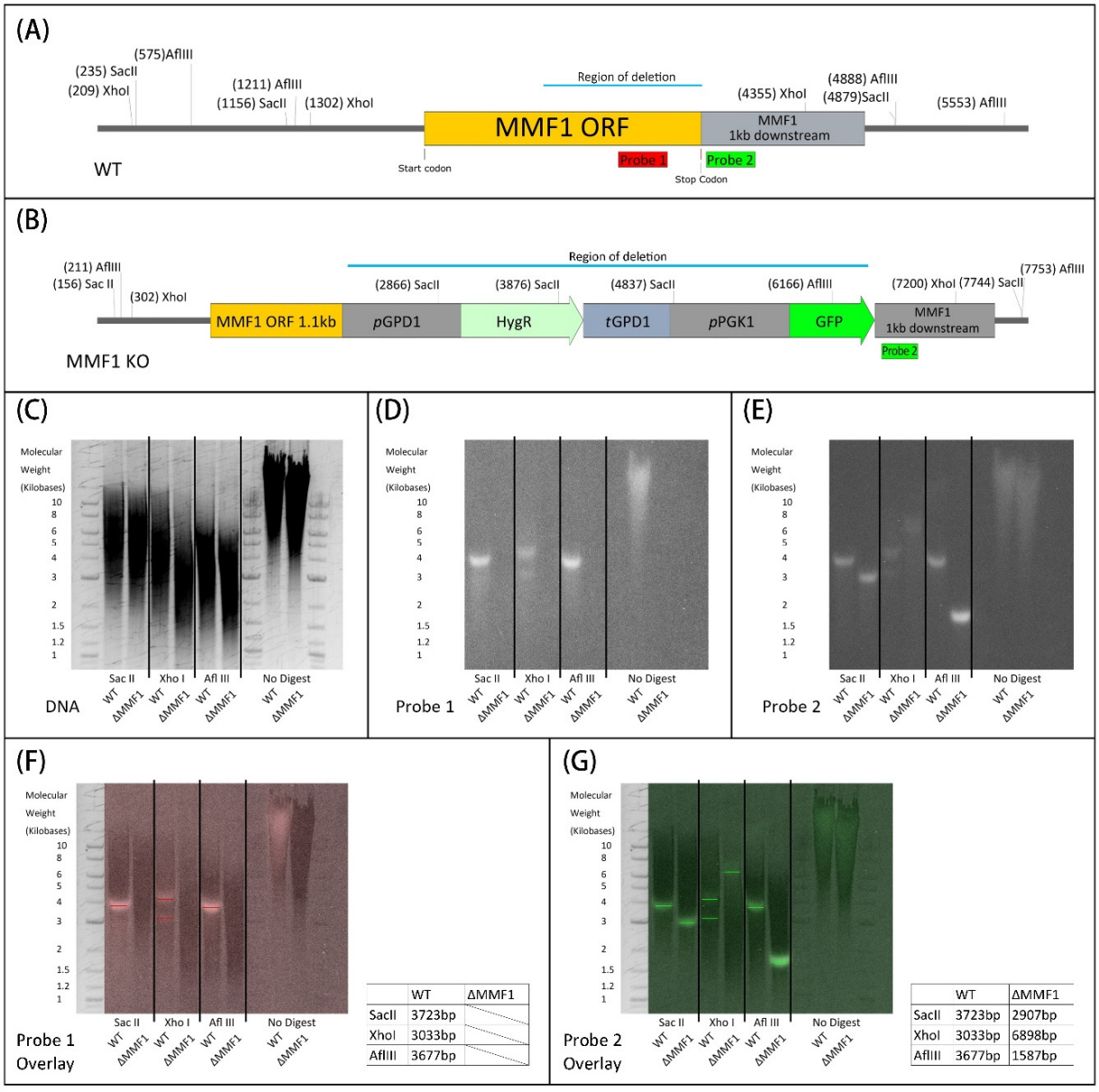

Figure 4.3. Southern blot verification of *Δmmf1* on *P. antarctica* digested genomic DNA. DNA map of (A) WT and (B)*Δmmf1* at the location of interest. Region of deletion through homologous recombination is indicated by the blue bar. Restriction enzyme site and position were labeled respectively. Probes are 300 bp in size. Probe 1 in red bind to -200 bp of the stop codon, and probe 2 in green bind to +30 bp of the stop codon. c) Agarose gel electrophoresis of

WT and *Δmmf1* undigested DNA and DNA digested with Sac II (10 minutes); Xho I (15 minutes); Afl III (15 minutes). Southern blot image of membrane probed with probe 1 (D) and probe 2 (E). Probe 1 (F) and probe 2 (G) overlayed with agarose gel. The predicted size after restriction digestion with respected enzyme is labeled on the side.

4.3. Phenotype evaluation of *MMF1 KO*

4.3.1. TLC analysis of MEL secretion by the *mmf1::HYGRO* mutant strain

After confirming the *MMF1 KO* genotype, thin-layer chromatography was employed to investigate the impact of *MMF1* knockout on the MEL production and secretion profile using water-soluble carbon sources as feed stock. MEL production trials were performed with an *MMF1* and *mmf1::HYGRO* strain using glucose or glycerol as the carbon source for MEL biosynthesis. On day 3 of the production trial, samples were collected and the cell pellet was separated from the culture medium fraction. The cells and media were extracted independently and analyzed by TLC. MEL was produced in all carbon sources tested, including 4% glucose, 12% glucose, and 6% glycerol. However, in the *MMF1 KO* samples, we observed that MEL could be extracted from the cell pellets but was absent from the culture medium fractions (**Fig. 4.4 A, B, C**). The absence of MEL secretion determined by the lack of staining on the TLC sample from the medium fractions, suggested that *MMF1* is required for MEL secretion.

Despite the lack of secreted MEL, the total amount of MEL accumulated within the cells was not significantly affected by the *MMF1 KO* genotype. In fact, the MEL-A stain in the cellular fraction of *MMF1 KO* for all carbon sources was slightly larger than that of the wild-type, indicating an accumulation of MEL-A within the cell. We also observed a shift in MEL species in the cellular fraction of *MMF1 KO*, where the spot representing MEL-C was lighter than that in the wild-type, suggesting that the absence of *MMF1* may impact the forms of MEL species that accumulate.

Close inspection of the TLC plates revealed the presence of an orcinol staining spot in the medium fractions that was greatly enriched in the *MMF1 KO* samples (**Fig. 4.4 A, B, C**). This spot is highlighted by the red arrow in the figure and is not detectable or at least not prominent in the wild-type samples. This spot could be a novel MEL species or a by-product of MEL biosynthesis. Previous research on *P. tsukubaensis MMF1 KO* has also observed a similar species that does not migrate with the conventional MEL species during TLC analysis [31]. It is known that *P.*

tsukubaensis produces a single di-acylated MEL-B species, and an uncharacterized species was only detected when the *MMF1* gene was removed. Further structural analysis by LC-MS has revealed that this spot corresponds to a mono-acylated derivative of MEL-B produced from *P. tsukubaensis Δmmf1* [31]. The presence of this unknown MEL species in the *MMF1 KO* may suggest that the knockout of *MMF1* may have altered the biosynthetic pathway of MEL-B, leading to the production of this novel derivative that does not require Mmf1 for secretion.

The production experiment comparing wild-type *MMF1* with *MMF1 KO* was continued for 5 days in 12% glucose culture. Similar to the results after three days of culture it was observed that MEL could be readily extracted from the cell pellets of either wild-type *MMF1* or *MMF1 KO* but no MEL could be detected in the medium fraction from the *MMF1 KO* strain (**Fig. 4.4 D, E**) The MEL staining in the cellular fraction of the *MMF1 KO* for all carbon sources was still slightly more prominent than in wild-type *MMF1*, suggesting that MEL accumulated within the cell. Furthermore, the shift in MEL species in the cellular fraction of *MMF1 KO* was still observed, with the spot representing MEL-C appearing lighter than in samples extracted from wild-type cells. The stain representing the uncharacterized MEL species was darker, indicating that more of this unknown MEL species was produced under 12% glucose conditions if cultured for a prolonged time. These findings suggest that the absence of *MMF1* may affect MEL secretion and accumulation within the cell and potentially alter the MEL species produced.

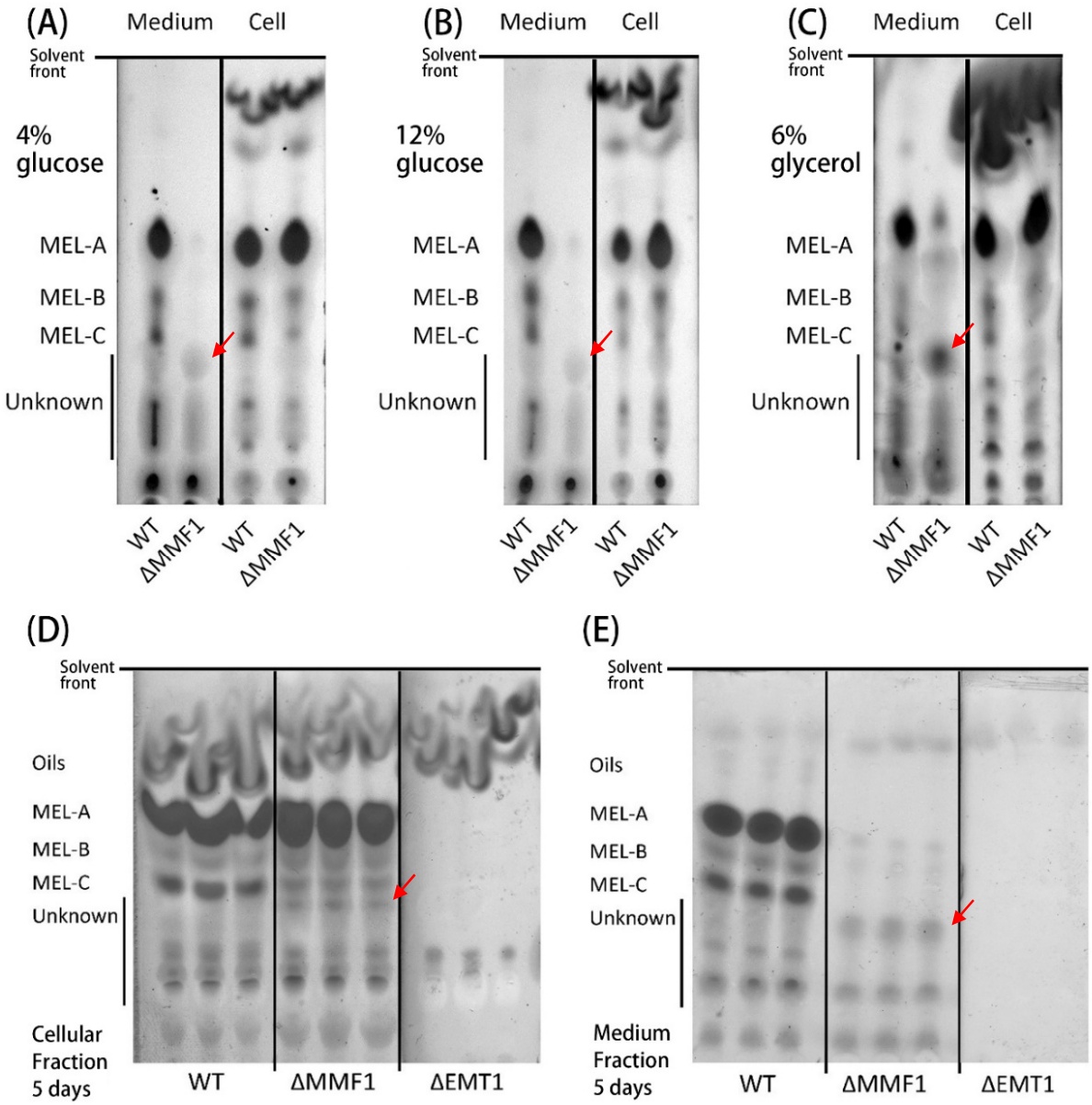

Figure 4.4. Thin layer chromatography profile of *MMF1 KO* in water-soluble carbon sources. MEL production of WT and *MMF1 KO* cells in 4% glucose (A), 12% glucose (B), and 6% glycerol (C) for the period of 3 days, unknown MEL species were marked by the red arrow. (D) cellular fraction and (E) medium fraction of MEL produced from WT, *MMF1* KO, and *EMT1* KO at day 5 with 12% glucose. Unknown MEL species were marked by the red arrow. The glycolipid species were visualized with orcinol-H_2SO_4 reagent.

4.3.2. Analysis of the effects of *MMF1* deletion on cell growth

The growth profile of the *MMF1 KO* strain was also determined in MEL production conditions to assess if the accumulation of MEL (caused by the absence of MEL transporter) affects cell proliferation. Wild-type cells, *EMT1 KO*, and *MMF1 KO* were cultured in MEL synthesis media with three different carbon sources: 4% glucose (**Fig 4.5 A**), 12% glucose (**Fig 4.5 B**), and 6% glycerol (**Fig 4.5 C**).

Overall, no significant difference in growth was observed between *MMF1 KO* and wild-type cells in any of the three carbon sources. Additionally, the *EMT1 KO* strain grew slower than the other two strains in all growth conditions. When the overall growth rates were compared, it was found that *P. antarctica* JCM10317 grew fastest in 6% glycerol, followed by 4% glucose and 12% glucose. The difference between the two glucose concentrations could be explained by osmotic pressure, which resulted in a significant delay in the growth curve of the 12% glucose group before 96 hours. The only significant difference in growth between wild-type and *MMF1 KO* was observed in the 6% glycerol group at 72 hours, although this significance was not observed at later time points.

These findings suggest that the absence of the *MMF1* gene does not significantly impact cell growth in culture conditions conducive to MEL production with different water-soluble carbon sources and that the *EMT1* gene may play a role in regulating growth in these conditions.

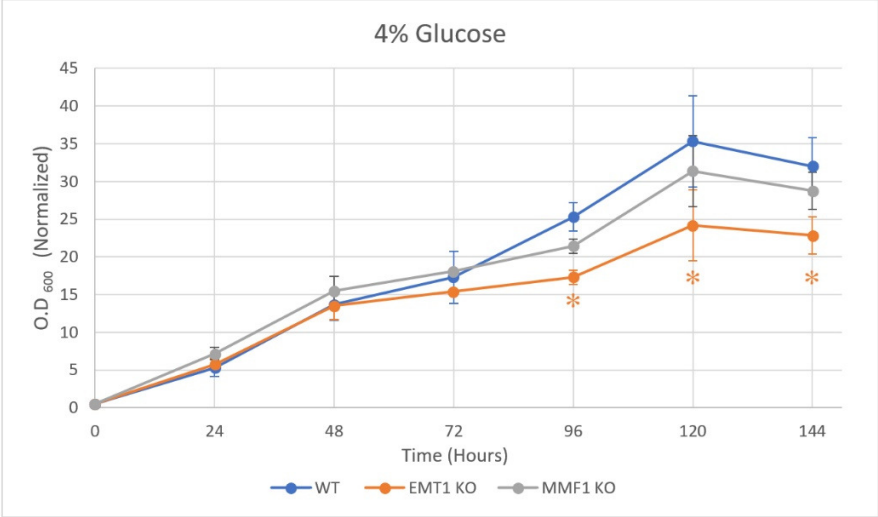
4% Glucose
O.D 600 (Normalized)
45
40
35
30
25
20
15
10
5
0
0
24
48
72
96
120
144
Time (Hours)
WT
EMT1 KO
MMF1 KO

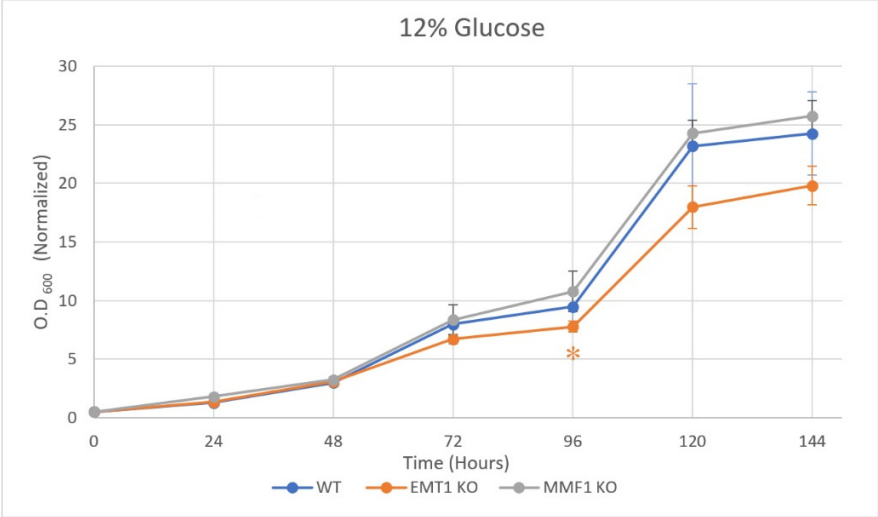
12% Glucose
O.D 600 (Normalized)
30
25
20
15
10
5
0
0
24
48
72
96
120
144
Time (Hours)
WT
EMT1 KO
MMF1 KO

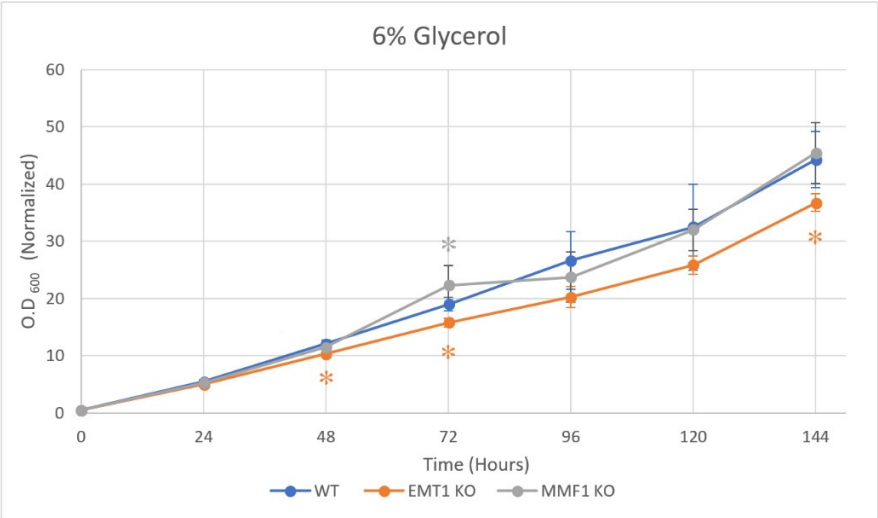
6% Glycerol
O.D 600 (Normalized)
60
50
40
30
20
10
0
0
24
48
72
96
120
144
Time (Hours)
WT
EMT1 KO
MMF1 KO

Figure 4.5. The growth profile of *P. antarctica* JCM10317 strains. Wild-type (WT), *emt1*::HYGRO (*EMT1 KO*), and *mmf1*::HYGRO (*MMF1 KO*), was measured by optical density at 600 nm (OD_{600}) in MEL production conditions. The strains were cultured with 4% glucose (A), 12% glucose (B), and 6% glycerol (C) over 144 hours. The OD_{600} values were normalized by multiplying the dilution factor, and each sample was measured in technical triplicates. The error bars reflecting standard deviation for each group are indicated by the same color as the corresponding line. The significance to WT was determined with t-Test (Two-Sample Assuming Equal Variances) and indicated by * symbol with corresponding color.

4.3.3. HPLC profile of secreted MEL

In a study involving *MMF1 KO*, TLC and orcinol staining was used to monitor MEL synthesis and secretion. The results showed that MEL-A/B/C were not detected on the TLC plate of the *MMF1 KO* group, indicating a significant suppression of MEL secretion in these samples. Additionally, an uncharacterized spot was detected in the medium and cellular fractions of the *MMF1 KO* samples, indicating a potentially new species of MEL was produced. HPLC analysis was performed on crude MELs extracted from the medium fraction of the 12% glucose group to investigate this observation further.

The results showed that the peak representing MEL-A/B/C in the WT samples was almost absent in the *MMF1 KO* samples, confirming the significant suppression of MEL secretion (**Fig. 4.6**). In contrast, a significant increase in the peak (WT: 4.745/ *MMF1 KO*: 4.758) representing the uncharacterized spot on the TLC plate was observed in the *MMF1 KO* samples compared to wild-type (**Fig. 4.6, blue arrow**). Finally, minor differences were observed at the retention times 4.210 (WT) - 4.215 (*MMF1 KO*) peak, although the significance of this peak is currently unknown.

Overall, HPLC results indicate a significant difference in the secretion of MEL between wild-type and *MMF1 KO* samples. These findings suggest that *Pa* Mmf1 plays a crucial role in the MEL secretion and MEL metabolism.

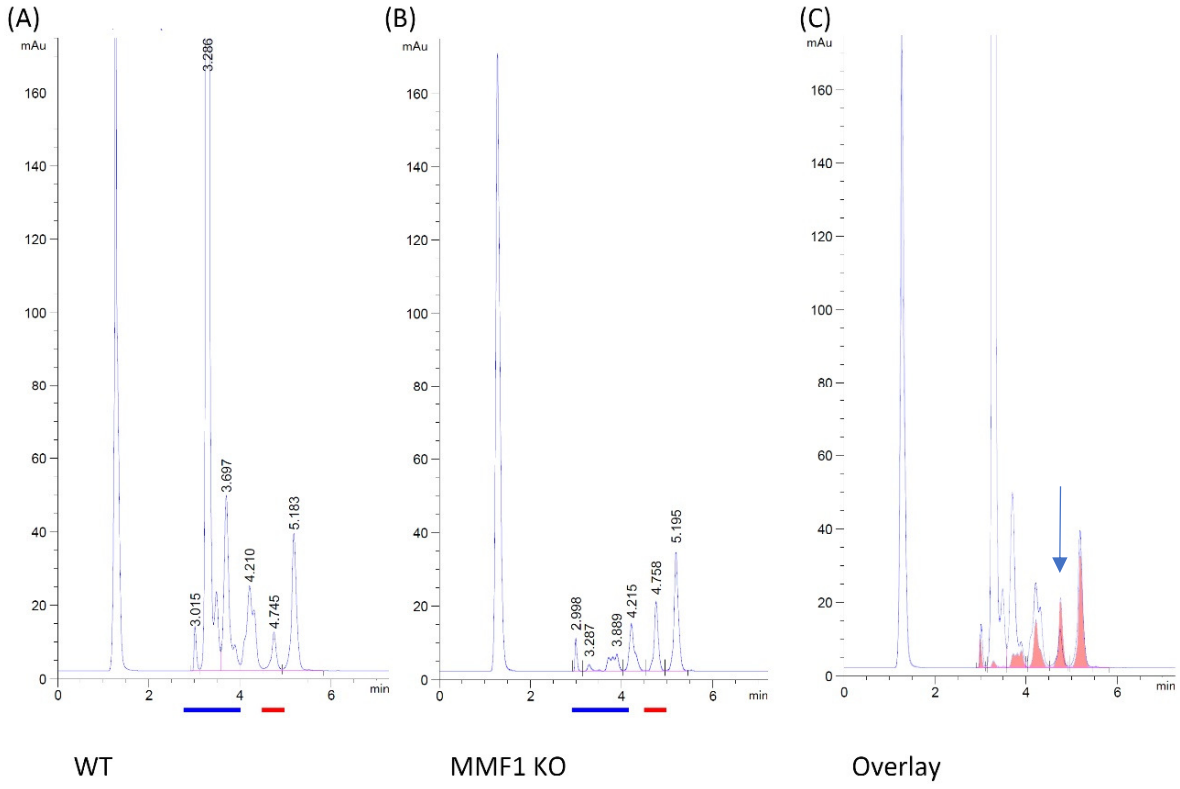

Figure 4.6 HPLC profile of crude MEL from *MMF1* and *mmf1:*HYGRO strains. MELs were extracted from the medium fraction of (A) WT, and (B) *MMF1 KO* after production for 3 days in MEL production medium with 12% glucose. The amount of MEL was normalized based on the intensity of the TLC stain. The blue line indicates MEL A/B/C, and the red solid fill indicates the unknown spot on the TLC plate. (C) The overlayed HPLC profile of WT and *MMF1 KO*, the HPLC profile of *MMF1 KO* was represented by solid red. Blue arrow indicates the unknown species of MEL.

Chapter 5

5. Sustainable MEL Biosynthesis Using Waste Cooking Oil and Brackish Water

5.1. *Pseudozyma antarctica* JCM10317 is salt tolerant and can produce MEL in 1M NaCl in the medium

In this study, we first investigated the ability of *P. antarctica* JCM10317 to grow in a MEL medium with 4% glucose at different NaCl concentrations and the MEL synthesis and secretion under salt stress conditions.

P. antarctica JCM10317 was previously isolated from a hypersaline lake in Antarctica, Lake Vanda, and is expected to be halotolerant [110]. However, the ability to convert carbon sources into MEL under salt stress was not tested before.

We began by testing the growth rate of *P. antarctica* JCM10317 under salt stress conditions by measuring its optical density at 600 nm ($O.D_{600}$) over 7 days in the MEL medium with 4% glucose and NaCl concentration from 0 M to 2 M. Our results showed that *P. antarctica* JCM10317 could grow in all salt concentrations tested, with varying performances (**Fig. 5.1 A**). In the first two days, all groups except the 2 M group grew rapidly (**Figure 5.1 A**, **dashed line**), then entered a plateau for 2 days (**Fig. 5.1 A, dotted line**) and grew rapidly again from day 5 to day 7 (**Fig. 5.1 A, solid line**). We observed a delay in the growth curve of the 2 M NaCl group, which was likely attributable to the high osmotic pressure. The first rapid growth phase was observed between day 1 and day 4, followed by a plateau until day 7 (**Fig. 5.1 A**).

To investigate the ability of *P. antarctica* JCM10317 to synthesize and secrete MEL under salt stress conditions, we tested MEL production in all groups. We found that all groups, except the 2 M NaCl group, produced a detectable amount of MEL (**Fig. 5.1 B**). For NaCl concentrations below 0.5 M, MEL secretion was efficient (**Fig. 5.1 B**). We observed that MEL production was correlated to the growth profile, with most MEL being produced during the second rapid growing phase. Since the 2 M NaCl group did not enter the second rapid-growing phase, MEL synthesis was limited. Additionally, excess osmotic pressure in groups with NaCl concentration above 0.2 M restricted the transportation of MEL to the extracellular space (**Fig. 5.1 B**).

In summary, this preliminary study provides evidence that the *P. antarctica* JCM10317 strain exhibits halotolerant characteristics and is capable of synthesizing MEL even in the presence of high osmotic pressure induced by the addition of NaCl.

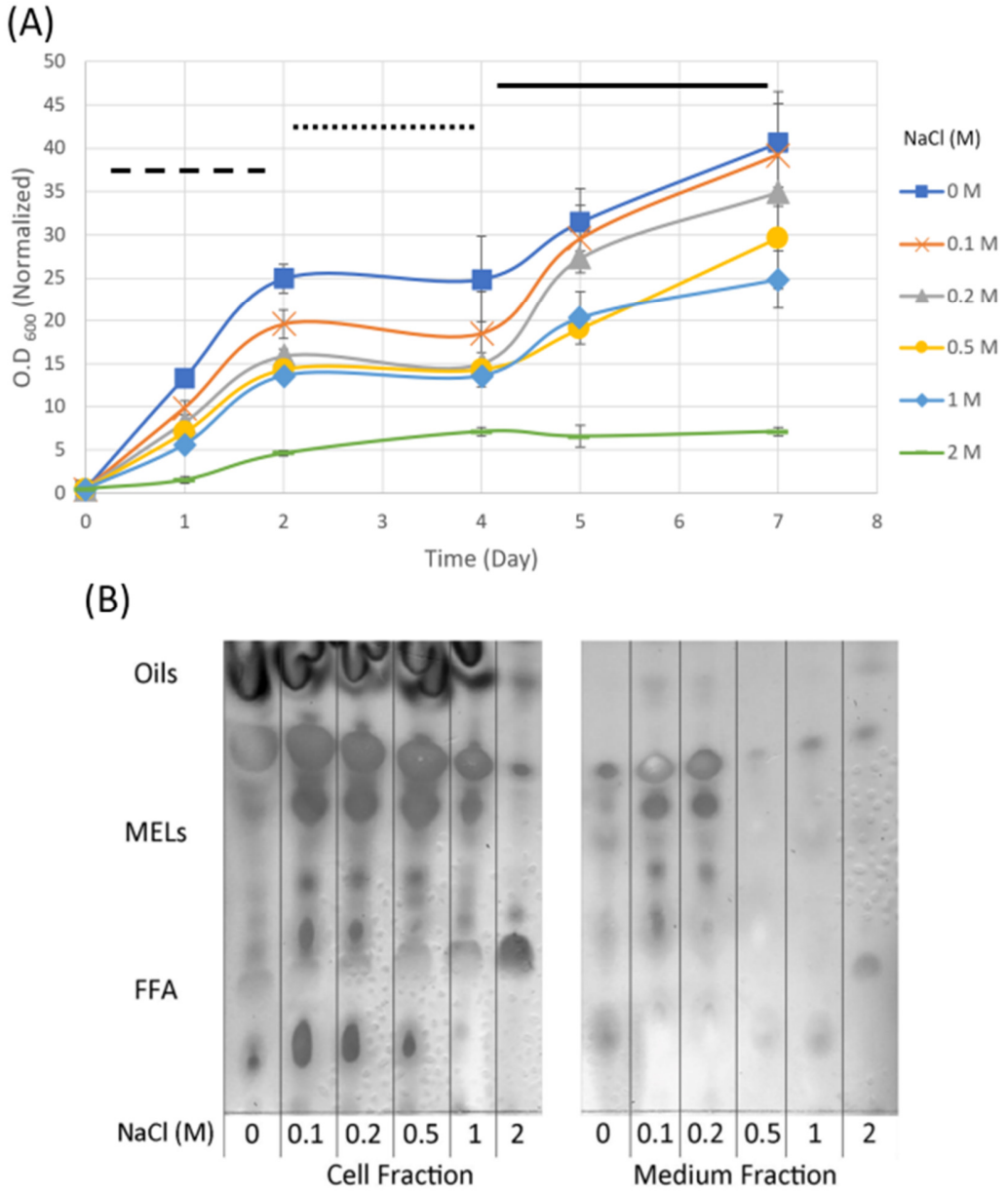

Figure 5.1. Salt tolerance and MEL synthesis of *Pseudozuma antarctica* JCM10317 in MEL seed medium with 4% glucose. (a) Growth curve of *P. antarctica* in seed medium with addition of different concentrations of NaCl. All samples started at an OD_{600} of 0.5. Dashed line: 1st rapid

growing phase; dotted line: plateau phase; solid line: 2nd rapid growth phase. (b) Thin-layer chromatography of mannosylerythritol lipid (MEL) obtained from ethyl acetate extractions after 7 days, the number represents NaCl concentration in M. MELs: mannosylerythritol lipids, FFA: free fatty acid.

5.2. Investigating the potential to use brackish water as a production medium for MEL biosynthesis.

Natural brackish water contains a range of nitrogen, organic carbon in addition to salts and micronutrients. The aim of this study is to investigate the possibility of using non-potable brackish water as the medium for MEL biosynthesis. Such a process would have the potential to reduce production costs and save the use of potable water for more appropriate purposes. As a first step, a sample of brackish water was obtained from Iona beach in Vancouver, British Columbia. The composition of the water sample used was determined by Natural Resources Analytical Lab at the University of Alberta (**Table 5.1**). A range of common ions as well as total nitrogen and carbon were analyzed. The water sample used in these experiments contained 38.37 mg/L potassium, 95.63 mg/L magnesium, and 788.37 mg/L sodium, making it unlikely that any of these ions would be limiting and could potentially be omitted from the medium prepared with this water. The total organic carbon content (TOC) was determined to be 3.77 mg/L. This low carbon content makes it unlikely that the natural content would make any significant contribution to any product formation. Additionally, the total nitrogen content was determined to be 45 mg/L and thus has the potential to be a limiting factor in cell growth, making it unlikely that supplementary nitrogen could be omitted. To determine whether the saline water could be used as the base for the MEL production medium, a "drop out" experiment was performed to determine what components of the standard MEL production medium components are not required when using brackish water rather than sterilized distilled water as for the production medium. Different combinations of salts, along with yeast extract and 4% glucose, were added to sterilized brackish water that had been collected. Wild-type *P. antarctica* was inoculated into various production media formulations and cultured over the course of four days. MEL production was observed in all groups, although a shift in MEL species was observed in the group with no KH_2PO_4 (**Fig. 5.2**). Specifically, there was a reduction in MEL-B and C, while there was a significant increase in MEL-D, and the amount of free fatty acids (FFA) was also significantly reduced (**Fig. 5.2**). This may be due to the difference in acetyl

groups between MEL-B/C and MEL-D. The feedstock used was glucose, which means that all the acyl-CoA and acetyl-CoA required for MEL synthesis had to be generated from the glycolytic metabolism, potentially limiting the availability of free fatty acids. However, this limitation was not observed in the control group or other samples, where there were spots on the TLC representing free fatty acids. It is suspected that the limitation of potassium or phosphate ions may be responsible for the reduced synthesis of free fatty acids. The limited availability of free fatty acids is then utilized in the synthesis of MELs, and there is no further acetylation of MEL-D due to the lack of free cytoplasmic acetyl-CoA. At the same time, we could not rule out the possibility that the limitation of potassium or phosphate is altering the activity of Mat1 acetyltransferase, resulting in either complete loss of acetylation or incomplete acetylation of MEL.

It is possible the potassium is limiting MEL production as the brackish water contains only 38 mg/L potassium, but phosphate could also be the limiting factor since the unsupplemented brackish water contains only 9.9 µg/L PO_4 (**Table 5.1**).

Additionally, the group with no addition of $NaNO_3$ showed a reduced amount of MEL production and secretion. This suggests that although nitrates are present in the brackish water sample, their concentration may not be sufficient to maintain the optimum C/N ratio for MEL production. The carbon sources were not analyzed to determine micronutrient, nitrogen or phosphate concentration and it is possible that some of the limiting nutrients may be provided from these sources. Nonetheless it is clear that magnesium can be omitted from the medium without a reduction in MEL biosynthesis but NO_3 or some other source of nitrogen must be supplemented.

Table 5.1. Water analysis of brackish water used in this experiment

Elements		Quantity	Unit
B	Boron	0.363	mg/L
Ca	Calcium	39.87	mg/L
Cu	Copper	0.002	mg/L
K	Potassium	38.868	mg/L
Mg	Magnesium	95.637	mg/L
Na	Sodium	788.371	mg/L
Ni	Nickel	0.001	mg/L
P	Phosphorus	0.015	mg/L
S	Sulfur	72.583	mg/L
Other			
PO4-P	Phosphate	9.890	µg/L
NO2-N	Nitrite	0.835	µg/L
NO3-N	Nitrate	45.85	mg/L
TOC	Total organic carbon	3.77	mg/L
TN	Total nitrogen	45	mg/L

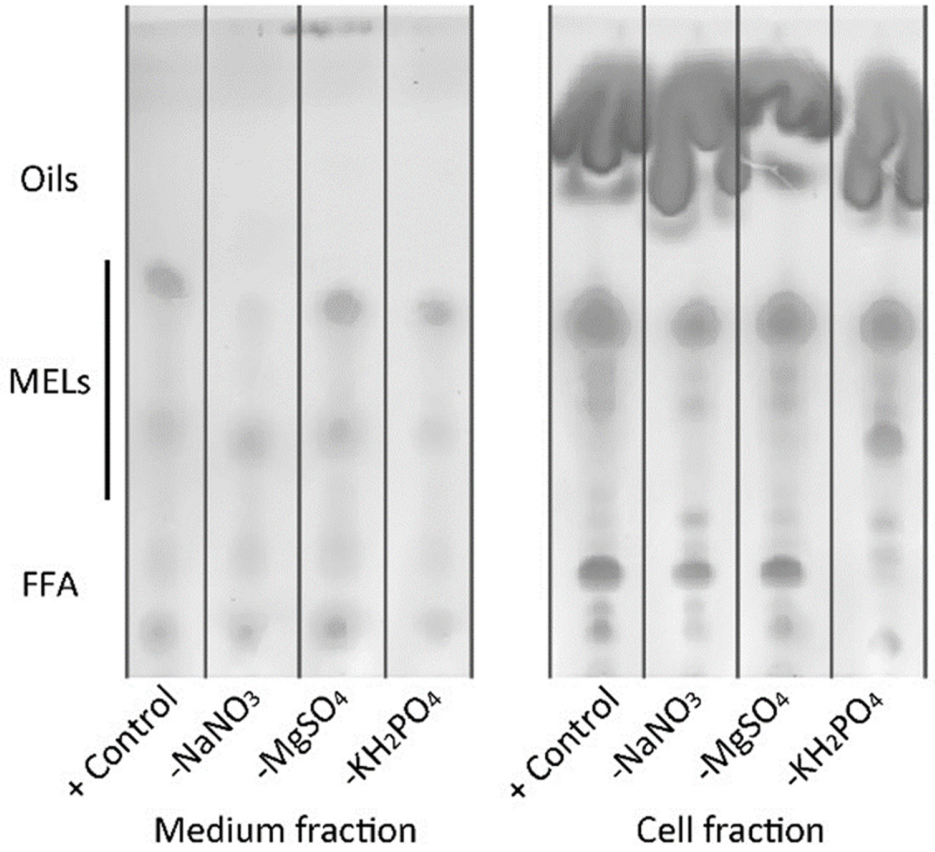

Figure 5.2 Thin-layer chromatography plate for MEL synthesis and secretion with subtraction of medium components (ions) using brackish water for medium. +Control: positive control with all ions supplemented; -$NaNO_3$: No addition of 0.3% $NaNO_3$; -$MgSO_4$: No addition of 0.03% $MgSO_4$; -KH_2PO_4: No addition of 0.03% KH_2PO_4; 4% glucose were used as carbon source.

5.3. Waste cooking oil is a reliable carbon source for MEL production with *P. antarctica*

To further investigate the potential to reduce the cost of MEL production, a study was performed to determine the suitability of waste cooking oil (WCO) as a carbon source for MEL production with *P. antarctica*. MEL production cultures were prepared with the standard MEL medium supplemented with either fresh canola oil or an equal amount of canola oil that had been extensively used for poutine preparation. The growth of *P. antarctica* in these two media was

monitored over seven days and at the completion of the experiment MEL was extracted from the culture (a sample that included the culture medium and the cells combined).

The shape of the growth curve was similar to that observed with glucose as the carbon source (**Fig. 5.3 A**). An initial growth phase followed by a plateau phase, and a second rapid growth phase. Interestingly, the second growth phase in the WCO group was initiated at around day 3, while the fresh canola oil group was delayed by 1 day (**Fig. 5.3 A**). This shortened delay may be explained by the presence of an elevated abundance of free fatty acids in the WCO culture (**Fig. 5.3 B**). The increased FFA concentration in the WCO sample may be attributed to hydrolysis of the triglyceride in the oil due to repeat high temperature treatments in frying and it is possible that some may originate in foods that were fried in oil. Without further analysis, samples of the oil prior to use and documentation of the foods that were cooked in the oil we cannot specifically determine the source of the elevated FFA. The *P. antarctica* cells may grow faster in the WCO supplemented medium since the FFA can be directly assimilated as a carbon source whereas the cells growing in fresh oil will need to rely on their secreted lipase to break down triglycerides in fresh canola oil before it can be absorbed, resulting in a delay of the second rapid growth phase.

Analysis of the total MEL produced after seven days of culture in the WCO and unused oil supplemented medium by TLC revealed that both carbon sources were effectively used and similar amounts of the MEL products were synthesized (**Fig. 5.3 B**). These observations suggest that WCO can be a low-cost and reliable carbon source for MEL production with *P. antarctica*. Overall, these findings suggest that waste cooking oil can be a promising alternative carbon source for MEL production.

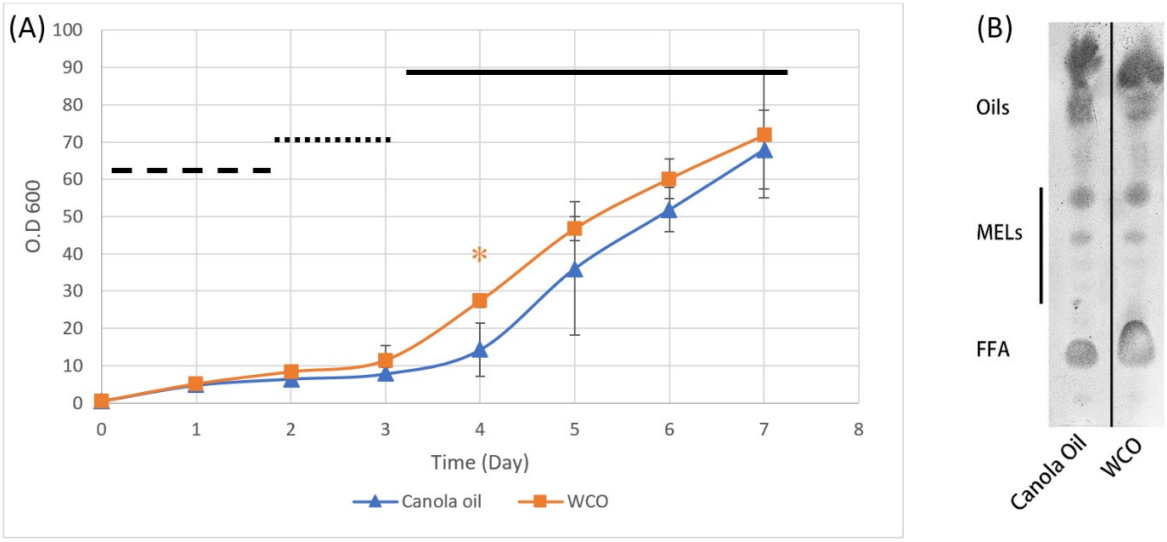

Figure 5.3 MEL production and growth curve of *P. antarctica* with waste cooking oil as carbon source. (a) *P. antarctica* growth curve in MEL production medium with distilled water and canola oil and waste cooking oil as carbon source, growth is measured with $O.D_{600}$. Dashed line: 1st rapid growing phase; dotted line: plateau phase; solid line: 2nd rapid growth phase. (b) Thin-layer chromatography of MEL total extract synthesis in MEL production medium with canola oil and WCO extracted on day 7. The significance to WT was determined with a t-Test (Two-Sample Assuming Equal Variances) and indicated by the * symbol with the corresponding color.

5.4. MEL production using unsterilized brackish water

P. antarctica displays a high tolerance for saltwater (**Fig. 5.1**). Since many microbial species are sensitive to high salt conditions, or rapid change in osmotic pressure, it seemed possible that unsterilized saline water could be used for MEL production without sterilization which contributes to the cost and energy use in this process. The brackish water sample collected from Iona beach was determined to have a conductivity of 5.2 mS/cm, corresponding to a salt concentration of 3640 ppm (~3.6 g/L); this is only about 0.1 times the concentration of salt measured in water collected from the open sea and less than 100 mM salt. As this low concentration of salt was unlikely to challenge the growth of contaminating microorganisms, NaCl was added to the unsterilized brackish water medium. The hypothesis behind this approach is that the sudden change in salinity would drastically alter the osmotic pressure, thereby preventing any bacteria present in the

unsterilized brackish water from growing. Waste cooking oil (WCO) was added as the alternative low-cost carbon source. Growth and MEL production by *P. antarctica* was investigated in these cultures with varying concentrations of added NaCl. In addition to monitoring MEL production, it was useful to determine if changing the salinity of the medium would inhibit the growth of competitive microorganisms naturally present in the brackish water, allowing *P. antarctica* to dominate and promote carbon assimilation and flow towards MEL production.

In the absence of added NaCl, bacteria in the brackish water could utilize WCO and outcompete *P. antarctica* (**Fig. 5.4 A**). However, when 0.3 M or 0.4 M NaCl was added to the water, bacterial growth was significantly inhibited (**Fig. 5.4 A**) After a prolonged incubation, contaminating microbes will outcompete *P. antarctica* even under these elevated salt conditions beyond day 7, resulting in an easily identifiable sticky gel-like medium, reducing MEL production. In contrast, adding 0.5 M or 0.6 M NaCl (the salt concentration of sea water) effectively inhibited bacterial growth and allowed *P. antarctica* to grow rapidly (**Fig. 5.4 A**). Analysis of MEL production from the culture (cellular fraction and medium fraction) was performed by TLC after a 10-day production period (**Fig. 5.4 B, C**). The amount and species of MEL produced were not significantly different between the sterilized brackish water (WCO) culture and the sterilized distilled water with canola oil (**Fig. 5.4B**). Little MEL could be detected in the cellular fraction of unsterilized unsupplemented brackish water (**Fig. 5.4 B**). This is consistent with the lack of accumulation of *P. antarctica* in this culture as it was rapidly overgrown by native microbes which presumable could deplete the available nutrients. TLC analysis demonstrated effective production of MEL in the brackish water samples that had been supplemented with 0.5 M and 0.6 M NaCl to inhibit the growth of the endogenous microbes (**Fig. 5.4 B, C**). Most of the MEL produced from the unsterilized water supplemented with 0.5 M and 0.6 M NaCl are within the cellular fraction (**Fig. 5.4 B**) and very little was detected in the medium fraction (**Fig. 5.4 C**). The yield of MEL within the cellular fraction was similar to control groups, indicating the MEL production was not significantly affected by the addition of NaCl.

Overall, these findings demonstrate that adding 0.5 M NaCl to unprocessed brackish water can effectively inhibit the growth of contaminating microorganisms, allowing *P. antarctica* to efficiently produce MEL from WCO without significant interference from bacterial competition.

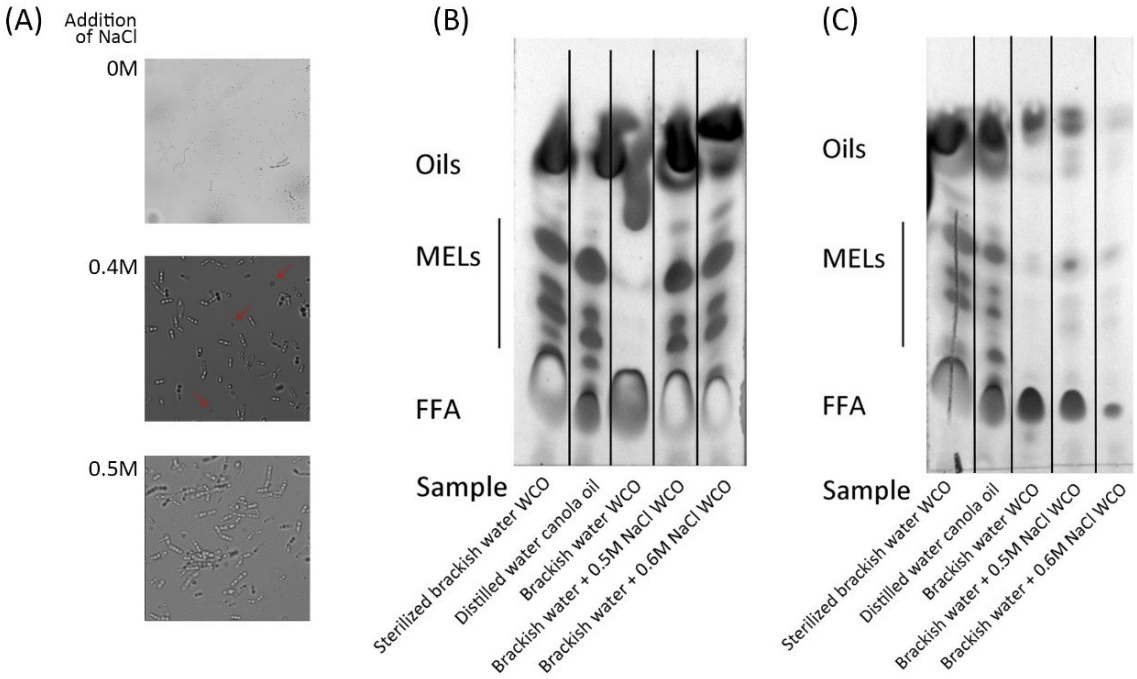

Figure 5.4 MEL production with *P. antarctica* JCM10317 strain using unsterilized brackish water and waste cooking oil. (a) Microscope image of brackish water with addition of NaCl at different concentrations, WCO was used as carbon source. Images were taken on day 6. Thin-layer chromatography of MEL production in cell fraction (B); and medium fraction (C) with brackish water and WCO with the addition of NaCl. Sterilized brackish water with WCO and distilled water with canola oil are positive control groups, and brackish water with WCO and no addition of salt is the negative control group. For experimental groups, 0.5 M and 0.6 M NaCl concentrations were tested. Samples for MEL analysis were collected after 10 days of culture.

5.5. Brackish water WCO production

In an industrial process the rate of product synthesis is an important consideration that influences cost and productivity. Figure 5.4 B shows that MEL can be synthesized in NaCl supplemented brackish water using WCO as a carbon source. The progress of MEL production in brackish water vs distilled water was compared at six and eight days of culture (**Fig. 5.5**). The experiment was conducted using a 10 mL culture with either brackish water supplemented with 0.5 M NaCl and

WCO as carbon source, or distilled water with fresh canola oil. Samples of the cellular fraction were collected and MEL extracted at day six, day eight, and day ten. The results showed that on day six, a large amount of MEL was detected in the distilled water group, whereas very little MEL was produced in the brackish water WCO culture (**Fig. 5.5 A**). One possibility to explain the delayed MEL production is that the increased osmotic pressure in brackish water with the addition of salt delayed the growth curve of *P. antarctica* relative to the distilled water culture, resulting in cells being at the plateau phase and very little MEL being produced (**Fig. 5.1 A**). On day eight, a very rapid increase in MEL content was observed in the brackish water group (**Fig. 5.5 B**). We hypothesize that cells entered the second rapid growth phase and due to the fact that WCO contains more free fatty acids, this supported faster growth and a rapid increase in MEL. These results suggest that adding salt to brackish water may delay the growth of *P. antarctica* initially, but eventually, it can support MEL production similar to distilled water and that WCO can be a potential low-cost carbon source for MEL production.

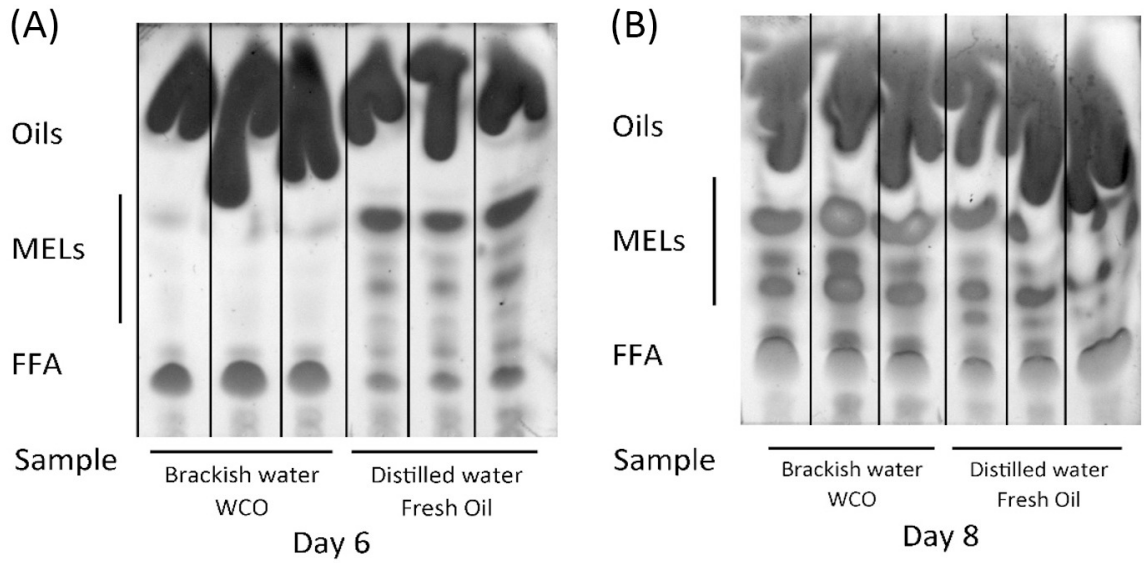

Figure 5.5 Thin-layer chromatography of MEL production with brackish water and waste cooking oil at day 6 and day 8 of production. The production medium was unsterilized brackish water and WCO with the addition of 0.5 M NaCl vs distilled water with fresh canola oil, MELs were extracted from the cellular fraction at (a) day 6; (b) day 8. Samples are in biological triplicates.

5.6. Mechanical lysis is not necessary for MEL extraction

In the previous MEL extraction method, the whole culture was subjected to either freeze-drying or mechanical lysis, followed by ethyl acetate extraction [4][5][6]. However, in brackish water with 0.5 M NaCl, MELs are not secreted and remain within the cells. To investigate the efficacy of MEL extraction with and without mechanical lysis, glass beads were added during the extraction process of cultures grown in brackish water with WCO for 10 days. The crude extracts were analyzed using TLC (**Fig. 5.6**). There were no significant differences in MEL species and yield, as well as FFA and oil content between samples with and without mechanical lysis. Therefore, it can be concluded that mechanical lysis is not necessary for MEL extraction. This is likely due to the fact that the use of ethyl acetate is sufficient to solubilize the cellular membranes and vacuoles, releasing MEL into the organic solvent phase.

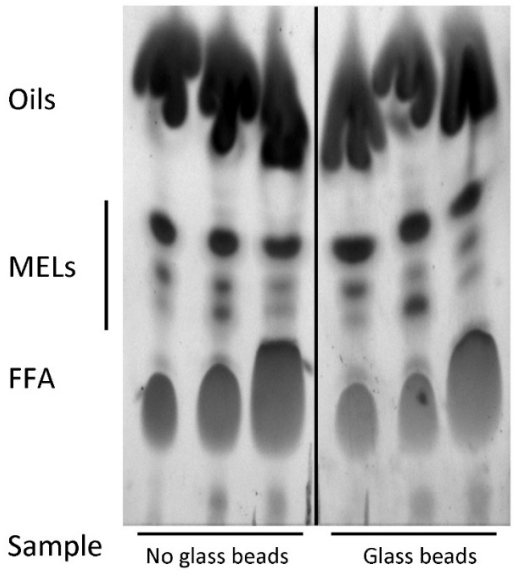

Figure 5.6 MEL extraction with or without mechanical lysis. Thin-layer chromatography of MEL samples fermented from WCO and brackish water, extracted with/without glass beads mechanical lysis. The samples are in biological triplicates.

5.7. Purification of MEL with silica column

MEL extracted from cell cultures or culture medium is a crude material contaminated with other hydrophobic cellular components. This is particularly an issue when MEL is extracted from an

unsterilized culture that may contain microbial species other than the MEL producer strain. To investigate whether MEL could be purified from other contaminating molecules, a silica gel chromatography method was tested. An experiment was performed with crude MEL extracted from *P. antarctica* cultured in brackish water with waste cooking oil (WCO) as a carbon source was tested and compared to MEL produced in distilled water with canola oil. The cultures were incubated for 10 days. Total culture, 10 mL (cells and medium) were collected, and the ethyl acetate extracts were applied to a silica gel column for purification.

Analysis of the chromatography fractions showed that both oil and free fatty acids were mostly eluted in the first 18 fractions, while MELs were eluted from fraction 20 onwards. Among the MEL species, MEL-A with the most hydrophobicity was eluted first, followed by MEL-B and MEL-C (**Fig. 5.7 A, B**). The oil, triglyceride, FFA and phospholipid can be largely separated from the MEL species although some of these contaminants do cofractionate with the MEL A species in fractions 20, 22 (**Fig. 5.7 A, B**).

Comparison between the brackish water with WCO and distilled water with canola oil showed that there were significantly more free fatty acids in the WCO samples from fractions 8 to 12. This was expected, as the WCO material had been subjected to repeated high temperature cooking applications that could be anticipated to induce hydrolysis of some portion of the triglyceride content. From fractions 12-18, the spots representing oil in the WCO groups were more complicated than in canola oil, which could be due to hydrolysis. Additionally, there were two spots in the free fatty acid region on the lower sections of the TLC plates that may represent hydrolyzed or modified fatty acid species. The identity of these species was not further investigated.

The chromatography fractions containing MELs (fractions 20-36) were pooled for both the brackish water with WCO and distilled water with canola oil samples. The MEL species were analyzed by fractionation on a TLC plate and detection with orcinol-H_2SO_4 reagent (**Fig. 5.7**). It is notable that the MEL species enriched from brackish water (WCO) are not significantly different from the species enriched from distilled water (canola oil) (**Fig. 5.7 C**). The final MEL yield from the brackish water with WCO culture was measured at 3.15±0.68 g/L after 10 days of culture, slightly lower than the control yield of 3.85±0.35 g/L isolated from distilled water with fresh canola oil. These results suggest that MEL production in brackish water with WCO can be purified

to produce similar MEL species as the traditional method, and the yield is slightly lower but still acceptable.

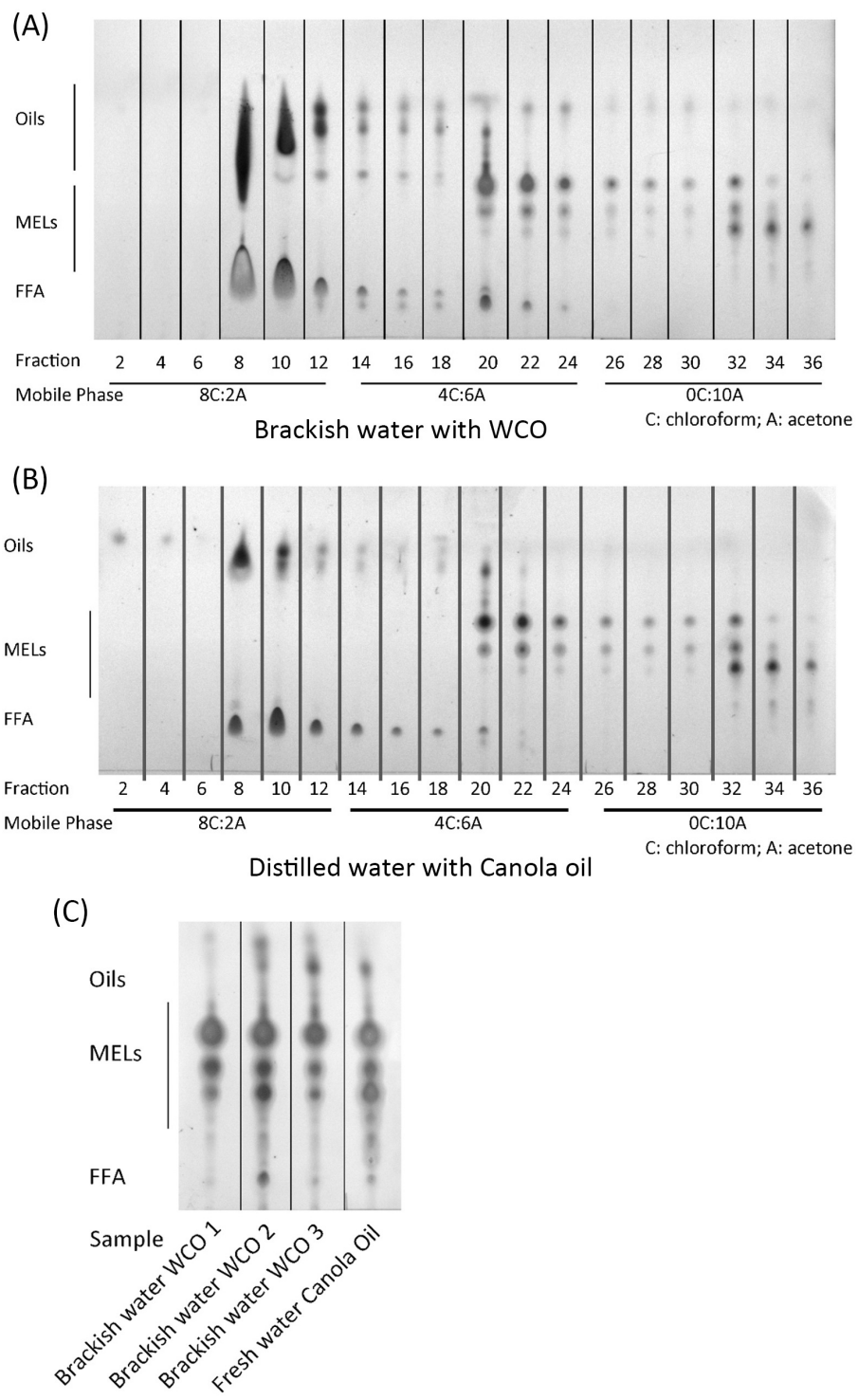

Figure 5.7 Silica gel liquid column purification of MEL produced from brackish water WCO production. Chromatography profile of MEL extracted from production with (a) brackish water with WCO and 0.5 M NaCl addition; (b) distilled water with canola oil for 10 days. Every 2 fractions were sampled and visualized with thin-layer chromatography (c) Thin-layer chromatography of purified MEL samples from brackish water (biological triplicates) and distilled water production. Glycolipids were visualized with orcinol-H_2SO_4 reagent.

Chapter 6

6. Discussion

6.1. General Summary

The work presented in this thesis demonstrates that the protein encoded by *PaMMF1* in the JCM10317 strain is necessary for the secretion of di-acylated MEL-A/B/C when the cells are utilizing water-soluble carbon sources. In this study, an unidentified species of MEL was found in both the cellular and medium fractions of the *MMF1 KO* strains.

P. antarctica JCM10317 has great potential as an industrial strain for the production of biosurfactant but little has been done to investigate conditions for strain engineering or the development of tools to modify the strain. In this study, conditions for effective transformation were developed with an emphasis on investigating optimal temperature conditions. Additionally, DNA cassettes with a suitable selectable marker were developed and it was determined that gene deletion by homologous recombination could be achieved.

To take advantage of the natural salt tolerance of this strain, it was demonstrated that JCM10317 could produce MEL with unsterilized brackish water as a production medium, with waste canola cooking oil as a carbon source. The fermented MEL obtained via the production of waste cooking oil and unsterilized brackish water can be purified using the standard silica liquid chromatography method. The purified MEL has a similar thin-layer chromatography profile to that of the MEL obtained from a sterile bioreactor culture using distilled water, defined nutrients and fresh refined canola oil.

6.2. *Pa MMF1* KO

6.2.1. *Pa MMF1* is necessary for MEL secretion in water-soluble carbon sources

The *Pa MMF1* gene has been found to play a crucial role in the secretion of mannosylerythritol lipid into the extracellular space in the JCM10317 strain (**Fig. 4.4**). This finding is a critical difference from previous research on *P. tsukubaensis,* and may be due to the existing selective pressure imposed by the environment. Specifically, the need for MEL secretion may not be present when the strain is growing in the presence of a water-soluble carbon source. In contrast, when

using plant-derived oil as a carbon source, the MELs play a crucial role in emulsifying these hydrophobic molecules. Such selective pressure may facilitate the extracellular production of MEL in an *MMF1*-independent mechanism such as lysis of some cells, or exocytosis. This study supports the hypothesis that at least for JCM10317, *MMF1* is necessary for MEL secretion, regardless of the type of carbon source used.

6.2.2. JCM10317 *MMF1* knockout exhibits normal growth rate and total MEL synthesis

The knockout of the *MMF1* gene resulted in the inhibition of MEL secretion and increased accumulation of MEL within the cell (**Fig. 4.4**). In the *P. tsukubaensis* strain, the total MEL production was significantly reduced in the *Pt MMF1* knockout compared to the wild-type strain and there was almost no accumulation of MEL in the cellular fraction. The researchers hypothesized that the intracellular accumulation of MEL could potentially damage the cells membranes or disrupt internal structures, leading to the halt of MEL synthesis to protect the cells from damage due to the accumulation of secondary metabolites. No mechanism for the control of MEL synthesis by product inhibition has been defined. However, in the JCM10317 strain, the growth rate of the *MMF1* knockout strain was not significantly affected compared to the wild-type strain (**Fig. 4.5**), and the amount of MEL in the cellular fraction of the knockout was equal to or more than that of the wild-type strain (**Fig. 4.4**). These results suggest that the rate of MEL synthesis was not significantly affected in JCM10317 *MMF1 KO*. The reason could be differences in the regulation of the MEL biosynthesis cluster and the mechanism of intracellular storage of MEL, but neither of these processes have been fully characterized.

In a previous study investigating the MEL producer, *Pseudozyma rugolosa* [119], Nile red staining with fluorescent microscopy were performed to examine the intracellular accumulation of lipids. When grown with glucose as the carbon source, lipid particles were observed inside the cell, forming a "peas in a pod" like structure under the microscope. In future experiments, we could analyze the difference between the number and size of lipid bodies in the wild-type *Pseudozyma antarctica* JCM10317 and *MMF1* knockout strains to investigate the difference in MEL intracellular accumulation. Additionally, we can compare the changes in lipid bodies between JCM10317 and *P. tsukubaensis* in wild-type and *MMF1* KO strains to understand the differences

in the mechanism of MEL accumulation.

In addition to the previous findings, a significant difference in the yield of MEL was observed between the *MMF1* KO strains of *P. tsukubaensis* and JCM10317. Specifically, the *P. tsukubaensis MMF1* KO strains produced significantly less MEL compared to their respective wild-type strains, while the JCM10317 strain did not exhibit a significant decrease in MEL production. This observation suggests the possibility of differences in the regulation of MEL biosynthesis pathways in the two strains. It is possible that a feedback mechanism involving the intracellular accumulation of MEL may be interfering with the activity of the MEL biosynthesis pathway. To further elucidate this difference, quantitative RT-PCR analysis can be performed on the MEL biosynthesis genes in *MMF1 KO* strains. This analysis can provide valuable insights into the difference in MEL biosynthesis gene regulation, and the regulatory role of *MMF1* in MEL biosynthesis. A more extensive investigation of this issue should make use of a more global gene expression analysis by RNAseq to identify changes to gene expression beyond the MEL biosynthesis genes to gain insight into potential gene regulatory mechanisms. Additionally, although it is more challenging, a proteomic analysis comparing wild-type and *MMF1* KO cells may provide more relevant information than could be obtained from the RNA analysis.

6.2.3. Decreased monoacetylated MEL species in *MMF1 KO* strain

In the *MMF1* KO strain, the MEL species in the cellular fraction display a shift towards more hydrophobic MEL-A in all three different cultivation conditions (**Fig. 4.4**). One possible explanation for this shift is the accumulation of monoacetylated MEL-B/C in the cell, leading to increased time and substrate availability for the acetyltransferase Mat1 to interact and acetylate the MEL-B/C. This would lead to an increase in the conversion of monoacetylated MEL-B/C to more hydrophobic MEL-A through the action of Mat1. To further validate this hypothesis, a potential experimental approach could be the utilization of metabolic tracing with C^{14} radioisotopes. By incorporating C^{14}-labeled precursors into the metabolic pathway, the dynamics of MEL synthesis and subsequent modifications could be monitored in the MMF1 KO strain.

This shift toward more hydrophobic MEL-A was not observed in the previous study on *P. tsukubaensis MMF1 KO*. This may be because the *P. tsukubaensis* strain only produces MEL-B and does not produce MEL-A, likely due to the specific activity of *Pt* Mat1.

6.2.4. Identification and hypothesized pathways of a novel MEL species in *MMF1 KO* strain

In the JCM10317 strain carrying *MMF1 KO*, a novel spot was detected on TLC plates loaded with samples from both intracellular and extracellular fraction (**Fig. 4.4**). Since this spot moves slower on the TLC plate, it suggests that it's less hydrophobic. Also, because it doesn't show up in the EMT1 KO lane (**Fig. 4.4 E**), which stops all MEL production, we believe it's a different type of mannosylerythritol lipid. In previous research on *P. tsukubaensis*, a similar finding was made, and LC-MS analysis of the less hydrophobic spot demonstrated it to be mono-acylated MEL-B [31]. Since JCM10317 preferentially produces MEL-A, we suspect that the unknown staining may represent mono-acylated MEL-A. For *P. antarctica* T-34 strain, when cultivated in excess glucose, an even less hydrophobic MEL, was discovered on TLC and HPLC, and was later identified as mono-acylated MEL-D in the previous research [10]. Upon comparing their HPLC data with our own, it was observed that the mono-acylated MEL-D obtained from their analysis corresponds to the last peak in our HPLC profile (**Fig. 4.6**, retention time: 5.183-5.195), further supporting the suspicion that the unknown spot in JCM10317 may be mono-acylated MEL-A, a slightly more hydrophobic MEL species. In *P. tsukubaensis*, di-acylated MEL-B was the only product from wild-type cells. Thus, there are two possible ways to produce mono-acylated MEL-B. The first is to synthesize di-acylated MEL-B, then de-acylate by unknown esterase, forming mono-acylated MEL-B; this will be referred as unknown esterase pathway. The second is to convert mannosylerythritol to mono-acylated MEL-D, then directly to mono-acylated MEL-B by *Pt* Mat1, this will be referred to as bypass Mac2 pathway.

The pathway for the production of this novel MEL species in JCM10317 is still unknown, however, I personally favor the unknown esterase pathway, where all mannosylerythritol in wild-type JCM10317 growing in glucose are first acylated by *Pa* Mac1 and *Pa* Mac2 acyltransferase, forming di-acylated MEL-D. Mat1 then acetylates MEL-D, forming MEL-A/B/C, and since there is a limitation of acyl-CoA when utilizing glucose as the sole carbon source, some acyl tails are stripped by an unknown esterase from the di-acylated MEL, leading to the production of mono-acylated MEL. This model is consistent with the unaltered activity of both acyltransferases Mac1 and Mac2 in the *MMF1* KO experiment. In *MMF1* KO of the JCM10317 strain, the transporter of di-acylated MEL was disrupted, leading to an accumulation of di-acylated MEL-A/B/C within the

cell. This resulted in more time for the unknown esterase to de-acylate the di-acylated MEL, resulting in an increase of mono-acylated MEL (**Fig. 6.1**) However, several factors need to be tested in future experiments to confirm this hypothesis, including whether the unknown spot is mono-acylated MEL-A and whether an unknown esterase is involved in the process.

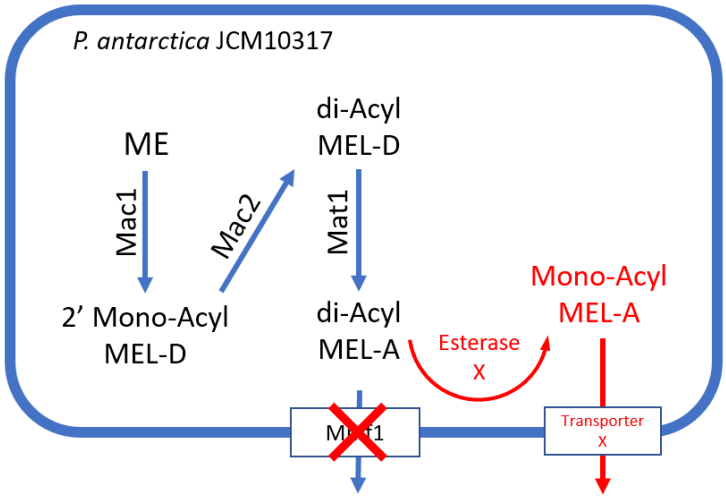

Figure 6.1 Proposed pathway for the synthesis of unknown MEL. ME: Mannosylerythritol; 2' Mono-Acyl MEL-D: 2' mono-acylated MEL-D; Di-Acyl MEL-D: di-acylated MEL-D; Di-Acyl MEL-A: di-acylated MEL-A; Mono-Acyl MEL-A: mono-acylated MEL-A; Esterase X: unknown esterase; Transporter X: unknown transporter

Investigating the specificity of Mat1 in the *P. antarctica* JCM10317 strain could provide valuable insight into distinguishing between the first and second pathways of synthesizing mono-acylated MEL. Specifically, if Mat1 selectively recognizes only di-acylated MEL-D, then the first pathway is likely responsible for the production of mono-acylated MEL, which involves an unknown esterase deacylating the di-acylated MEL-A. On the other hand, if Mat1 recognizes both mono-acylated and di-acylated MEL-D, the pathway for the production of the unknown species of MEL remains unknown.

The disruption of the transporter due to the *Pa MMF1* gene knockout led to the production of an unknown glycolipid species. One possible reason for this could be that the unknown glycolipid is less hydrophobic, which could lead to reduced cellular stress in the event of disrupted secretion,

thus diacylation is favored. Another possibility is that the accumulation of MELs within the cell led to an increased retention time for the unknown esterase to interact with MEL-A, which in turn resulted in the production of the unknown species. To further investigate these possibilities, a transcriptome analysis can be conducted to determine if gene expression is affected. In the case of an unknown esterase being involved, its expression might be upregulated. Alternatively, if a bypass pathway is responsible, the *MAC2* expression could be downregulated. Furthermore, the study found that *MMF1* knockout did not disrupt the secretion of the unknown MEL. This suggests that a different mechanism might be responsible for secreting the less hydrophobic variant of MEL. There are two possible explanations: (1) The unknown variant of MEL may not require a transporter to be secreted and may instead diffuse freely through the cell or be released through exocytosis. (2) A different type of transporter (Transporter X) may be involved in secreting the unknown variant of MEL (**Fig. 6.1**). Never the less, considering the nature of MEL is a biosurfactant, and excess accumulation can lead to many problems to the cell such as membrane disruption, osmotic imbalance, and cytotoxicity, it would be logically correct for the cells to modify such molecule and secrete them in alternative mechanism to reduce damage to the cell.

6.3. Transformation & homologous recombination efficiency of JCM10317

6.3.1. Optimization of transformation efficiency by elimination of the heat shock step.

In yeast transformation, the role of the heat shock step is to increase permeability and allow DNA to pass through the cell wall, thus increasing transformation efficiency. Transformation of *P. antarctica* GB-4(0) strain, another MEL producer, using the LiAc-PEG mediated method was similar to the established *S. cerevisiae* transformation protocol: the cells were heat shocked at 42 degrees for 5-60 minutes before chilling on the ice [122]. However, this method resulted in very low transformation efficiency in JCM10317. As mentioned, a critical difference between those two strains is that the GB-4(0) strain was initially isolated in Japan [124]. In contrast, the JCM10317 strain was isolated from the lake sediment in the Antarctic, so there might be a crucial difference in the optimal temperature range for growth and survival. Heat tolerance was tested on the JCM10317 strain, and it was determined that it could not tolerate temperatures greater than 37 °C for a prolonged time. By adjusting the heat shock temperature to 30 degrees, the transformation efficiency can reach up to 74.5CFU/μg DNA. No experiments were performed to

investigate the mechanisms that impose thermosensitivity on *P. antarctica*, but possibilities include a less robust system of heat-shock response proteins or a membrane composition that is not conducive to tolerating the increased fluidity induced by the elevated temperature.

6.3.2. Homologous sequences of 1kb or greater are required for efficient homologous recombination

In the context of a transformation/gene knockout study targeting *Pa EMT1* and *Pa MMF1*, a difference in homologous targeting efficiency was observed. In the *EMT1* knockout experiment, a PCR-amplified fragment with 1.1 kb of the homologous arm at each end was used, resulting in two out of eight transformed candidates being confirmed as *EMT1* knockout. On the other hand, in the *MMF1* knockout experiment, a fragment with 1.1 kb homology on the 5' end and 640 bp on the 3' end was used, resulting in a total of 15 candidates with hygromycin resistance, but only one sample was confirmed to have a complete replacement of the targeted gene. Although the sample size was small and the result was inconclusive, there may be a correlation between the length of the homologous arm and the homologous targeting efficiency.

In a previous experiment using CRISPR-Cas9 targeted gene replacement with homologous recombination in *P. antarctica* GB-4(0) strain, the targeting efficiency was found to increase from 7% with 0.5kb on each end to 32% with 1 kb homologous arm on each end [123]. This suggests that homologous recombination in the *P. antarctica* GB-4(0) strain is sensitive to the length of the homologous arm. To explore the correlation between homologous arm length and targeting efficiency in the JCM10317 strain, additional investigations could be performed by utilizing primers to amplify fragments with varying homologous arm lengths, ranging from 1.5 kb to 0.5 kb, from the YEplac195-*EMT1*::[Hyg] plasmid. The targeting efficiency could then be evaluated for each fragment, thus identifying any associations between arm length and targeting efficiency. This study should provide valuable information for the requirements for a efficient genetic modification experiment in the future.

6.4. Brackish water MEL production with JCM10317 strain

6.4.1. Summary

In this experiment, we demonstrated the possibility of utilizing unsterilized brackish water as a production medium and waste cooking oil as the carbon source to ferment mannosylerythritol lipid with the *P. antarctica* JCM10317 strain. The resulting final product is purifiable with liquid chromatography and demonstrated similar MEL profile to conventional method of production.

Biosurfactants are still relatively rare and expensive and have only taken a very small share of the surfactant market. The primary reason is the cost of the fermentative process, including water processing, sterilization, and feedstock. Currently, the commercially deployed MEL production uses food substances such as vegetable oil and olive oil as feedstock, which may aggravate the food crisis. The use of non-food substrates, such as waste cooking oil, and non-potable brackish water, could be a game-changer in the biosurfactant industry. With cost being one of the primary limitations for biosurfactants currently, this process has the potential to bring down the price and make biosurfactants a more attractive option for industries. Additionally, utilizing waste products rather than food crops as feedstock can help mitigate concerns about food crisis, and make use of a byproduct that ultimately becomes nuisance waste that becomes costly to dispose of. The possibility of lowering the cost and utilizing sustainable resources would make biosurfactants a more attractive alternative to traditional surfactants, opening up a wider range of applications in various industries.

6.4.2. MEL can be effectively produced in brackish water supplemented with waste cooking oil

The use of brackish water in MEL production has not been extensively studied, but the results of this study suggest that it could be a viable option for future research.

One potential advantage of brackish water in MEL production is its abundance in coastal areas, which can be obtained at relatively low costs. Brackish water is an underutilized water source and has fewer applications than freshwater. It is not intended for drinking, meaning that it does not have to compete with drinking water resources for use in production processes. Another potential advantage is that the production process demonstrated in this study does not require sterilization, which can save a significant amount of money on the energy required for sterilization, and the infrastructure necessary for sterile production. In addition, the process of adding NaCl to inhibit

bacterial growth in brackish water is sustainable and easy to operate. NaCl is non-toxic, readily available at a low cost, and does not cause pollution after production.

Using WCO as an alternative to food-related substances also has important implications for sustainability. First of all, by using a waste product instead of a food crop as a feedstock, this study demonstrates a more environmentally friendly approach to biosurfactant production. This approach has the potential to ease concerns about the use of food crops for non-food purposes and contribute to a more sustainable future for the industry. Secondly, this experiment demonstrated that WCOs could be directly added to the fermentative medium without any pre-treatment. This process can convert a waste product into a value-added product, further contributing to sustainability efforts. Additionally, using WCOs saves the costs and effort of processing those oils, leading to more efficient use of resources.

Utilizing brackish water and waste cooking oil for biosurfactant production represents a promising way to a more sustainable and economical production process. Further research needs to be conducted to fully understand the impact of using brackish water and waste cooking oil on the MEL production process and the quality of the final product.

6.4.3. MEL yields from brackish water cultivations can be further optimized

This study is preliminary and has not fully considered yield optimization. However, the MEL yield in brackish water with waste cooking oil (WCO) can be further improved to achieve a more efficient production.

MEL production was found to be most efficient during the stationary phase; however, achieving stationary phase production of MEL in this situation is not possible. In our experiment using brackish water with 0.5 M of salt and *P. antarctica* cells, when the *P. antarctica* culture reaches the stationary phase, the bacteria will outgrow yeast in a few days, leading to a significant decrease in MEL yield. Nevertheless, the yield of brackish water production can be increased through other methods, such as adjusting the pH, pretreating the WCO, pretreating the brackish water, and adjusting the supply of micronutrients in the culture medium.

The initial pH of the culture is a crucial factor in the production of biosurfactants such as MELs.

Previous studies on MEL production have suggested that the optimal pH range is slightly acidic, preferably between 5.5-7. In our brackish water sample, the initial pH was measured at 7.58, slightly above the preferred range. To further improve the yield of MELs in brackish water production, buffering the pH to a more optimal range may be necessary.

Waste cooking oil contains degradation products from the repeated high temperature treatment of the oil. These may impact the yield of MEL. Previous studies have shown that treating WCO with activated earth and charcoal can significantly reduce the peroxide value. For example, in the production of rhamnolipids with *Pseudomonas aeruginosa* ATCC 10145, the pretreatment of WCO in such a manner resulted in a 2.2-fold increase in growth and a 2.7-fold increase in rhamnolipid yield, with a final yield of 7.51 g/L in 96 hours [94]. It is assumed that reducing the peroxide value in WCO can also aid in the faster growth of *P. antarctica*, leading to an increase in MEL yield.

In addition to the listed micronutrient salts, some studies have suggested that adding additional micronutrients, such as manganese and copper, can significantly increase MEL yield. For example, Fan et al. demonstrated that by replacing the nitrogen source with peptone at 4 g/L and adding 2 g/L of manganese sulfate and 0.4 g/L of copper sulfate to the basic MEL production medium, MEL yield was increased by 1.4-fold with *Pseudozyma aphidis* ZJUDM34 using soybean oil as the carbon source [95]. In our brackish water sample, there were very few copper ions and no manganese ions detected. An increase in MEL yield might be achieved by adding these ions while adding little cost.

6.4.4. Applications of MELs from brackish water

Mannosylerythritol lipids produced from the production of brackish water and waste cooking oil may not be as competitive in the cosmetic market due to their low cost and origin from "dirty" resources. However, they can be utilized in other industrial applications that require MELs on a large scale.

Ice slurry systems are a type of cooling technology that utilizes a mixture of ice particles and a liquid medium, which can be transported through pipelines, and wildly used in commercial air conditioning systems, but ice agglomeration can lead to complications such as blocked pipes,

decreased efficiency, and instability. MEL-B, added to the system at a low concentration of 10 mg/L, was found to be effective in preventing ice agglomeration by being absorbed onto the ice surface [88]. This method has been successfully demonstrated in small scale systems, outperforming traditional additives that require high concentrations (>10%).

MELs have been demonstrated to exhibit excellent antimicrobial activity against gram-positive bacteria. Recent studies have shown that MELs produced from *Pseudozyma aphids* are highly effective against *Staphylococcus aureus* ATCC 6538 by disrupting biomass, reducing metabolic activity, and exhibiting bactericidal effects on mature biofilm after 24 hours without harming human keratinocyte cells [13][127]. This property is particularly valuable in settings such as hospitals, where traditional antimicrobial agents are becoming less effective. Considering these properties, the possibility of integrating MELs as a key ingredient in the development of novel surface disinfectants should be explored in the future.

Overall, cheaper MEL production can expand the range of applications in situations that require large quantities at a lower price.

Chapter 7

7. Future directions

7.1. Investigating the synthesis of mono-acylated MEL:

Mat1 is an acetyltransferase that plays a crucial role in the biosynthesis of MELs in *P. antarctica* JCM10317. It is responsible for acetylating MEL-D to form the more hydrophobic MEL-A/B/C. However, the specificity of *Pa* Mat1 in recognizing its substrates is still unclear, and this has implications for understanding the pathway of synthesizing mono-acylated MEL in the JCM10317 strain with *MMF1 KO*. If *Pa* Mat1 selectively recognizes only di-acylated MEL-D, then the pathway, in which di-acylated MEL-B is first formed and then de-acylated by an unknown esterase to form mono-acylated MEL-B, is likely responsible for the production of mono-acylated MEL (**Fig. 7.1 A)**. In contrast, if Mat1 recognizes both mono-acylated and di-acylated MEL-D, then the pathway for the production of the unknown species of MEL remains unknown. To explore the specificity of Mat1 in the JCM10317 strain, future experiments could involve creating gene knockouts of either Mac1 or Mac2 in *MMF1* KO background and analyzing the resulting changes in MEL synthesis and acetylation. This could be accomplished by generating Mac1 or Mac2 knockout strains using homologous recombination knockout and comparing the MEL profile of *Δmmf1 Δmac1* or *Δmmf1 Δmac2* double mutant to the wild-type strain and *MMF1* KO strain. If the double mutant still produces mono-acylated MEL-A, it would suggest that Mat1 recognizes both mono-acylated and di-acylated MEL-D, and there is no requirement for the esterase X for the synthesis of mono-acylated MEL-A (**Fig. 7.1 B**). On the other hand, if knockout strains only produce mono-acylated MEL-D, it would suggest that Mat1 selectively recognizes di-acylated MEL-D, thus the mono-acylated MEL-A must be derived from di-acylated MEL-A with an unknown esterase (**Fig. 7.1 A**).

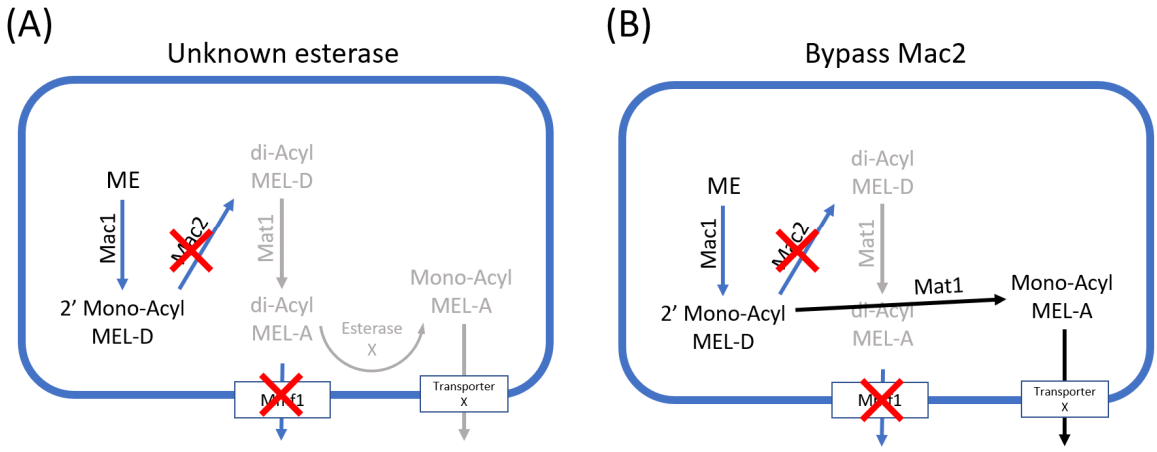

Figure 7.1 The MEL biosynthesis schematic of proposed *MMF1 MAC2* double mutant study. (A) Unknown esterase pathway: Mat1 does not recognize mono-acylated MEL, there will be no production of mono-acylated MEL-A. (B) Bypass Mac2 pathway: Mat1 recognize mono-acylated MEL, there will be synthesis of mono-acylated acetylated MEL-A, there is no requirement for unknown esterase in this pathway. ME: Mannosylerythritol; Mono-Ac MEL-D: mono-acylated MEL-D; Di-Acyl MEL-D: di-acylated MEL-D; Di-Acyl MEL-A: di-acylated MEL-A; Mono-Ac MEL-A: mono-acylated MEL-A. Esterase X: unknown esterase. Transporter X: unknown transporter.

The secretion of the presumed mono-acylated MEL appears to be independent of the Mmf1 transporter, as shown by unchanged secretion of unknown MEL in *MMF1* knockout strains in JCM10317. It is possible that an alternate transport mechanism exists for mono-acylated MEL (**Fig. 7.1**). Mmf1 belongs to the major facilitator superfamily transporters, and MFS transporters are known to accommodate a wide range of substrates, including sugars, amino acids, organic acids, and ions. Bioinformatic studies can be conducted to identify such transporters. A genome-wide alignment could be performed based on the *MMF1* gene sequence or protein sequence to locate proteins with similar sequences. Homologs of such candidates that already have assigned functions in other species could then be removed from the potential candidates. Finally, knockout studies could be conducted in the *MMF1* knockout background strain to identify which transporter impact the secretion of mono-acylated MEL.

The MEL gene cluster is conserved in many MEL-producing species, including distantly related

species outside the *Ustilaginaceae* family of yeast [22][23][116]. This suggests the possibility of horizontal gene transfer, similar to other gene clusters involved in secondary metabolites. We can transfer the MEL genes into other yeast species, such as *S. cerevisiae*, which is a convenient model organism for genetic manipulation. This can be achieved by constructing MEL gene cassettes with *S. cerevisiae* inducible promoters and selectable markers on a plasmid. Simulated knockouts can be generated by controlling the plasmid that the gene is carried on, as well as the promoter inducer. The precursors required for MEL biosynthesis could either be supplied from the medium or generated by introducing the corresponding biosynthesis genes. This approach provides a powerful tool to investigate the biological processes of MEL biosynthesis and broaden our understanding of secondary metabolite gene clusters.

7.2. Optimizing MEL production conditions in brackish water & WCO

Optimization of production conditions is a crucial aspect of developing a viable biosurfactant production process. This can involve exploring the effects of various parameters such as pH, temperature, water treatment and WCO treatment on MEL production yields. Additionally, we should also explore the possibility of increasing MEL yield by adding secondary water-soluble carbon sources.

One potential experiment to optimize production conditions could involve JCM10317 strain MEL production at different pH levels. A preliminary experiment could involve using brackish water and WCO and a range of pH levels, ranging from 5.0 to 7.0, and observing the effects of each level on MEL production yields. If acidic conditions are preferred for MEL production, acidic nitrogen sources such as ammonium chloride can be used for nitrogen supply while maintaining acidic condition. A similar test with ranges of production temperature can also be done to determine the optimum production temperature for JCM10317 strain.

Flocculation is the process of aggregating suspended particles into larger clusters or masses that can be easily removed. This process involves adding flocculants such as aluminum sulfate that cause the small particles to group together and form larger, more visible clumps that can be easily removed. In a previous study with the addition of 6-15 mg/L aluminum sulfate, over 95% of the culturable bacteria was removed from lake water [121]. According to current market prices, aluminum sulfate costs approximately 240 US dollars per ton [125], while water treatment costs

0.6 cents per ton, or 6 dollars per thousand tons of brackish water at the maximum concentration of 25 mg/L for water flocculation. In the context of MEL production, adding flocculants to brackish water can potentially remove most of the bacteria from unsterilized brackish water, thus increase the production time, leading to increased MEL yield through stationary phase production; or lower the NaCl required to inhibit bacterial growth, thereby reducing overall production costs. Moreover, implementing flocculation techniques in the MEL production process could potentially contribute to more efficient utilization of brackish water resources if stationary phase production is achieved. However, the effects of aluminum salts on MEL production of JCM10317 strain require further investigation.

Untreated WCO may contain degradation compounds and peroxides that can negatively impact MEL yield. To improve the yield of MELs during production, one potential experiment could involve treatment of WCO with activated earth and charcoal and evaluating its effects on MEL production yields. Treating WCO with activated earth and charcoal could effectively remove impurities and degradation compounds, potentially enhancing the quality of the feedstock and ultimately resulting in higher MEL production yields.

WCO is a suitable substrate for the lipid tail of MEL production due to its high content of hydrophobic carbon. However, gluconeogenesis pathway is needed to produce sugar moiety that is required for MEL synthesis, which can limit the rate of MEL production. To address this issue, several previous experiments have suggested that the addition of molasses to the production process can be advantageous. Molasses contains high amounts of sugars and micronutrients, consisting of nitrogen and metal ions, which aid and supplement the MEL production process. An experiment conducted with *P. aphidis* using soapstock and molasses without other micronutrients recorded a high yield of up to 90 g/L MEL [104]. Replacing yeast extract and other purified salts with molasses can further reduce the cost of MEL production and may lead to a higher yield when used with waste cooking oil as primary carbon source. In summary, incorporating molasses into the MEL production process can potentially enhance the product yield and reduce production costs by providing necessary sugars, micronutrients, and nitrogen source when combined with waste cooking oil as the primary carbon source.

Chapter 8

8. References

1. Haskins, R. H., Thorn, J. A., & Boothroyd, B. (1955). Biochemistry of the Ustilaginales: XI. Metabolic Products of *Ustilago zeae* in Submerged Culture. *Canadian Journal of Microbiology*, *1*(9), 749–756. https://doi.org/10.1139/m55-089
2. Boothroyd, B., Thorn, J. A., & Haskins, R. H. (1956). Biochemistry of the Ustilaginales: XII. Characterization of Extracellular Glycolipids Produced by *Ustilago sp*. *Canadian Journal of Biochemistry and Physiology*, *34*(1), 10–14. https://doi.org/10.1139/o56-003
3. Fluharty, A. L., & O'Brien, J. S. (1969). A mannose- and erythritol-containing glycolipid from Ustilago maydis. *Biochemistry*, *8*(6), 2627–2632. https://doi.org/10.1021/bi00834a056
4. Kitamoto, D., Haneishi, K., Nakahara, T., & Tabuchi, T. (1990). Production of mannosylerythritol lipids by Candida antarctica from vegetable oils.. *Agricultural and Biological Chemistry*, 54(1), 37–40. https://doi.org/10.1271/bbb1961.54.37
5. Fukuoka, T., Morita, T., Konishi, M., Imura, T., & Kitamoto, D. (2008). A basidiomycetous yeast, *Pseudozyma tsukubaensis*, efficiently produces a novel glycolipid biosurfactant. The identification of a new diastereomer of mannosylerythritol lipid-B. *Carbohydrate Research*, *343*(3), 555–560. https://doi.org/10.1016/j.carres.2007.11.023
6. Fukuoka, T., Kawamura, M., Morita, T., Imura, T., Sakai, H., Abe, M., & Kitamoto, D. (2008). A basidiomycetous yeast, *Pseudozyma crassa*, produces novel diastereomers of conventional mannosylerythritol lipids as glycolipid biosurfactants. *Carbohydrate Research*, *343*(17), 2947–2955. https://doi.org/10.1016/j.carres.2008.08.034
7. Morita, T., Fukuoka, T., Konishi, M., Imura, T., Yamamoto, S., Kitagawa, M., Sogabe, A., & Kitamoto, D. (2009). Production of a novel glycolipid biosurfactant, mannosylmannitol lipid, by Pseudozyma parantarctica and its interfacial properties. *Applied Microbiology and Biotechnology*, *83*(6), 1017–1025. https://doi.org/10.1007/s00253-009-1945-4
8. Morita, T., Fukuoka, T., Imura, T., & Kitamoto, D. (2012). Formation of the two novel glycolipid biosurfactants, mannosylribitol lipid and mannosylarabitol lipid, by *Pseudozyma parantarctica* JCM 11752T. *Applied Microbiology and Biotechnology*, *96*(4), 931–938. https://doi.org/10.1007/s00253-012-4230-x

9. Fukuoka, T., Morita, T., Konishi, M., Imura, T., & Kitamoto, D. (2007). Characterization of new glycolipid biosurfactants, tri-acylated mannosylerythritol lipids, produced by *Pseudozyma* yeasts. *Biotechnology Letters*, *29*(7), 1111–1118. https://doi.org/10.1007/s10529-007-9363-0
10. Fukuoka, T., Morita, T., Konishi, M., Imura, T., Sakai, H., & Kitamoto, D. (2007). Structural characterization and surface-active properties of a new glycolipid biosurfactant, mono-acylated mannosylerythritol lipid, produced from glucose by *Pseudozyma antarctica*. *Applied Microbiology and Biotechnology*, *76*(4), 801–810. https://doi.org/10.1007/s00253-007-1051-4
11. Beck, A., Werner, N., & Zibek, S. (2019). Mannosylerythritol Lipids: Biosynthesis, Genetics, and Production Strategies. In *Biobased Surfactants* (pp. 121–167). Elsevier. https://doi.org/10.1016/B978-0-12-812705-6.00004-6
12. Morita, T., Ito, E., Kitamoto, H. K., Takegawa, K., Fukuoka, T., Imura, T., & Kitamoto, D. (2010). Identification of the gene *PaEMT1* for biosynthesis of mannosylerythritol lipids in the basidiomycetous yeast *Pseudozyma antarctica*. *Yeast*, *27*(11), 905–917. https://doi.org/10.1002/yea.1794
13. Coelho, A. L. S., Feuser, P. E., Carciofi, B. A. M., de Andrade, C. J., & de Oliveira, D. (2020). Mannosylerythritol lipids: antimicrobial and biomedical properties. *Applied Microbiology and Biotechnology*, *104*(6), 2297–2318. https://doi.org/10.1007/s00253-020-10354-z
14. Yoshida, S., Morita, T., Shinozaki, Y., Watanabe, T., Sameshima-Yamashita, Y., Koitabashi, M., Kitamoto, D., & Kitamoto, H. (2014). Mannosylerythritol lipids secreted by phyllosphere yeast Pseudozyma antarctica is associated with its filamentous growth and propagation on plant surfaces. *Applied Microbiology and Biotechnology*, *98*(14), 6419–6429. https://doi.org/10.1007/s00253-014-5675-x
15. Hewald, S., Josephs, K., & Bölker, M. (2005). Genetic Analysis of Biosurfactant Production in *Ustilago maydis*. *Applied and Environmental Microbiology*, *71*(6), 3033–3040. https://doi.org/10.1128/AEM.71.6.3033-3040.2005
16. Keller, N. P. (2019). Fungal secondary metabolism: regulation, function and drug discovery. *Nature Reviews Microbiology*, *17*(3), 167–180. https://doi.org/10.1038/s41579-018-0121-1

17. Hewald, S., Linne, U., Scherer, M., Marahiel, M. A., Kämper, J., & Bölker, M. (2006). Identification of a Gene Cluster for Biosynthesis of Mannosylerythritol Lipids in the Basidiomycetous Fungus *Ustilago maydis*. *Applied and Environmental Microbiology*, *72*(8), 5469–5477. https://doi.org/10.1128/AEM.00506-06
18. Saika, A., Koike, H., Fukuoka, T., Yamamoto, S., Kishimoto, T., & Morita, T. (2016). A Gene Cluster for Biosynthesis of Mannosylerythritol Lipids Consisted of 4-O-β-D-Mannopyranosyl-(2R,3S)-Erythritol as the Sugar Moiety in a Basidiomycetous Yeast Pseudozyma tsukubaensis. *PLOS ONE*, *11*(6), e0157858. https://doi.org/10.1371/journal.pone.0157858
19. Hohn, T. M., McCormick, S. P., & Desjardins, A. E. (1993). Evidence for a gene cluster involving trichothecene-pathway biosynthetic genes in Fusarium sporotrichioides. *Current Genetics*, *24*(4), 291–295. https://doi.org/10.1007/BF00336778
20. Tudzynski, B., & Hölter, K. (1998). Gibberellin Biosynthetic Pathway inGibberella fujikuroi:Evidence for a Gene Cluster. *Fungal Genetics and Biology*, *25*(3), 157–170. https://doi.org/10.1006/fgbi.1998.1095
21. Deml, G., Anke, T., Oberwinkler, F., Max Giannetti, B., & Steglich, W. (1980). Schizonellin A and B, new glycolipids from Schizonella melanogramma. *Phytochemistry*, *19*(1), 83–87. https://doi.org/10.1016/0031-9422(80)85018-7
22. Kurz, M., Eder, C., Isert, D., Li, Z., Paulus, E. F., Schiell, M., Toti, L., Vértesy, L., Wink, J., & Seibert, G. (2003). Ustilipids, Acylated .BETA.-D-Mannopyranosyl D-Erythritols from Ustilago maydis and Geotrichum candidum. *The Journal of Antibiotics*, *56*(2), 91–101. https://doi.org/10.7164/antibiotics.56.91
23. Kakugawa, K., Tamai, M., Imamura, K., Miyamoto, K., Miyoshi, S., Morinaga, Y., Suzuki, O., & Miyakawa, T. (2002). Isolation of Yeast *Kurtzmanomyces* sp. I-11, Novel Producer of Mannosylerythritol Lipid. *Bioscience, Biotechnology, and Biochemistry*, *66*(1), 188–191. https://doi.org/10.1271/bbb.66.188
24. Saika, A., Koike, H., Fukuoka, T., Yamamoto, S., Kishimoto, T., & Morita, T. (2016). A Gene Cluster for Biosynthesis of Mannosylerythritol Lipids Consisted of 4-O-β-D-Mannopyranosyl-(2R,3S)-Erythritol as the Sugar Moiety in a Basidiomycetous Yeast Pseudozyma tsukubaensis. *PLOS ONE*, *11*(6), e0157858. https://doi.org/10.1371/journal.pone.0157858

25. Freitag, J., Ast, J., Linne, U., Stehlik, T., Martorana, D., Bölker, M., & Sandrock, B. (2014). Peroxisomes contribute to biosynthesis of extracellular glycolipids in fungi. *Molecular Microbiology*, *93*(1), 24–36. https://doi.org/10.1111/mmi.12642
26. Morita, T., Fukuoka, T., Kosaka, A., Imura, T., Sakai, H., Abe, M., & Kitamoto, D. (2015). Selective formation of mannosyl-l-arabitol lipid by *Pseudozyma tsukubaensis* JCM16987. *Applied Microbiology and Biotechnology*, *99*(14), 5833–5841. https://doi.org/10.1007/s00253-015-6575-4
27. Deinzer, H.-T., Linne, U., Xie, X., Bölker, M., & Sandrock, B. (2019). Elucidation of substrate specificities of decorating enzymes involved in mannosylerythritol lipid production by cross-species complementation. *Fungal Genetics and Biology*, *130*, 91–97. https://doi.org/10.1016/j.fgb.2019.05.003
28. Saika, A., Utashima, Y., Koike, H., Yamamoto, S., Kishimoto, T., Fukuoka, T., & Morita, T. (2018). Biosynthesis of mono-acylated mannosylerythritol lipid in an acyltransferase gene-disrupted mutant of *Pseudozyma tsukubaensis*. *Applied Microbiology and Biotechnology*, *102*(4), 1759–1767. https://doi.org/10.1007/s00253-017-8698-2
29. Konishi, M., & Makino, M. (2018). Selective production of deacetylated mannosylerythritol lipid, MEL-D, by acetyltransferase disruption mutant of *Pseudozyma hubeiensis*. *Journal of Bioscience and Bioengineering*, *125*(1), 105–110. https://doi.org/10.1016/j.jbiosc.2017.08.003
30. Morita, T., Takashima, M., Fukuoka, T., Konishi, M., Imura, T., & Kitamoto, D. (2010). Isolation of basidiomycetous yeast *Pseudozyma tsukubaensis* and production of glycolipid biosurfactant, a diastereomer type of mannosylerythritol lipid-B. *Applied Microbiology and Biotechnology*, *88*(3), 679–688. https://doi.org/10.1007/s00253-010-2762-5
31. Saika, A., Fukuoka, T., Koike, H., Yamamoto, S., Sugahara, T., Sogabe, A., Kitamoto, D., & Morita, T. (2020). A putative transporter gene PtMMF1-deleted strain produces mono-acylated mannosylerythritol lipids in *Pseudozyma tsukubaensis*. *Applied Microbiology and Biotechnology*, *104*(23), 10105–10117. https://doi.org/10.1007/s00253-020-10961-w
32. Kitamoto, D., Ikegami, T., Suzuki, G. T., Sasaki, A., Takeyama, Y. I., Idemoto, Y., Koura, N., & Yanagishita, H. (2001). Microbial conversion of n-alkanes into glycolipid biosurfactants, mannosylerythritol lipids, by *Pseudozyma (Candida antarctica)*. *Biotechnology Letters*, *23*(20). https://doi.org/10.1023/A:1012464717259

33. Morita, T., Ishibashi, Y., Hirose, N., Wada, K., Takahashi, M., Fukuoka, T., Imura, T., Sakai, H., Abe, M., & Kitamoto, D. (2011). Production and characterization of a glycolipid biosurfactant, mannosylerythritol lipid B, from sugarcane juice by *Ustilago Scitaminea* NBRC 32730. *Bioscience, Biotechnology and Biochemistry*, *75*(7). https://doi.org/10.1271/bbb.110221
34. Faria, N. T., Marques, S., Fonseca, C., & Ferreira, F. C. (2015). Direct xylan conversion into glycolipid biosurfactants, mannosylerythritol lipids, by *Pseudozyma antarctica* PYCC 5048T. *Enzyme and Microbial Technology*, *71*, 58–65. https://doi.org/10.1016/j.enzmictec.2014.10.008
35. Schuler, D., Wahl, R., Wippel, K., Vranes, M., Münsterkötter, M., Sauer, N., & Kämper, J. (2015). Hxt1, a monosaccharide transporter and sensor required for virulence of the maize pathogen *Ustilago maydis* . *New Phytologist*, *206*(3), 1086–1100. https://doi.org/10.1111/nph.13314
36. Rzechonek, D. A., Dobrowolski, A., Rymowicz, W., & Mirończuk, A. M. (2018). Recent advances in biological production of erythritol. *Critical Reviews in Biotechnology*, *38*(4), 620–633. https://doi.org/10.1080/07388551.2017.1380598
37. Moon, H.-J., Jeya, M., Kim, I.-W., & Lee, J.-K. (2010). Biotechnological production of erythritol and its applications. *Applied Microbiology and Biotechnology*, *86*(4), 1017–1025. https://doi.org/10.1007/s00253-010-2496-4
38. Dunn, M. F., Ramírez-Trujillo, J. A., & Hernández-Lucas, I. (2009). Major roles of isocitrate lyase and malate synthase in bacterial and fungal pathogenesis. *Microbiology*, *155*(10), 3166–3175. https://doi.org/10.1099/mic.0.030858-0
39. Kitamoto, H. K., Shinozaki, Y., Cao, X., Morita, T., Konishi, M., Tago, K., Kajiwara, H., Koitabashi, M., Yoshida, S., Watanabe, T., Sameshima-Yamashita, Y., Nakajima-Kambe, T., & Tsushima, S. (2011). Phyllosphere yeasts rapidly break down biodegradable plastics. *AMB Express*, *1*(1), 44. https://doi.org/10.1186/2191-0855-1-44
40. Faria, N. T., Santos, M. v., Fernandes, P., Fonseca, L. L., Fonseca, C., & Ferreira, F. C. (2014). Production of glycolipid biosurfactants, mannosylerythritol lipids, from pentoses and d-glucose/d-xylose mixtures by *Pseudozyma* yeast strains. *Process Biochemistry*, *49*(11). https://doi.org/10.1016/j.procbio.2014.08.004

41. Stehlik, T., Sandrock, B., Ast, J., & Freitag, J. (2014). Fungal peroxisomes as biosynthetic organelles. *Current Opinion in Microbiology*, *22*, 8–14. https://doi.org/10.1016/j.mib.2014.09.011
42. Kitamoto, D., Yanagishita, H., Haraya, K. et al. Contribution of a chain-shortening pathway to the biosynthesis of the fatty acids of mannosylerythritol lipid (biosurfactant) in the yeast *Candida antarctica*: Effect of β-oxidation inhibitors on biosurfactant synthesis. *Biotechnology Letters 20*, 813–818 (1998). https://doi.org/10.1023/A:1005347022247
43. Kitamoto, D., Nemoto, T., Yanagishita, H., Nakane, T., Kitamoto, H., & Nakahara, T. (1993). Fatty-acid Metabolism of Mannosylerythritol Lipids as Biosurfactants Produced by Candida antarctica. *Journal of Japan Oil Chemists' Society*, *42*(5), 346–358. https://doi.org/10.5650/jos1956.42.346
44. Kitamoto, D., Yokoshima, T., Yanagishita, H., Haraya, K., & Kitamoto, H. K. (1999).Formation of Glycolipid Biosurfactant, Mannosylerythritol Lipid, by *Candida antarctica* from Aliphatic Hydrocarbons via Subterminal Oxidation Pathway. *Journal of Japan Oil Chemists' Society*, *48*(12). https://doi.org/10.5650/jos1996.48.1377
45. Rau, U., Nguyen, L. A., Schulz, S., Wray, V., Nimtz, M., Roeper, H., Koch, H., & Lang, S. (2005). Formation and analysis of mannosylerythritol lipids secreted by *Pseudozyma aphidis*. *Applied Microbiology and Biotechnology*, *66*(5). https://doi.org/10.1007/s00253-004-1672-9
46. Kitamoto, D., Yanagishita, H., Haraya, K., & Kitamoto, H. K. (1995). Effect of cerulenin on the production of mannosyl-erythritol lipids as biosurfactants by *Candida antarctica*. *Biotechnology Letters*, *17*(1), 25–30. https://doi.org/10.1007/BF00134190
47. Ortiz, C., Ferreira, M. L., Barbosa, O., dos Santos, J. C. S., Rodrigues, R. C., Berenguer-Murcia, Á., Briand, L. E., & Fernandez-Lafuente, R. (2019). Novozym 435: the "perfect" lipase immobilized biocatalyst? *Catalysis Science & Technology*, *9*(10), 2380–2420. https://doi.org/10.1039/C9CY00415G
48. Fukuoka, T., Yanagihara, T., Imura, T., Morita, T., Sakai, H., Abe, M., & Kitamoto, D. (2011). Enzymatic synthesis of a novel glycolipid biosurfactant, mannosylerythritol lipid-D and its aqueous phase behavior. *Carbohydrate Research*, *346*(2), 266–271. https://doi.org/10.1016/j.carres.2010.11.025

49. Fukuoka, T., Yanagihara, T., Imura, T., Morita, T., Sakai, H., Abe, M., & Kitamoto, D. (2012). The diastereomers of mannosylerythritol lipids have different interfacial properties and aqueous phase behavior, reflecting the erythritol configuration. *Carbohydrate Research*, *351*, 81–86. https://doi.org/10.1016/j.carres.2012.01.019
50. Morita, T., Konishi, M., Fukuoka, T., Imura, T., & Kitamoto, D. (2007). Microbial conversion of glycerol into glycolipid biosurfactants, mannosylerythritol lipids, by a basidiomycete yeast, Pseudozyma antarctica JCM 10317T. *Journal of Bioscience and Bioengineering*, *104*(1), 78–81. https://doi.org/10.1263/jbb.104.78
51. Hiok, C., Tabuchi, T., Kitamoto, D., & Akiba, S. (1990). Extracellular Accumulation of Mannosylerythritol Lipids by a Strain of Candida Antarctica. *Agricultural and Biological Chemistry*, *54*(1). https://doi.org/10.1271/bbb1961.54.31
52. Morita, T., Konishi, M., Fukuoka, T., Imura, T., & Kitamoto, D. (2007). Physiological differences in the formation of the glycolipid biosurfactants, mannosylerythritol lipids, between Pseudozyma antarctica and Pseudozyma aphidis. *Applied Microbiology and Biotechnology*, *74*(2), 307–315. https://doi.org/10.1007/s00253-006-0672-3
53. Morita, T., Koike, H., Hagiwara, H., Ito, E., Machida, M., Sato, S., Habe, H., & Kitamoto, D. (2014). Genome and Transcriptome Analysis of the Basidiomycetous Yeast Pseudozyma antarctica Producing Extracellular Glycolipids, Mannosylerythritol Lipids. *PLoS ONE*, *9*(2), e86490. https://doi.org/10.1371/journal.pone.0086490
54. Spoeckner, S., Wray, V., Nimtz, M., & Lang, S. (1999). Glycolipids of the smut fungus Ustilago maydis from cultivation on renewable resources. *Applied Microbiology and Biotechnology*, *51*(1), 33–39. https://doi.org/10.1007/s002530051359
55. Günther, M., Grumaz, C., Lorenz, S., Stevens, P., Lindemann, E., Hirth, T., Sohn, K., Zibek, S., & Rupp, S. (2015). The transcriptomic profile of Pseudozyma aphidis during production of mannosylerythritol lipids. *Applied Microbiology and Biotechnology*, *99*(3), 1375–1388. https://doi.org/10.1007/s00253-014-6359-2
56. Mortazavi, A., Williams, B. A., McCue, K., Schaeffer, L., & Wold, B. (2008). Mapping and quantifying mammalian transcriptomes by RNA-Seq. *Nature Methods*, *5*(7), 621–628. https://doi.org/10.1038/nmeth.1226
57. Kitamoto, D., Yanagishita, H., Shinbo, T., Nakane, T., Kamisawa, C., & Nakahara, T. (1993). Surface active properties and antimicrobial activities of mannosylerythritol lipids as

biosurfactants produced by Candida antarctica. *Journal of Biotechnology*, *29*(1–2), 91–96. https://doi.org/10.1016/0168-1656(93)90042-L

58. Kitamoto, D., Isoda, H., & Nakahara, T. (2002). Functions and potential applications of glycolipid biosurfactants — from energy-saving materials to gene delivery carriers —. *Journal of Bioscience and Bioengineering*, *94*(3). https://doi.org/10.1016/s1389-1723(02)80149-9
59. McDowell RH, Sands EM, Friedman H. Bacillus Cereus. [Updated 2022 Sep 12]. In: StatPearls [Internet]. Treasure Island (FL): StatPearls Publishing; 2022 Jan-. Available from: https://www.ncbi.nlm.nih.gov/books/NBK459121/
60. Shu, Q., Niu, Y., Zhao, W., & Chen, Q. (2019). Antibacterial activity and mannosylerythritol lipids against vegetative cells and spores of Bacillus cereus. *Food Control*, *106*, 106711. https://doi.org/10.1016/j.foodcont.2019.106711
61. Yoshida, S., Koitabashi, M., Nakamura, J., Fukuoka, T., Sakai, H., Abe, M., Kitamoto, D., & Kitamoto, H. (2015). Effects of biosurfactants, mannosylerythritol lipids, on the hydrophobicity of solid surfaces and infection behaviours of plant pathogenic fungi. *Journal of Applied Microbiology*, *119*(1), 215–224. https://doi.org/10.1111/jam.12832
62. Kitamoto, D., Morita, T., Fukuoka, T., Konishi, M., & Imura, T. (2009). Self-assembling properties of glycolipid biosurfactants and their potential applications. *Current Opinion in Colloid & Interface Science*, *14*(5), 315–328. https://doi.org/10.1016/j.cocis.2009.05.009
63. Morita, T., Kitagawa, M., Suzuki, M., Yamamoto, S., Sogabe, A., Yanagidani, S., Imura, T., Fukuoka, T., & Kitamoto, D. (2009). A Yeast Glycolipid Biosurfactant, Mannosylerythritol Lipid, Shows Potential Moisturizing Activity toward Cultured Human Skin Cells: The Recovery Effect of MEL-A on the SDS-damaged Human Skin Cells. *Journal of Oleo Science*, *58*(12), 639–642. https://doi.org/10.5650/jos.58.639
64. Yamamoto, S., Morita, T., Fukuoka, T., Imura, T., Yanagidani, S., Sogabe, A., Kitamoto, D., & Kitagawa, M. (2012). The Moisturizing Effects of Glycolipid Biosurfactants, Mannosylerythritol Lipids, on Human Skin. *Journal of Oleo Science*, *61*(7), 407–412. https://doi.org/10.5650/jos.61.407
65. Worakitkanchanakul, W., Imura, T., Fukuoka, T., Morita, T., Sakai, H., Abe, M., Rujiravanit, R., Chavadej, S., Minamikawa, H., & Kitamoto, D. (2009). Phase behavior of ternary

mannosylerythritol lipid/water/oil systems. *Colloids and Surfaces B: Biointerfaces*, *68*(2), 207–212. https://doi.org/10.1016/j.colsurfb.2008.10.009

66. Santana, R. C., Perrechil, F. A., & Cunha, R. L. (2013). High- and Low-Energy Emulsifications for Food Applications: A Focus on Process Parameters. *Food Engineering Reviews*, *5*(2), 107–122. https://doi.org/10.1007/s12393-013-9065-4
67. Morita, T., Kitagawa, M., Yamamoto, S., Sogabe, A., Imura, T., Fukuoka, T., & Kitamoto, D. (2010). Glycolipid Biosurfactants, Mannosylerythritol Lipids, Repair the Damaged Hair. *Journal of Oleo Science*, *59*(5), 267–272. https://doi.org/10.5650/jos.59.267
68. Morita, T., Kitagawa, M., Yamamoto, S., Suzuki, M., Sogabe, A., Imura, T., Fukuoka, T., & Kitamoto, D. (2010). Activation of Fibroblast and Papilla Cells by Glycolipid Biosurfactants, Mannosylerythritol Lipids. *Journal of Oleo Science*, *59*(8), 451–455. https://doi.org/10.5650/jos.59.451
69. Reynolds, A. J., & Jahoda, C. A. (1992). Cultured dermal papilla cells induce follicle formation and hair growth by transdifferentiation of an adult epidermis. *Development*, *115*(2), 587–593. https://doi.org/10.1242/dev.115.2.587
70. Kawai, N; Nomura,Y. Hair Nourishing agent. Japanese Patent No.3772190. 05/10/2006
71. Takahashi, M., Morita, T., Fukuoka, T., Imura, T., & Kitamoto, D. (2012). Glycolipid Biosurfactants, Mannosylerythritol Lipids, Show Antioxidant and Protective Effects against H2O2-Induced Oxidative Stress in Cultured Human Skin Fibroblasts. *Journal of Oleo Science*, *61*(8), 457–464. https://doi.org/10.5650/jos.61.457
72. Inoh, Y., Kitamoto, D., Hirashima, N., & Nakanishi, M. (2001). Biosurfactants of MEL-A Increase Gene Transfection Mediated by Cationic Liposomes. *Biochemical and Biophysical Research Communications*, *289*(1), 57–61. https://doi.org/10.1006/bbrc.2001.5930
73. Ghosh, S., Brown, A. M., Jenkins, C., & Campbell, K. (2020). Viral Vector Systems for Gene Therapy: A Comprehensive Literature Review of Progress and Biosafety Challenges. *Applied Biosafety*, *25*(1), 7–18. https://doi.org/10.1177/1535676019899502
74. Isoda, H., Shinmoto, H., Kitamoto, D., Matsumura, M., & Nakahara, T. (1997). Differentiation of human promyelocytic leukemia cell line HL60 by microbial extracellular glycolipids. *Lipids*, *32*(3), 263–271. https://doi.org/10.1007/s11745-997-0033-0
75. Wang Q-M, Begerow D, Groenewald M, Liu X-Z, Theelen B, Bai F-Y, Boekhout T (2015) Multigene phylogeny and taxonomic revision of yeasts and related fungi in

the Ustilaginomycotina. *Studies in Mycology 81*: 55−83. https://doi.org/10.1016/j.simyco.2015.10.004

76. Hakomori, S. (1990). Bifunctional role of glycosphingolipids. Modulators for transmembrane signaling and mediators for cellular interactions. *Journal of Biological Chemistry*, *265*(31), 18713–18716. https://doi.org/10.1016/S0021-9258(17)30565-3
77. Iwabuchi, K., Nakayama, H., Iwahara, C., & Takamori, K. (2010). Significance of glycosphingolipid fatty acid chain length on membrane microdomain-mediated signal transduction. *FEBS Letters*, *584*(9), 1642–1652. https://doi.org/10.1016/j.febslet.2009.10.043
78. Isoda, H., Nakahara, T. (1997).Mannosylerythritol lipid induces granulocytic differentiation and inhibits the tyrosine phosphorylation of human myelogenous leukemia cell line K562. *Cytotechnology 25*, 191–195. https://doi.org/10.1023/A:1007982909932
79. Zhao, X., Geltinger, C., Kishikawa, S. et al. (2000). Treatment of mouse melanoma cells with phorbol 12-myristate 13-acetate counteracts mannosylerythritol lipid-induced growth arrest and apoptosis. *Cytotechnology 33, 123–130.* https://doi.org/10.1023/A:1008129616127
80. Carson, D. A., & Ribeiro, J. M. (1993). Apoptosis and disease. *The Lancet*, *341*(8855), 1251–1254. https://doi.org/10.1016/0140-6736(93)91154-E
81. Livneh, E., & Fishman, D. D. (1997). Linking Protein Kinase C to Cell-Cycle Control. *European Journal of Biochemistry*, *248*(1), 1–9. https://doi.org/10.1111/j.1432-1033.1997.t01-4-00001.x
82. Kalal, B. S., Upadhya, D., & Pai, V. R. (2017). Chemotherapy resistance mechanisms in advanced skin cancer. *Oncology Reviews*. https://doi.org/10.4081/oncol.2017.326
83. Im, J. H., Yanagishita, H., Ikegami, T., Takeyama, Y., Idemoto, Y., Koura, N., & Kitamoto, D. (2003). Mannosylerythritol lipids, yeast glycolipid biosurfactants, are potential affinity ligand materials for human immunoglobulin G. *Journal of Biomedical Materials Research*, *65A*(3), 379–385. https://doi.org/10.1002/jbm.a.10491
84. Gülich, S., Uhlén, M., & Hober, S. (2000). Protein engineering of an IgG-binding domain allows milder elution conditions during affinity chromatography. *Journal of biotechnology, 76 2-3*, 233-44. https://doi.org/10.1016/s0168-1656(99)00197-2
85. Evans, S. v., & Roger MacKenzie, C. (1999). Characterization of protein-glycolipid recognition at the membrane bilayer. *Journal of Molecular Recognition*, *12*(3), 155–168. https://doi.org/10.1002/(SICI)1099-1352(199905/06)12:3<155::AID-JMR456>3.0.CO;2-S

86. Im, J.H., Nakane, T., Yanagishita, H. et al. (2001). Mannosylerythritol lipid, a yeast extracellular glycolipid, shows high binding affinity towards human immunoglobulin G. *BMC Biotechnol* 1, 5 https://doi.org/10.1186/1472-6750-1-5
87. Sajna, K. V., Sukumaran, R. K., Jayamurthy, H., Reddy, K. K., Kanjilal, S., Prasad, R. B. N., & Pandey, A. (2013). Studies on biosurfactants from Pseudozyma sp. NII 08165 and their potential application as laundry detergent additives. *Biochemical Engineering Journal*, *78*, 85–92. https://doi.org/10.1016/j.bej.2012.12.014
88. Kitamoto, D., Yanagishita, H., Endo, A., Nakaiwa, M., Nakane, T., & Akiya, T. (2001). Remarkable Antiagglomeration Effect of a Yeast Biosurfactant, Diacylmannosylerythritol, on Ice-Water Slurry for Cold Thermal Storage. *Biotechnology Progress*, *17*(2), 362–365. https://doi.org/10.1021/bp000159f
89. Bart, J. C. J., Palmeri, N., & Cavallaro, S. (2010). Processes for biodiesel production from unrefined oils and fats. In *Biodiesel Science and Technology* (pp. 386–433). Elsevier. https://doi.org/10.1533/9781845697761.386
90. Advances in Eco-Fuels for a Sustainable Environment. (2019). Elsevier. https://doi.org/10.1016/C2017-0-04211-8
91. Bednarski, W., Adamczak, M., Tomasik, J., & Płaszczyk, M. (2004). Application of oil refinery waste in the biosynthesis of glycolipids by yeast. *Bioresource Technology*, *95*(1), 15–18. https://doi.org/10.1016/j.biortech.2004.01.009
92. Wan Azahar, W. N. A., Bujang, M., Jaya, R. P., Hainin, M. R., Mohamed, A., Ngad, N., & Jayanti, D. S. (2016). THE POTENTIAL OF WASTE COOKING OIL AS BIO-ASPHALT FOR ALTERNATIVE BINDER â€“ AN OVERVIEW. *Jurnal Teknologi*, *78*(4). https://doi.org/10.11113/jt.v78.8007
93. Fleurackers, S. J. J. (2006). On the use of waste frying oil in the synthesis of sophorolipids. *European Journal of Lipid Science and Technology*, *108*(1), 5–12. https://doi.org/10.1002/ejlt.200500237
94. Haba, E., Espuny, M. J., Busquets, M., & Manresa, A. (2000). Screening and production of rhamnolipids by Pseudomonas aeruginosa 47T2 NCIB 40044 from waste frying oils. *Journal of Applied Microbiology*, *88*(3), 379–387. https://doi.org/10.1046/j.1365-2672.2000.00961.x
95. Niu, Y., Wu, J., Wang, W., & Chen, Q. (2019). Production and characterization of a new glycolipid, mannosylerythritol lipid, from waste cooking oil biotransformation by

Pseudozyma aphidis ZJUDM34. *Food Science and Nutrition*, *7*(3). https://doi.org/10.1002/fsn3.880

96. Morita, T., Ishibashi, Y., Hirose, N., Wada, K., Takahashi, M., Fukuoka, T., Imura, T., Sakai, H., Abe, M., & Kitamoto, D. (2011). Production and Characterization of a Glycolipid Biosurfactant, Mannosylerythritol Lipid B, from Sugarcane Juice by *Ustilago scitaminea* NBRC 32730. *Bioscience, Biotechnology, and Biochemistry*, *75*(7), 1371–1376. https://doi.org/10.1271/bbb.110221
97. Singh, A., Lal, U., Mukhtar, H., Singh, P., Shah, G., & Dhawan, R. (2015). Phytochemical profile of sugarcane and its potential health aspects. *Pharmacognosy Reviews*, *9*(17), 45. https://doi.org/10.4103/0973-7847.156340
98. Avancini, S. R. P., Faccin, G. L., Vieira, M. A., Rovaris, A. A., Podestá, R., Tramonte, R., de Souza, N. M. A., & Amante, E. R. (2007). Cassava starch fermentation wastewater: Characterization and preliminary toxicological studies. *Food and Chemical Toxicology*, *45*(11), 2273–2278. https://doi.org/10.1016/j.fct.2007.06.006
99. Maróstica Jr., M. R., & Pastore, G. M. (2006). Biotransformation of citronellol in rose-oxide using cassava wastewater as a medium. *Ciência e Tecnologia de Alimentos*, *26*(3), 690–696. https://doi.org/10.1590/S0101-20612006000300032
100. Andrade, C. J. de, Andrade, L. M. de, Rocco, S. A., Sforça, M. L., Pastore, G. M., & Jauregi, P. (2017). A novel approach for the production and purification of mannosylerythritol lipids (MEL) by Pseudozyma tsukubaensis using cassava wastewater as substrate. *Separation and Purification Technology*, *180*, 157–167. https://doi.org/10.1016/j.seppur.2017.02.045
101. Morita, T., Ishibashi, Y., Fukuoka, T., Imura, T., Sakai, H., Abe, M., & Kitamoto, D. (2009).Production of Glycolipid Biosurfactants, Mannosylerythritol Lipids, Using Sucrose by Fungal and Yeast Strains, and Their Interfacial Properties. *Bioscience, Biotechnology, and Biochemistry*, *73*(10), 2352–2355. https://doi.org/10.1271/bbb.90439
102. Barile, D., Tao, N., Lebrilla, C. B., Coisson, J.-D., Arlorio, M., & German, J. B. (2009). Permeate from cheese whey ultrafiltration is a source of milk oligosaccharides. *International Dairy Journal*, *19*(9), 524–530. https://doi.org/10.1016/j.idairyj.2009.03.008
103. Tsermoula, P., Bechshøft, M. R., Friis, C., Engelsen, S. B., & Khakimov, B. (2023). Screening of non-protein nitrogen compounds in lactose refining streams from industrial

whey permeate processing. *Food Chemistry, 405*, 134716. https://doi.org/10.1016/j.foodchem.2022.134716

104. Dzięgielewska, E., & Adamczak, M. (2013). Evaluation of waste products in the synthesis of surfactants by yeasts. *Chemical Papers*, *67*(9). https://doi.org/10.2478/s11696-013-0349-1

105. Jamir, L., Kumar, V., Kaur, J., Kumar, S., & Singh, H. (2021). Composition, valorization and therapeutical potential of molasses: a critical review. *Environmental Technology Reviews*, *10*(1), 131–142. https://doi.org/10.1080/21622515.2021.1892203

106. Tovar-Herrera, O. E., Batista-García, R. A., Sánchez-Carbente, M. del R., Iracheta-Cárdenas, M. M., Arévalo-Niño, K., & Folch-Mallol, J. L. (2015). A Novel Expansin Protein from the White-Rot Fungus Schizophyllum commune. *PLOS ONE*, *10*(3), e0122296. https://doi.org/10.1371/journal.pone.0122296

107. Wada, K., Koike, H., Fujii, T., & Morita, T. (2020). Targeted transcriptomic study of the implication of central metabolic pathways in mannosylerythritol lipids biosynthesis in Pseudozyma antarctica T-34. *PLOS ONE*, *15*(1), e0227295. https://doi.org/10.1371/journal.pone.0227295

108. Saika, A., Koike, H., Hori, T., Fukuoka, T., Sato, S., Habe, H., Kitamoto, D., & Morita, T. (2014). Draft Genome Sequence of the Yeast *Pseudozyma antarctica* Type Strain JCM10317, a Producer of the Glycolipid Biosurfactants, Mannosylerythritol Lipids. *Genome Announcements*, *2*(5). https://doi.org/10.1128/genomeA.00878-14

109. Katsivela, E., Kleppe, F., Lang, S., & Wagner, F. (1995). Ustilago maydis lipase I. Hydrolysis and ester-synthesis activities of crude enzyme preparation. *Enzyme and Microbial Technology, 17(8)*, 739–745. https://doi.org/10.1016/0141-0229(94)00127-D

110. Sugiyama, J., Sugiyama, Y., Iizuka, H., and Torii, T. (1967). Report of the Japanese summer parties in dry valleys, Victoria Land, 1963–1965. IV. Mycological studies of the Antarctic fungi. Part. 2. Mycoflora of Lake Vanda, an ice-free lake. *Antarct. Rec. 28*, 23–32.

111. Goossens, E., Wijnants, M., Packet, D., & Lemière, F. (2016). Enhanced separation and analysis procedure reveals production of tri-acylated mannosylerythritol lipids by Pseudozyma aphidis. *Journal of Industrial Microbiology and Biotechnology*, *43*(11), 1537–1550. https://doi.org/10.1007/s10295-016-1838-3

112. Gibson, D., Young, L., Chuang, RY. *et al.* Enzymatic assembly of DNA molecules up to several hundred kilobases. *Nat Methods* **6**, 343–345 (2009). https://doi.org/10.1038/nmeth.1318

113. Kawai, S., Hashimoto, W., & Murata, K. (2010). Transformation of *Saccharomyces cerevisiae* and other fungi. *Bioengineered Bugs*, *1*(6), 395–403. https://doi.org/10.4161/bbug.1.6.13257

114. Lõoke, M., Kristjuhan, K., & Kristjuhan, A. (2011). Extraction of genomic DNA from yeasts for PCR-based applications. *BioTechniques*, *50*(5), 325–328. https://doi.org/10.2144/000113672

115. Goldstein, A. L., & McCusker, J. H. (1999). Three new dominant drug resistance cassettes for gene disruption in Saccharomyces cerevisiae. *Yeast*, *15*(14), 1541–1553. https://doi.org/10.1002/(SICI)1097-0061(199910)15:14<1541::AID-YEA476>3.0.CO;2-K

116. Deml, G., Anke, T., Oberwinkler, F., Max Giannetti, B., & Steglich, W. (1980). Schizonellin A and B, new glycolipids from *Schizonella melanogramma*. *Phytochemistry*, *19*(1), 83–87. https://doi.org/10.1016/0031-9422(80)85018-7

117. Dincer, I., & Erdemir, D. (2021). Heat Storage Methods. In *Heat Storage Systems for Buildings* (pp. 37–90). Elsevier. https://doi.org/10.1016/B978-0-12-823572-0.00010-2

118. Ma, H., Kunes, S., Schatz, P. J., & Botstein, D. (1987). Plasmid construction by homologous recombination in yeast. *Gene*, *58*(2–3), 201–216. https://doi.org/10.1016/0378-1119(87)90376-3

119. Morita, T., Konishi, M., Fukuoka, T. *et al.* (2006). Discovery of *Pseudozyma rugulosa* NBRC 10877 as a novel producer of the glycolipid biosurfactants, mannosylerythritol lipids, based on rDNA sequence. *Appl Microbiol Biotechnol* **73**, 305–313 https://doi.org/10.1007/s00253-006-0466-7

120. Sambrook, J., & Russell, D. W. (2006). The Inoue Method for Preparation and Transformation of Competent *E. Coli* : "Ultra-Competent" Cells. *Cold Spring Harbor Protocols*, *2006*(1), pdb.prot3944. https://doi.org/10.1101/pdb.prot3944

121. Bulson, P. C., Johnstone, D. L., Gibbons, H. L., & Funk, W. H. (1984). Removal and inactivation of bacteria during alum treatment of a lake. *Applied and Environmental Microbiology*, *48*(2), 425–430. https://doi.org/10.1128/aem.48.2.425-430.1984

122. Yarimizu, T., Shimoi, H., Sameshima-Yamashita, Y., Morita, T., Koike, H., Watanabe, T., & Kitamoto, H. (2017). Targeted gene replacement at the *URA3* locus of the basidiomycetous yeast *Pseudozyma antarctica* and its transformation using lithium acetate treatment. *Yeast*, *34*(12), 483–494. https://doi.org/10.1002/yea.3251

123. Kunitake, E., Tanaka, T., Ueda, H., Endo, A., Yarimizu, T., Katoh, E., & Kitamoto, H. (2019). CRISPR/Cas9-mediated gene replacement in the basidiomycetous yeast *Pseudozyma antarctica*. *Fungal Genetics and Biology*, *130*, 82–90. https://doi.org/10.1016/j.fgb.2019.04.012

124. Watanabe, T., Suzuki, K., Sato, I., Morita, T., Koike, H., Shinozaki, Y., Ueda, H., Koitabashi, M., & Kitamoto, H. K. (2015). Simultaneous bioethanol distillery wastewater treatment and xylanase production by the phyllosphere yeast *Pseudozyma antarctica* GB-4(0). *AMB Express*, *5*(1), 36. https://doi.org/10.1186/s13568-015-0121-8

125. Alerts, I. (n.d.). Aluminum sulfate prices - historical & forecast data in several countries. Intratec.us. Retrieved April 17, 2023, from https://www.intratec.us/chemical-markets/aluminum-sulfate-price

126. Piepenbring, M., Stoll, M. & Oberwinkler, F. The generic position of *Ustilago maydis*, *Ustilago scitaminea*, and *Ustilago esculenta (Ustilaginales)*. Mycol Progress 1, 71–80 (2002). https://doi.org/10.1007/s11557-006-0006-y

127. Shu, Q., Lou, H., Wei, T., Zhang, X., & Chen, Q. (2021). Synergistic antibacterial and antibiofilm effects of ultrasound and MEL-A against methicillin-resistant *Staphylococcus aureus*. *Ultrasonics Sonochemistry*, 72, 105452. https://doi.org/10.1016/j.ultsonch.2020.105452